MODELING AND ANALYSIS OF ENERGY CONSUMPTION IN CHEVROLET VOLT GEN II HYBRID ELECTRIC VEHICLE

By

Rajeshwar Yadav

A THESIS

Submitted in partial fulfillment of the requirements for the degree of

MASTER OF SCIENCE

In Mechanical Engineering

MICHIGAN TECHNOLOGICAL UNIVERSITY

2018

This thesis has been approved in partial fulfillment of the requirements for the Degree of MASTER OF SCIENCE in Mechanical Engineering.

Department of Mechanical Engineering-Engineering Mechanics

Thesis Co-advisor: *Dr.Mahdi Shahbakhti*

Thesis Co-advisor: *Dr.Darell Robinette*

Committee Member: *Dr.Bo Chen*

Department Chair: *Dr. Willian W. Predebon*

Dedication

To my father Girja Shankar Yadav, mother Prabhavati Yadav,Archana Yadav ,Arati Yadav and Tejashree Gundeti

Contents

List of Figures

List of Tables

Acknowledgments

I would like to thank my family for their support,motivation and encouragement.

I would extend my gratitude to my advisor Dr. Mahdi Shahbakhti and Dr. Robinette for giving me the opportunity to be part of prestigious NEXTCAR project and guiding throughout my research term at Michigan Tech.

I would like to thank Dr. Bo Chen for being the part of my committee.

I would also like to thank other members of NEXTCAR project Chris Morgan, Joe Oncken,Kovid Sachdeva,Josh Orlando, Pradeep Bhatt, Drew Hannover and Saurabh Bhasme for their support and advice.

I would like thank my friends and colleagues for their support and encouragement.

List of Abbreviations

TPIM	Traction power inverter module
SI	Spark ignition
ICE	Internal Combustion engine
GM	General Motors
SOC	State of charge
ANL	Argonne National Laboratory
US	United States
GHG	Green house gases
GDI	Gasoline Direct Injection
OEM	Original Equipment Manufacturer
EPA	Environmental Protection Agency
MY	Manufacturing year
HEV	Hybrid electric vehicle
PHEV	Plug in hybrid electric vehicle
FCV	Fuel cell vehicle
ARPA-E	Advanced Research Projects Agency-Energy
NEXTCAR	NEXT- Generation Energy Technologies for Connected and Automated On–Road
MPC	Model predictive control

ANL	Argonne National Laboratory
BEV	Battery electric vehicle
APRF	Advanced Powertrain Research Facility
BSFC	Brake specific fuel consumption
APSRC	Advanced Power Systems Research Center
CSV	Comma–separated values
DBC	Data Base Container
ECU	Electric control unit
EGR	Exhaust gas recirculation
WOT	Wide open throttle
R–C	Resistance capacitance
MGA	Motor generator A
MGB	Motor generator B
DC	Direct current
AC	Alternating current
LVD	Longitudinal vehicle dynamics
UDDS	Urban Dynamometer Driving Schedule
HWFET	Highway Fuel Economy Test
CS	Charge sustaining
CD	Charge depleting
DOHC	Dual over head cam

SA	Spark advance
TWC	Three way catalyst
OBD	On-board diagnostics
OCV	Open circuit voltage
OCW	One way clutch
PG	Planetary gear
LHV	Lower heating value
TWC	Three Way Catalyst
HVAC	Heating, ventilation , and air conditioning

Symbols

C_D	Discharge coefficient
T	Temperature (K)
P	Pressure (kPa)
p_r	Pressure ratio (-)
R	Universal Gas Constant (kJ/kg.k)
γ	Specific heat ratio (-)
$\dot{m}$	mass flow rate (g/s)
V	Volume (cc)

η_{vol}	Efficiency (%)
N	Engine speed (RPM)
T_{br}	Brake torque (Nm)
T_L	Engine load (Nm)
J_{eff}	Effective moment of inertia of engine (kg/m^3)
R_{TS}	Resistance of shorter time constant RC circuit (ohm)
C_{TS}	Capacitance of shorter time constant RC circuit (F)
V_{CTS}	Voltage drop in shorter time constant RC circuit (V)
R_{TL}	Resistance of longer time constant RC circuit (ohm)
C_{TL}	Capacitance of longer time constant RC circuit (F)
V_{CTL}	Voltage drop in longer time constant RC circuit (V)
R_s	Series resistance (ohm)
w	Angular velocity (rev/sec)
S	Radius of sun gear (m)
R	Radius of ring gear (m)
I	Inertia ($kg.m^2$)
F	Force (N)
$\dot{\omega}$	Angular acceleration (rev/sec^2)
P	Power (W)
v	Vehicle velocity (m/s)
α	fraction of fuel energy supplied to coolant heating (-)

Q_{LHV}	Lower heating value of gasoline (kJ/kg)
M	Mass (kg)
C	Specific heat capacity (J/kg.K)
h	Convective heat transfer coefficient ($W/(K.m^2)$)
A	Area of coolant exposed to air (m^2)
δT	difference between coolant temperature and ambient air temperature (K)
E	Energy consumed (MJ)

Subscripts

at	intake
0	Ambient
man	Manifold
ac	In–cylinder
vol	Volumetric
d	Displaced
$e\dot{f}f$	Effective
V	Volume (cc)
L	Load
$batt$	Battery

i	Initial
1	Planetary gear 1
2	Planetary gear 2
e	engine
R	Resistance
$R, front$	Front rolling resistance
$R, front$	Rear rolling resistance
$aero$	Aerodynamic
f	fuel

Abstract

A high fidelity vehicle model is important to predict energy consumption of vehicle and to implement control strategies for further improvement in performance of vehicle. The work in this thesis, describes modeling procedure for developing a high fidelity model of plug in hybrid electric vehicle (PHEV) Chevrolet Volt Gen II using parameters provided by General Motors, is as a part of Advanced Research Projects Agency Energy (ARPA-E) group's "NEXT-Generation Energy Technologies for Connected and Automated On-Road Vehicles (NEXTCAR)" project. Each powertrain component , namely; internal combustion engine (ICE), motor generators, battery, traction power inverter module (TPIM) and drive unit, have been developed using high fidelity parameters in MATLAB/ Simulink.

In addition to major powertrain components development process, several energy affecting components/ conditions were modeled. To enhance accuracy of energy consumption prediction of battery, a regression fit drive unit auxiliary pump model, dependent on vehicle speed, axle torque and operating mode, was developed using experimental Argonne National Laboratory (ANL) test data. Further improvement in engine fuel energy prediction was improved by incorporating rule based fuel penalties (catalyst lightoff , coldstart and cranking) that depends on three way catalyst

(TWC) and engine coolant temperatures. In–vehicle testing was carried out to accomplish this task. To predict engine coolant temperature, a lumped coolant model was developed which will be necessary for predicting coldstart fuel penalty. Catalyst thermal model was develop to predict TWC temperature.

This thesis walks through validation process of each subsystem developed with experimental ANL test data and, validated components were integrated to develop a Chevy Volt Gen II model. The developed model was validated for US06 and Highway Fuel Economy Test (HWFET) drive cycles provided ANL for both charge sustaining (CS) and charge depleting (CD) test cases. The total energy (sum of electrical and fuel energy) of developed model is well with 5 % error compared to ANL test data. Further analysis of engine transient operation, causing transient fuel penalty, has been performed which a map-based engine model is incapable to predict. Using this analysis, an engine transient fuel penalty map was developed which will make a map–based model to mimic as a dynamic engine model. Moreover, mode switch fuel penalties have been analyzed and incorporated in the model.

Chapter 1

Introduction

According to Inventory of U.S. Greenhouse Gas Emissions and Sinks 1990 - 2015, transportation sector is the largest contributor of U.S.greenhouse gas (GHG) (shown in Figure 1.1), about 27% [1]. About 60 percent (shown in Figure 1.2) of total Transportation Sector GHG Emissions is contributed by Light-Duty Vehicles [1]. By 2025, Light duty vehicles have to achieve fleet-wide fuel economy of 54.5 miles per gallon (mpg) in order meet CO2 emission standards setup by EPA [20].

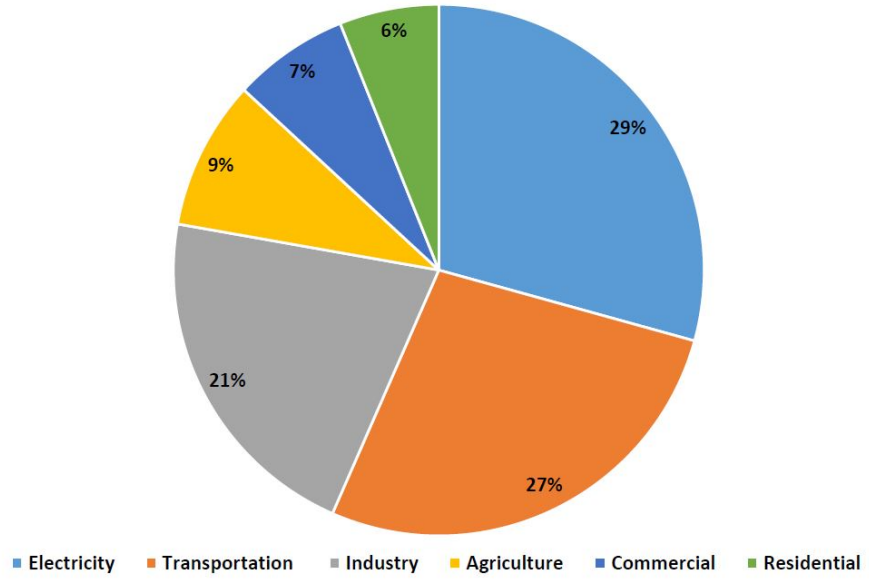

Figure 1.1: 2015 U.S. GHG Emissions by Sector. The data is taken from [1]

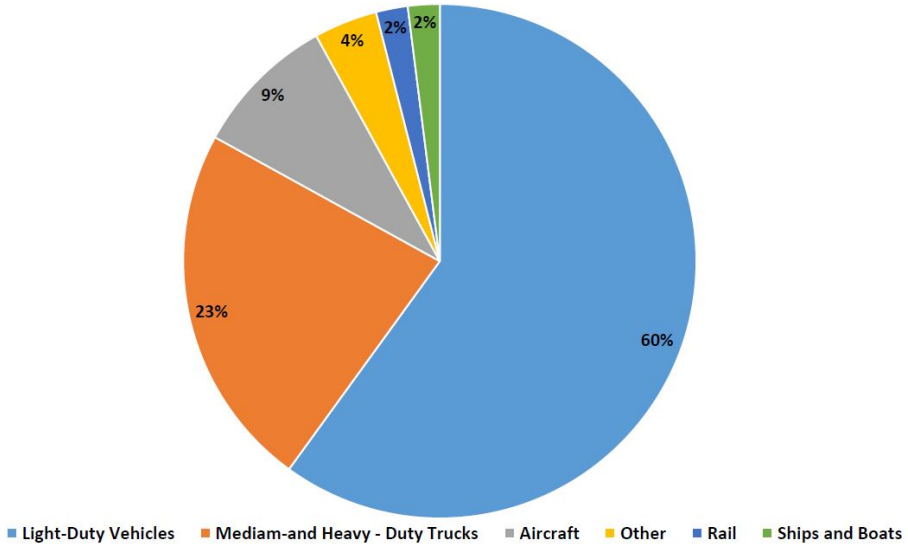

Figure 1.2: 2015 U.S. GHG Emissions by Source. The data is taken from [1]

Automotive industries have started utilizing technologies to achieve CO2 emissions, fuel economy and performance goals. Technologies like Gasoline Direct Injection (GDI), turbochargers and transmissions with seven or more speeds, have been used extensively in vehicles presently. Figure 1.3 shows the emerging technologies that major Original Equipment Manufacturers (OEM) have utilized in their vehicles in MY2017.

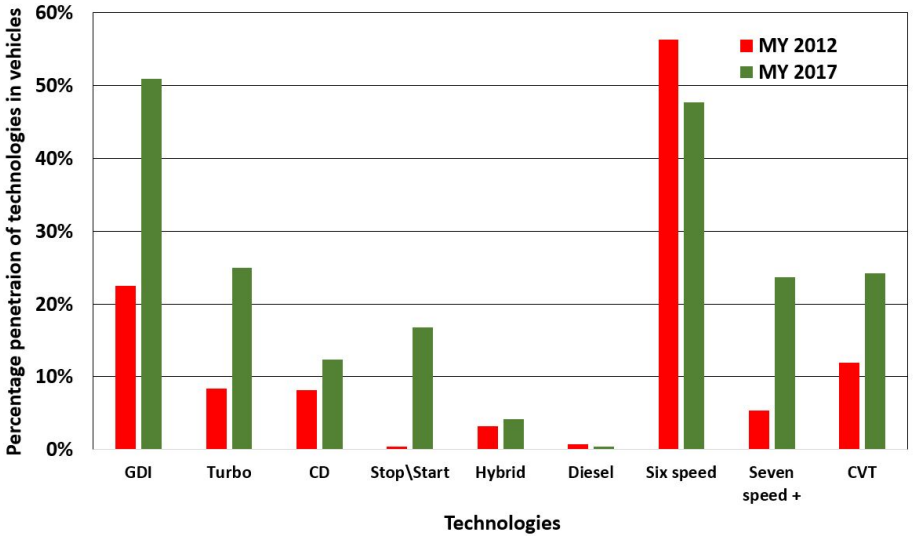

Figure 1.3: Comparison of Technologies in MY 2012 & MY 2017. The data is taken from[2]

According to the report by EPA [21], these technological enhancements have decreased CO2 emissions by 22 percent and increased fuel economy by 28 percent in MY2016 compared to MY 2004. Shift towards alternate vehicle technologies have been observed in recent years. Many OEMs and start-ups are coming up with new models of Hybrid Electric Vehicles (HEV), Plug in Hybrid Electric Vehicles (PHEV)

and Electric Vehicles (EV). This can be inferred from Figure 1.4 which compares number of alternate fuel vehicle models in MY2012 and MY2017.

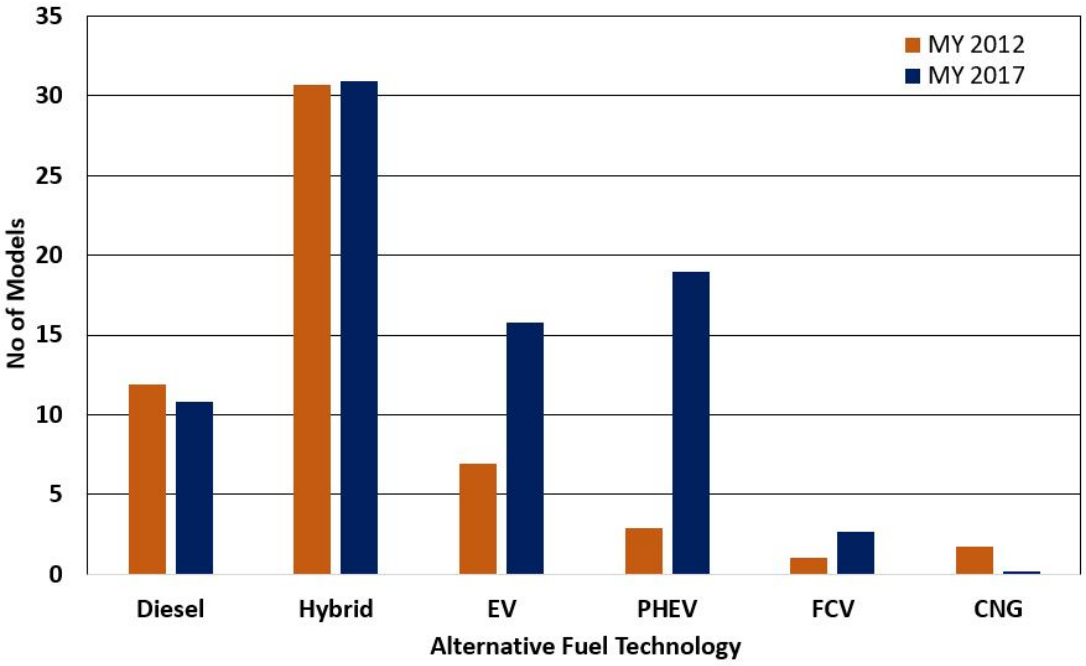

Figure 1.4: Alternate Fuel Vehicle Models in MY 2012 & MY 2017. The data is taken from[2]

It is projected that 5 % of MY 2017 production could achieve MY 2025 CO2 emissions targets, though this will rely only on HEV, PHEV, EV and Hydrogen Fuel Cell Vehicles (FCV)[21]. This shift from conventional vehicles demands improvement in the existing technologies in electric and hybrid vehicles. HEV have become popular segment in vehicle models. It uses engine as well as battery to propel the vehicle. This results in improved fuel economy and less emissions as electrical energy is cleaner and efficient compared to Gasoline/ Diesel, assuming renewable sources are used to generate electricity. Apart from these merits, vehicle can store regenerative braking

energy in the battery and utilize later to propel the vehicle. Presence of battery as an energy source also provides the flexibility to run the engine at efficient operating points. Figure 1.5 shows comparison of hybrid and non-hybrid midsize cars [2] on the basis of adjusted fuel economy.

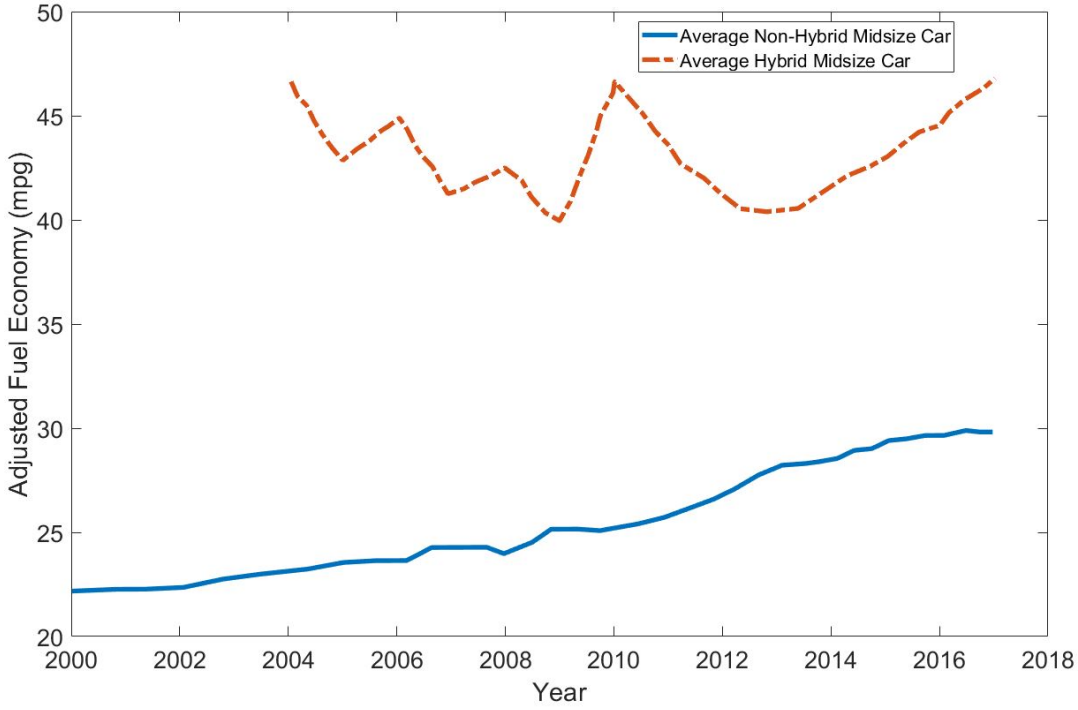

Figure 1.5: Trend in adjusted fuel economy variations for hybrid and non-hybrid midesize cars [2]

1.1 NEXTCAR Project

The work in this thesis is based on ARPA-E's NEXTCAR project, which stands for "NEXT-Generation Energy Technologies for Connected and Automated On-Road Vehicles", funded by the U.S Department of Energy (DOE). This project aims to use connectivity and automation among the vehicle fleet to optimize vehicle dynamics and powertrain controls of each vehicle, and reduce overall energy consumption by 20%.

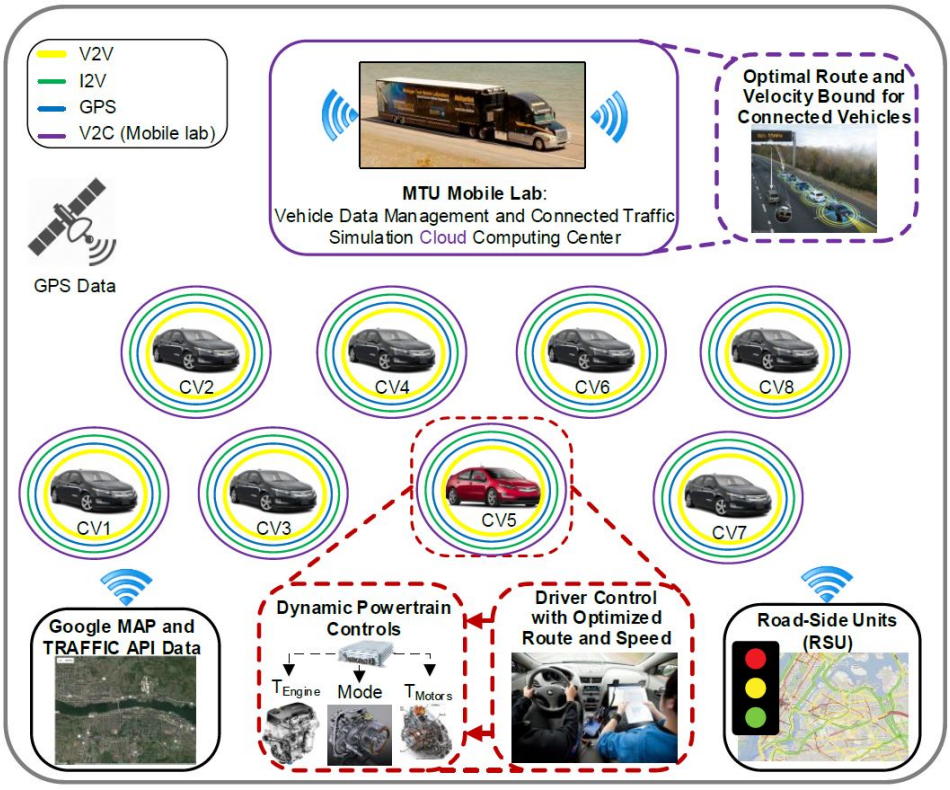

Figure 1.6: Overview of NEXTCAR project

Michigan Technological University with GM, is working on a fleet of eight Chevy GEN II Volts. The team aims to successfully implement a model-based predictive control (MPC) on Chevy Volt GEN II powertrain, to achieve desired target of 20 % energy consumption reduction by utilizing connectivity and autonomy. Vehicle connectivity, traffic simulation and eco-routing with MPC based dynamic powertrain model of vehicle will enable optimization of propulsion system operation.

The project estimates that connected and automated HEV technology has potential to reduce energy consumption by 20% and improve EV range by 6%. Moreover this will also lead to reduction in emissions which will help OEM to achieve strict emission norms setup by EPA. Furthermore economic strengthening can be expected as this technology will reduce dependency of U.S on oil imports by improving vehicular fuel economy.

1.2 Objectives of Thesis

Integral part of the project is development of a high fidelity vehicle dynamics and powertrain model which can predict energy consumption of the vehicle with an error less than 5% when compared to experimental data. A high fidelity model is necessary tool for testing energy management control strategies and deriving a simplified control oriented model, and finally implementing it in a vehicle. This thesis discusses the powertrain components of Chevy Volt GEN II and walks through the model development process of each component.

The model was developed in MATLAB/SIMULINK using high fidelity parameters provided by GM and implementing vehicle control logics understood from in-vehicle testing and Argonne National Laboratory (ANL) experimental data. Each powertrain component is dependent on either maps or dynamic equations. Model validation was carried out using the ANL experimental data. To further enhance the model accuracy different energy consuming components like drive unit auxiliary pump model is simulated. Special operating scenarios like ICE startup (coldstart, cranking and catalyst heating) have been incorporated to improve the accuracy of ICE dynamic model. This level of accuracy will enhance energy consumption prediction and help in analysis of transient fuel penalty in ICE. Following are the objectives of the thesis:

† To develop a dynamic model of PHEV Chevy Volt Gen II and validate with experimental data

† To develop fuel penalty terms to capture required extra fueling for catalyst lightoff, engine coldstart and engine cranking (for vehicle energy management)

† To characterize and simulate fuel penalty associated with engine transients from one speed and load to another speed and load

† To study different mode operation for charge depleting and charge sustaining drive cycles

† To analyze mode switching in Chevy Volt and develop appropriate energy penalties for vehicle energy management

1.3 Literature review

Automotive researchers have conducted numerous studies on vehicle components, performance and energy consumption analysis through modeling and simulation. Modeling is performed based on the level of details and accuracy required. Figure 1.7 shows different levels of model that are developed for EV/HEV research.

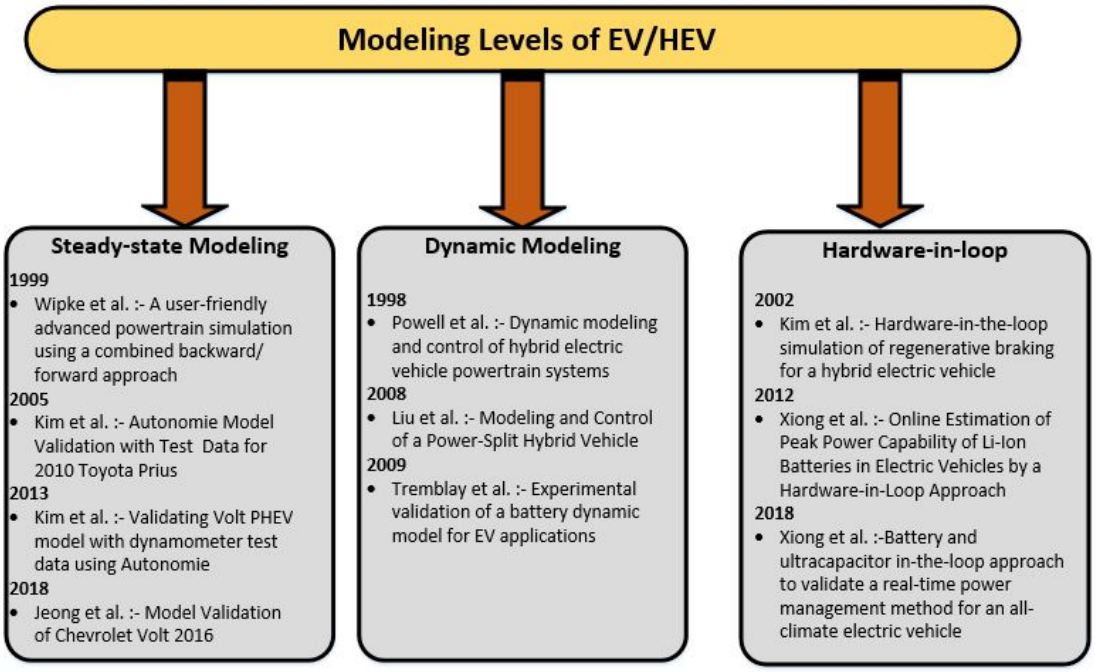

Figure 1.7: Modeling levels of EV/HEV used in automotive research [3][4] [5][6][7][8][9][10][11][12][13]

Steady-state modeling is simple modeling which include steady state maps that are obtained through vehicle testing. The models are computationally inexpensive requiring less simulation duration. The main disadvantage of these models is lack of dynamics resulting in inaccurate performance prediction for transient operations. ANL have conducted powertrain and control algorithm studies on Toyota Prius (MY 2010) [3] and PHEV Volt (MY 2010) [4] using Autonomie software which is used to develop map based models.

Dynamic modeling include physics based models which have high accuracy compared to steady state model and are capable to predict transient behavior. [5] have discussed

dynamic modeling of Toyota Hybrid system and, have incorporated and analyzed control algorithms in the model. [7] have discussed dynamic modeling and validation of battery for EV applications.

Hardware-in-loop (HIL) models are the most advanced model which include complex equations and depend on large number of parameters. Though these models are highly accurate, they are computationally expensive. [8] [9] and [10] use HIL simulation to analyze and evaluate real time behavior of powertrain components.

The work in this thesis utilizes dynamic modeling methods ([5], [22]) to model and simulate powertrain components of PHEV Chevy Volt GEN II.

1.4 Organization of Thesis

Overview of this thesis is shown in the Figure 1.8. Chapter2 discusses experimental setup for data acquisition from Chevy Volt GEN II.

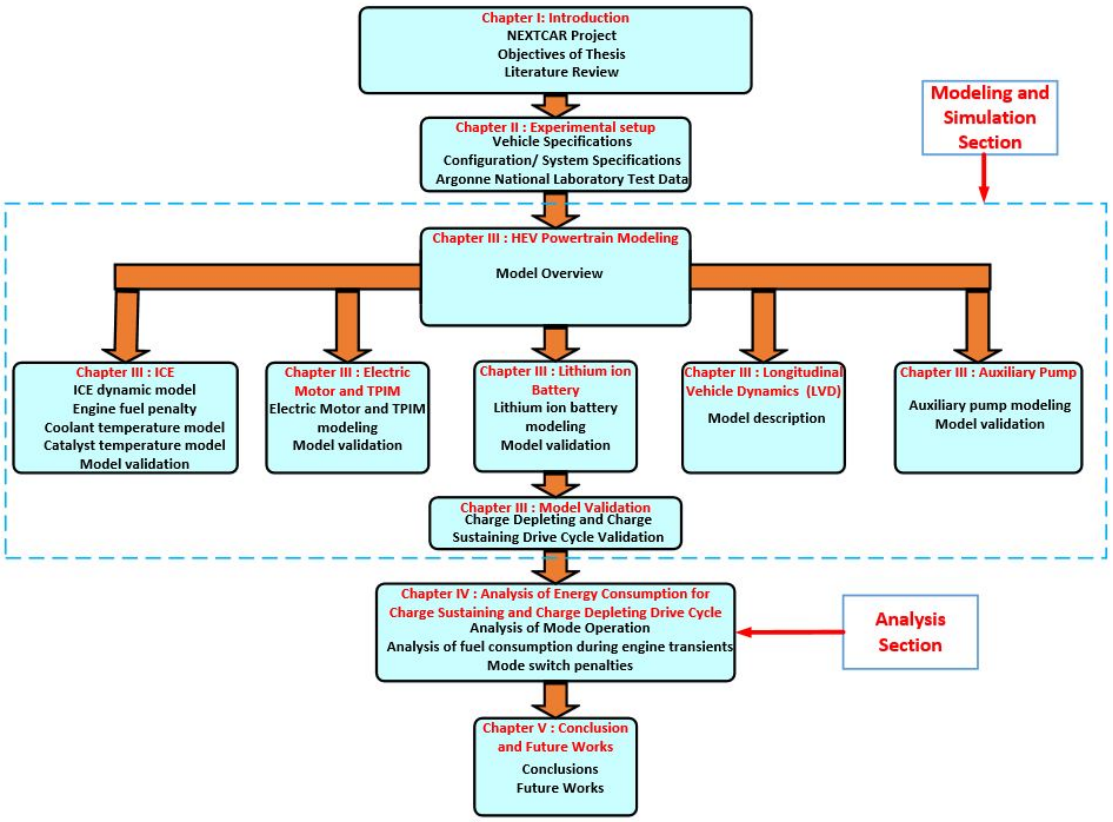

Figure 1.8: Organization of thesis

Chapter3 discusses modeling procedure and validation with ANL test data of each powertrain component. Chapter 4 discusses mode operation during charge depleting and charge sustaining drive cycles, engine transient fuel penalty and mode switch fuel

penalty. Chapter 5 describes the conclusion of this thesis and future works that has been planned by the NEXTCAR project team.

Chapter 2

Experimental Setup

2.1 Vehicle Specifications

The work in this thesis is based on PHEV Chevy Volt Gen II which is produced by Chevrolet (General Motors). The vehicle went into sale in October 2015 in US and Canada. Figure 2.1 shows Chevy Volt Gen II and Table 2.1 includes the vehicle specifications of powertrain components (engine, motor-generators and Lithium-ion battery) and other vehicle components.

Figure 2.1: Chevy Volt Gen II [14]

Table 2.1
Specifications of Chevy Volt Gen II [18]

Model	Chevrolet Volt
Driveline	Front-wheel-drive
EPA vehicle class	Compact car
Battery chemistry	Lithium-ion
Battery energy	18.4 kWh
Engine type	1.5L DOHC I-4
Compression ratio	12.5:1
Output engine (kW/hp @ rpm)	75/101 @ 5600
Motor power (kW/hp)	111/149
Motor torque (Nm)	294/398
Performance (0-60 mph)	8.4 sec
EV range (city)	53 miles/ 85 km (based on estimated fuel economy)
EV/extended range	420 miles/ 675 km including EV on fully charged battery and full tank of fuel
Tires	Michelin Energy Saver A/S 215/50R17 all-season
Wheelbase (in / mm)	106.1 / 2694
Vehicle length (in / mm)	180.4 / 4582
Vehicle width (in / mm)	71.2 / 1809
Vehicle height (in / mm)	56.4 / 1432
Curb weight (lb / kg)	3543 / 1607

2.2 Configuration/ System Specifications

Data acquisition was carried out using Vector CANoe VN5610A through the On board diagnostic (OBD) port of Chevy Volt Gen II. Specifications of Vector CANoe tool have been shown in Table 2.2. Figures 2.2 and 2.3 show data acquisition during in-vehicle testing carried out at Advanced Power Systems Research Center (APSRC) Laboratory, Houghton and OBD port connection in Chevy Volt Gen II.

Table 2.2
Specifications of Vector CAN tool (VN5610A) used for data acquisition

Ethernet: Channels/transceiver	2x BCM89811, 2x BCM54810
Ethernet: Physical layer	100 BASE-T1 (Broad-Reach) and 10BASE-T/100BASE-TX
Baudrates %	10Mbit/s ,100 Mbit/s ,1000 Mbit/s
CAN (FD) : Physical layer	CAN Highspeed(CAN FD capable)
CAN (FD) : Connectors	1x D-SUB9 (dual channel)
Analog and Digital I/O	1x Digital in/out, e.g. for DoIP Activation Line
Mean reaction time	250 s

Figure 2.2: Data Acquisition using Vector CANoe VN5610A

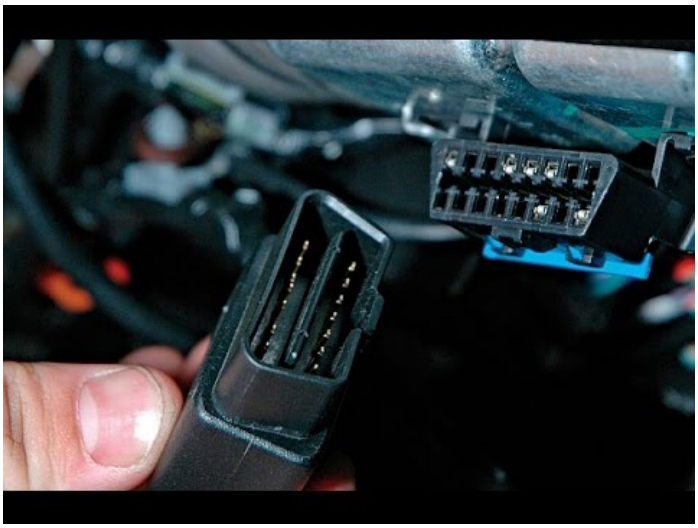

Figure 2.3: OBD port of Chevy Volt Gen II [15]

CAN messages were recorded and stored as comma-separated values (CSV) file for model development and validation. Post processing of acquired data (engine fuel flow rate, coolant temperature, engine speed, etc) was carried out in MATLAB 2017b. Table 2.3 shows the parameters that were recorded using Vector CANoe tool.

Table 2.3
Parameters recorded / measured using Vector CANoe tool

Paramters	**Units**
Engine speed	RPM
Engine fuel flow rate	g/s
Engine coolant temperature	°C
Engine catalyst temperature	°C

A Data Base Container (DBC) file was provided by GM and it contains information of CAN messages and signals which are needed to be recorded for model development and validation. GM also provided CAN messages IDs which where included in the DBC file for data acquisition. CANdb++ Editor in Vector CANoe software allows users to visualize messages in engineering units and store data for later validation / calibration purpose. Figure 2.4 shows sample data recorded using Vector CANoe tool at APS Labs.

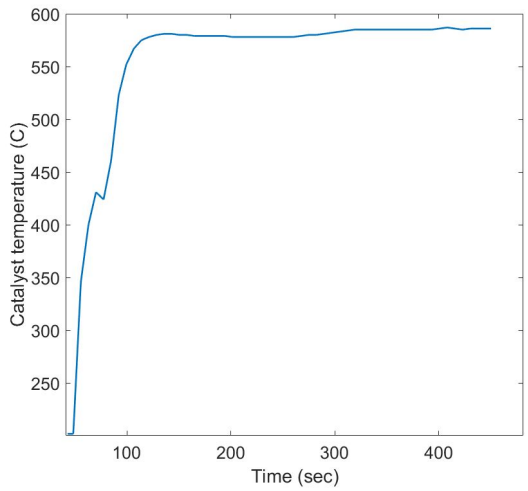

(a) Catalyst temperature Vs Time

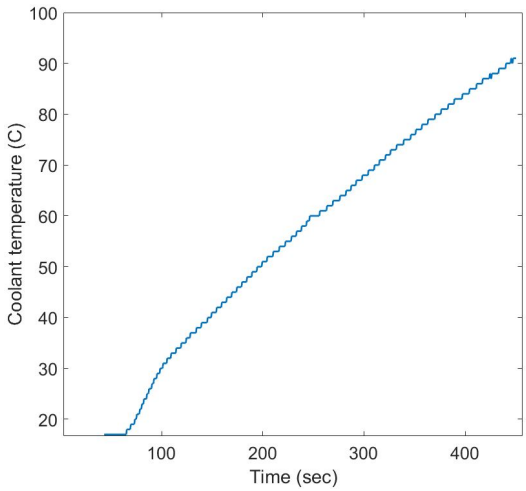

(b) Coolant temperature Vs Time

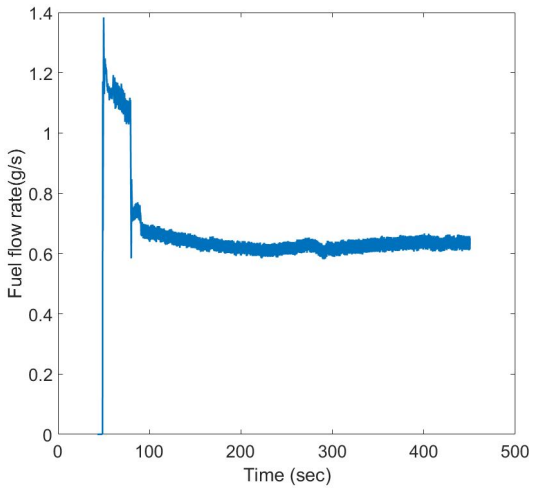

(c) Fuel flow rate Vs Time

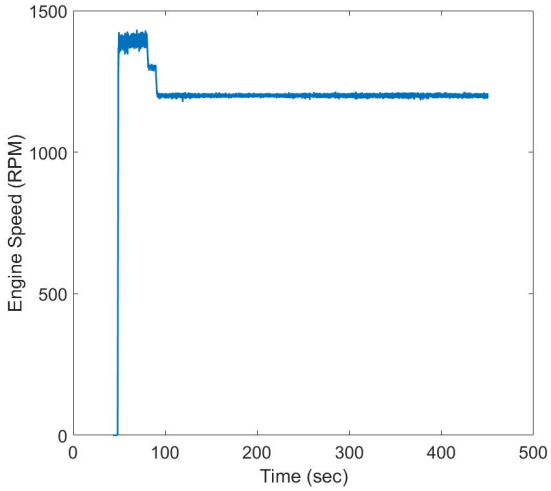

(d) Engine speed Vs Time

Figure 2.4: Data acquired using Vector CANoe tool at APS Labs

2.3 Argonne National Laboratory (ANL) Test Data for Model Validation

Argonne National Laboratory (ANL) conducted several dynamometer tests on Chevy Volt GEN II volt and provided data to NEXTCAR team of Michigan Tech. The data, consisting of several performance parameter channels recorded for different driving conditions, was used for validation of powertrain components of vehicle model and also in understanding the control logics behind vehicle operation. Table 2.4 shows vehicle data summary provided by ANL:

Table 2.4
ANL vehicle data summary

Number of test cycles	25
Drive cycles	UDDS FCT
	HWY FCT
	US–06
	Passing maneuvers
Performance test	Charge depleting
	Charge sustaining
Engine start conditions	Cold–start
	Warm–start
Grade-ability	0%
	6%
	25%

During each ANL dynamometer test, vehicle performance parameters were recorded

which have been used in validation of each component. Figure 2.5 shows ANL test data usage for vehicle model validation.

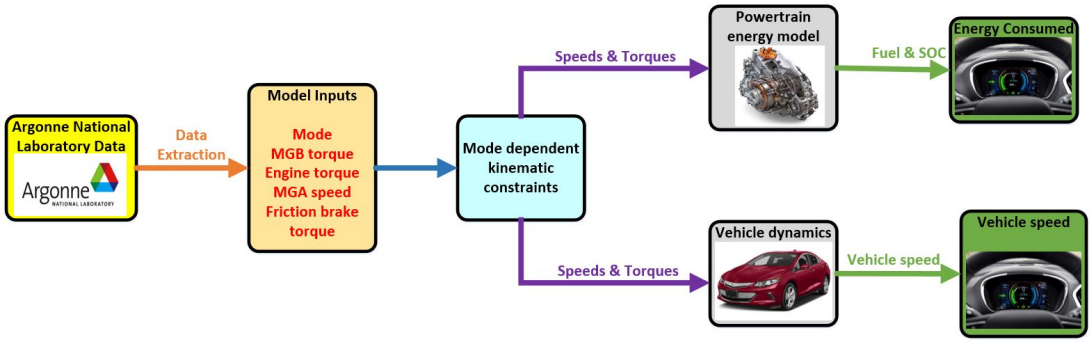

Figure 2.5: ANL data for vehicle model validation

ANL test data was used for validation of engine fuel flow rate, SOC of battery and vehicle speed. From a test cycle data, six inputs (commanded by the supervisory controller) are extracted and fed to the model. For component wise model validation, performance parameters (shown in Table 2.5) were validated before integrating into the whole model.

Table 2.5
Components modeled and corresponding performance parameters validated

Components	Performance parameters
ICE	Engine torque
	Fuel flow rate
	Intake air flow rate
MGA and MGB	Battery power load
Lithium ion battery	SOC (%)
Auxiliary pump	Auxiliary pump power
Engine coolant model	Coolant temperature
Catalyst Temperature model	Catalyst temperature

Chapter 3

HEV Powertrain Modeling

3.1 Model Overview

Chevy Volt Gen II model overview is shown in the Figure 3.1 with its subsystems, propulsion energy flows developed in SIMULINK/MATLAB®. Each subsystem has been discussed in detail in the following sections.

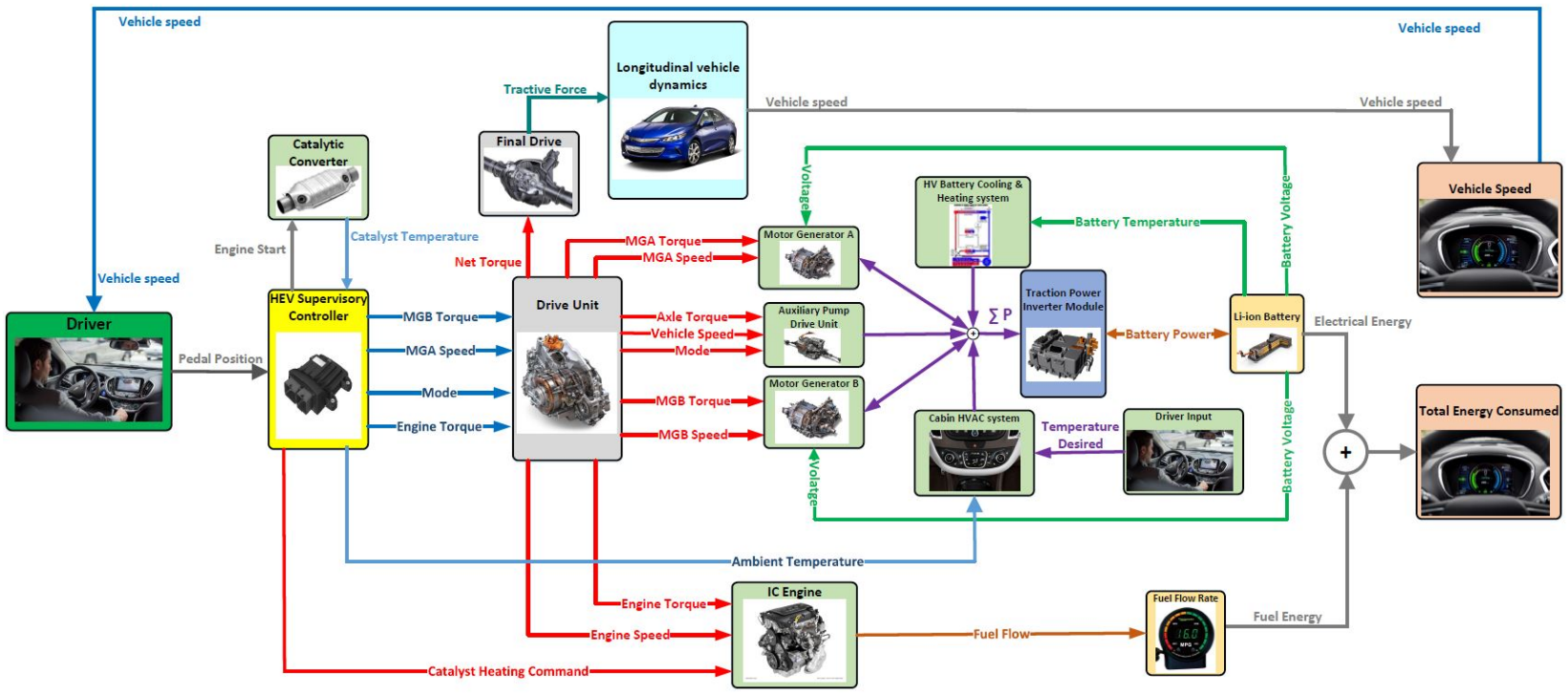

Figure 3.1: Schematic of a powertrain and vehicle dynamic model for Chevy Volt Gen II

3.2 Model Description

This section discusses modeling of ICE, electric motor generators, Li-ion battery, longitudinal vehicle dynamics (LVD), drive unit and drive unit auxiliary pump.

The vehicle model was created using the component parameters provided by GM. The parameters were initially requested to GM on the basis of the powertrain development requirements (ICE and battery specifications). Few models like drive unit auxiliary pump model requires high level of information which is difficult to implement. In such case, a regression model was created by identifying relevant dependent parameters. Table 3.1 shows parameters that were received from GM for dynamic ICE model development:

Table 3.1
Parameters from GM for ICE dynamic modeling

Parameters	**Component modeled**
Throttle discharge coefficient	Throttle body
Throttle diameter	Throttle body
Throttle position %	Engine ECU
Intake manifold volume	Intake manifold
Steady state Brake torque, engine speed, intake airflow	Torque generation
Steady state EGR %, brake torque and engine speed	EGR model
Engine inertia	Rotational dynamics
Wide open throttle (WOT)	Engine brake torque limits

Table 3.2 shows parameters that were received from GM for Li-Ion battery modeling:

Table 3.2
Parameters from GM for Li-Ion battery modeling

Parameters	Component modeled
SOC and temperature dependent resistance and capacitance	Shorter time constant R-C circuit
SOC and temperature dependent resistance and capacitance	Longer time constant R-C circuit
Battery capacity	SOC

Table 3.3 shows parameters that were received from GM for MGA and MGB modeling:

Table 3.3
Parameters from GM for MGA and MGB modeling

Parameters	Component modeled
Motor speed, torque dependent voltage dependent motor losses	MGA and MGB efficiency maps
MGA and MGB max and min torque tables dependent on voltage	MGA and MGB torque limits

Table 3.4 shows parameters that were received from GM for traction power inverter module A (TPIMA) and traction power inverter module B (TPIMB):

Table 3.4
Parameters from GM for TPIMA and TPIMB modeling

Parameters	Component modeled
MGA speed, torque dependent voltage dependent DC power motor AC current	TPIMA efficiency map
MGB speed, torque dependent voltage dependent DC power motor AC current	TPIMB efficiency map

Table 3.5 shows parameters that were received from GM for drive unit:

Table 3.5
Parameters from GM for drive unit

Parameters	Component modeled
Gear mesh efficiency	Transmission
Final drive ratio	Transmission
Number of sun and ring teeth	Planetary gear one
Number of sun and ring teeth	Planetary gear two
Inertias	Planetary gears
Spin and parasitic losses	Transmission

Table 3.6 shows parameters that were received from GM for longitudinal vehicle dynamics (LVD):

Table 3.6
Parameters from GM for LVD

Parameters	Component modeled
Road load profile includes	LVD
Aerodynamic coefficient and rolling resistance	
Mass	LVD

3.2.1 Internal Combustion Engine Model

A dynamic ICE model of 1.5 liter l-4 naturally aspirated DI SI engine has been developed using the parameters provided by GM. The model specifications and schematic diagram are shown in Table 3.7 and Figure 3.2, respectively. The ICE model is a feedback model consisting sub–models with ICE dynamics including intake air flow dynamics and rotational dynamics and others with static maps like torque generation and exhaust gas recirculation (EGR) map.

Table 3.7
Engine specifications of 1.5 L l-4 Ecotec engine [17]

Parameters	Value
Number of cylinders (–)	4
Displacement volume (cc)	1490
Bore x stroke (mm x mm)	74 x 86.6
Connecting rod length (mm)	128.8
Compression ratio	12.5:1
Number of valves per cylinder	4
Peak torque (Nm)	140 @ 4300 rpm
Peak power (kW)	75 @ 5600 rpm
Valve train	DOHC, intake and exhaust high authority cam phasing
EGR system	Cooled external and internal
Fuel injection	Direct injection
Fuel	Regular unleaded

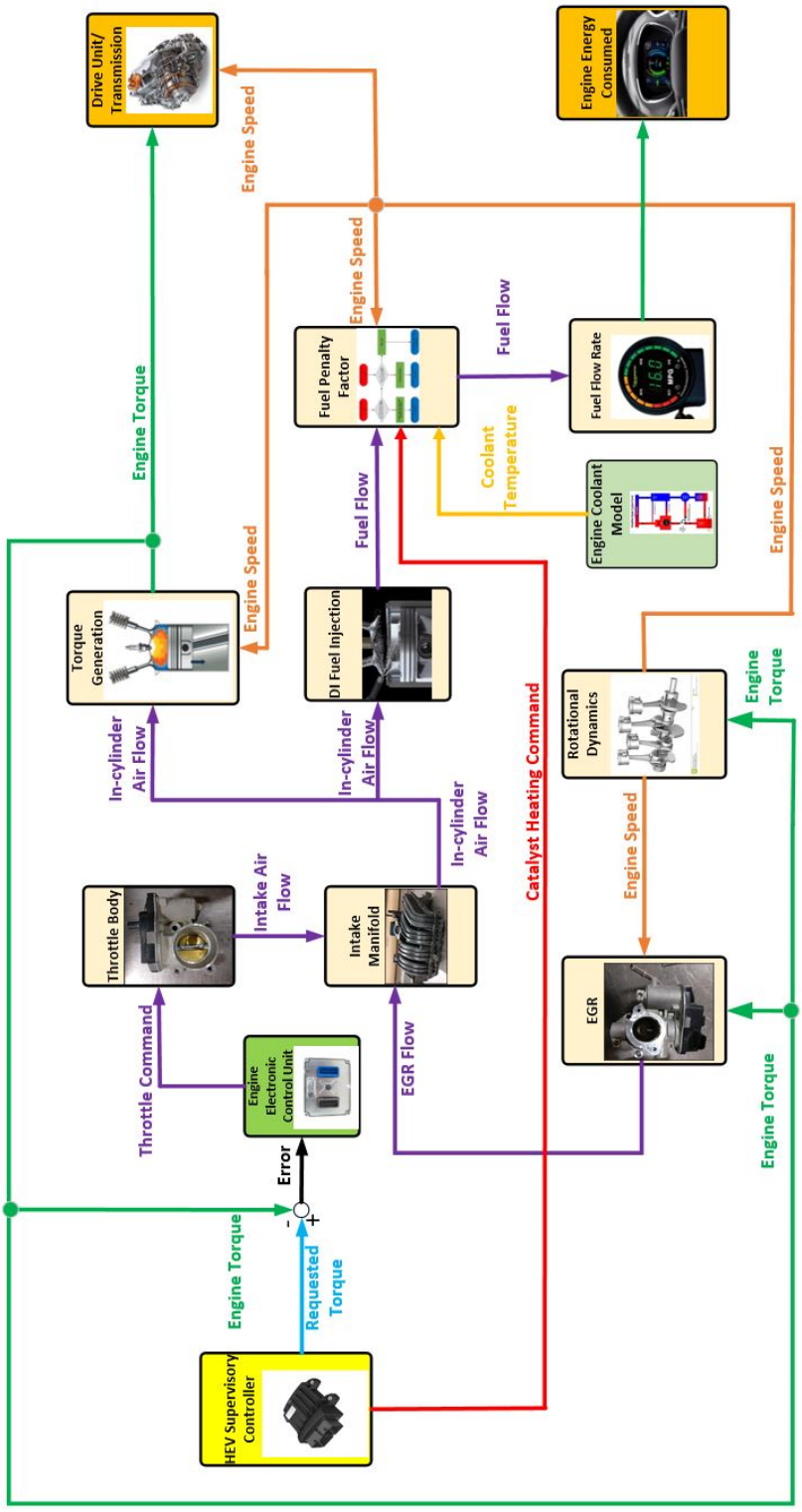

Figure 3.2: Dynamic ICE Model

As shown in the Figure 3.2, supervisory controller gives torque request to engine ECU. The ECU commands throttle command to throttle body, leading to opening of throttle valve to supply intake air flow rate to achieve desired torque. Intake air flow enters intake manifold and, depending on engine speed and torque, EGR flow also enters intake manifold and mixes with fresh intake air flow. This mixture enters engine cylinder during intake process and engine torque is produced in torque generation subsystem. The amount of fuel injected is obtained in DI fuel injection subsystem and fuel penalty subsystem estimates fuel penalty based on engine thermal conditions. Engine speed is determined in rotational dynamics subsystem. Engine speed and torque are the outputs of engine model and is fed to drive unit / transmission subsystem. Each subsystem is discussed in detail in the following sections.

3.2.1.1 Intake Air Flow Dynamics

Air flow rate ($\dot{m}_{at}$) through the throttle body is given by [22] :

$$\dot{m}_{at} = \frac{C_D A_T P_0 p_r}{\sqrt{RT_0}} \gamma^{1/2} \left\{ \frac{2\gamma}{\gamma - 1} \left[1 - \left(p_r \right)^{(\gamma-1)/\gamma} \right] \right\}^{0.5} \tag{3.1}$$

For choked flow:

$$\dot{m}_{at} = \frac{C_D A_T P_0 p_r}{\sqrt{RT_0}} \gamma^{1/2} \left(\frac{2\gamma}{\gamma + 1} \right)^{\gamma + 1/2(\gamma-1)} \tag{3.2}$$

where, C_D is the discharge coefficient, P_0 and T_0 are ambient pressure and temperature respectively, A_T is throttle angle dependent area, p_r is ratio of intake manifold pressure to ambient pressure and γ is specific heat ratio. Depending on the pressure ratio, Equations 3.1 (p_r greater than 0.532) and 3.2 (p_r less than 0.532) are switched in the model [22].

The intake manifold subsystem estimates manifold pressure (P_{man}) by using conservation of mass law for the control volume as intake manifold, with throttle air flow ($\dot{m}_{at}$) and EGR flow ($\dot{m}_{EGR}$) coming in and in–cylinder air flow ($\dot{m}_{ac}$) going out, yielding [23][24]:

$$\frac{\dot{P}V_{man}}{RT_{man}} = \dot{m}_{at} + \dot{m}_{EGR} - \dot{m}_{ac} \tag{3.3}$$

where, V_{man} is intake manifold volume, T_{man} is manifold temperature and R is the Universal Gas Constant. In-cylinder air flow rate is calculated using Speed-Density equation as below:

$$\dot{m}_{ac} = \frac{\eta_{vol}\rho_{a,m}V_d N}{2} \tag{3.4}$$

where, η_{vol} is volumetric efficiency, $\rho_{a,m}$ is air density, N is the engine speed. Volumetric efficiency, depends on manifold pressure and engine speed, is estimated using regression [25] of steady state experimental engine data provided by GM:

$$\eta_{vol}(N, P_{man}) = \eta_{vol0} + \eta_{vol1}N + \eta_{vol2}N^3 + \eta_{vol3}P_{man} \tag{3.5}$$

where, η_{vol0} , η_{vol1} , η_{vol2} and η_{vol3} are coefficients derived by regression of experimental data.

3.2.1.2 Torque Generation

Engine torque generation model is a function of in–cylinder mass flow rate, air fuel ratio, spark advance (SA) and engine speed [26]. The engine brake torque is given by the following regression function:

$$T_{br} \;=\; F(\dot{m}_{ac}, A/F, SA, N) \tag{3.6}$$

where, $\dot{m}_{ac}$ is in-cylinder mass flow rate, A/F is air fuel ratio, SA is spark advance and N is engine speed.

3.2.1.3 Rotational Dynamics

The rotational dynamics subsystem, a lumped model with constant inertia, estimates engine speed using Newton's second law. Since a simple engine model is being developed, effect of variable inertia and crankshaft torsional have been neglected [25][27].The rotational dynamics to determine engine speed is based on the following equation:

$$\frac{d\omega_{eng}}{dt} = \frac{T_{br} - T_L}{J_{eff}} \tag{3.7}$$

where, J_{eff} is the effective moment of inertia of engine, T_L is the engine load and w_{eng} is angular velocity of crankshaft.

3.2.1.4 Exhaust Gas Recirculation (EGR)

The EGR subsystem developed is an external EGR model which is actuated by the EGR valve. Internal EGR is controlled by camshaft timing and is not included in the model. EGR subsystem is a static map based model, depending on the engine speed and engine torque [28]. This map was developed using GM parameters and incorporated in the model.

The amount of EGR that flows in the intake manifold is calculated using the following equation [29]:

$$EGR\% = \frac{\dot{m}_{EGR}}{\dot{m}_{EGR} + \dot{m}_{at}} \times 100 \tag{3.8}$$

where, $\dot{m}_{egr}$ and $\dot{m}_{at}$ are mass flow rate of EGR and intake air flow rate.

3.2.1.5 Engine Electronic Control Unit

Engine torque control is done by an electronic control unit (ECU) which is a feedback controller. Here, engine torque control is simulated by a combined feed forward and feed back controller, as shown in the Figure 3.3. The engine ECU commands throttle opening percentage depending on the error between the delivered and requested torque. A throttle 3-D map, dependent on engine torque and speed, was developed using GM parameters and incorporated in the model.

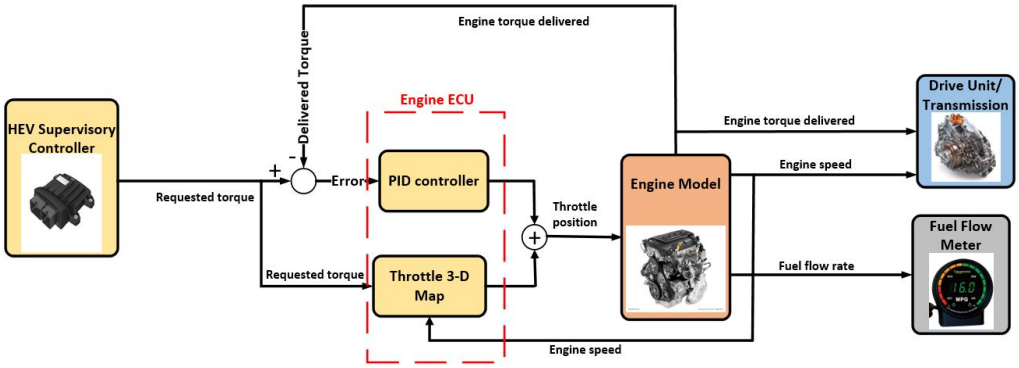

Figure 3.3: Overview of torque control using engine ECU

3.2.1.6 Engine Fuel Penalty

Engine thermal conditions and three way catalyst (TWC) temperature play an important role in ECU strategies. These directly affect the fuel flow rate and have

to be included in the engine and TWC model to improve vehicle fuel consumption prediction.

Three fuel penalty factors were determined for the engine to account ECU strategies for:

† Catalyst heating to minimize light-off period

† Engine cold-start leads to increased fuel consumption due to following reasons[30]:

  – Low cylinder wall temperature resulting in poor combustibility of injected fuel

  – Viscosity of lubricant between piston and liner interface high, resulting in increased friction losses

† Cranking is defined as the start of engine crankshaft rotation from rest position until engine achieves certain engine speed (600-700 RPM)

TWC must be above 250 to 300° C (light-off temperature) to achieve a conversion efficiency of 50 % and any temperature less than this will make the catalyst inefficient, leading to high CO, HC and NOx emissions [22]. To achieve the required high TWC temperature, catalyst warm up command is given by ECU.

These fuel penalties were found by conducting in-vehicle tests on Chevy Volt in cold and normal conditions. Vector CANoe tool was used for data acquisition through the On–board diagnostics (OBD). Temperature threshold (Catalyst light off at 300°C and Coldstart at 55°C) were determined by vehicle tests and also through discussion with GM engineers. Figure 3.4 shows the fuel penalty strategy implemented in the engine.

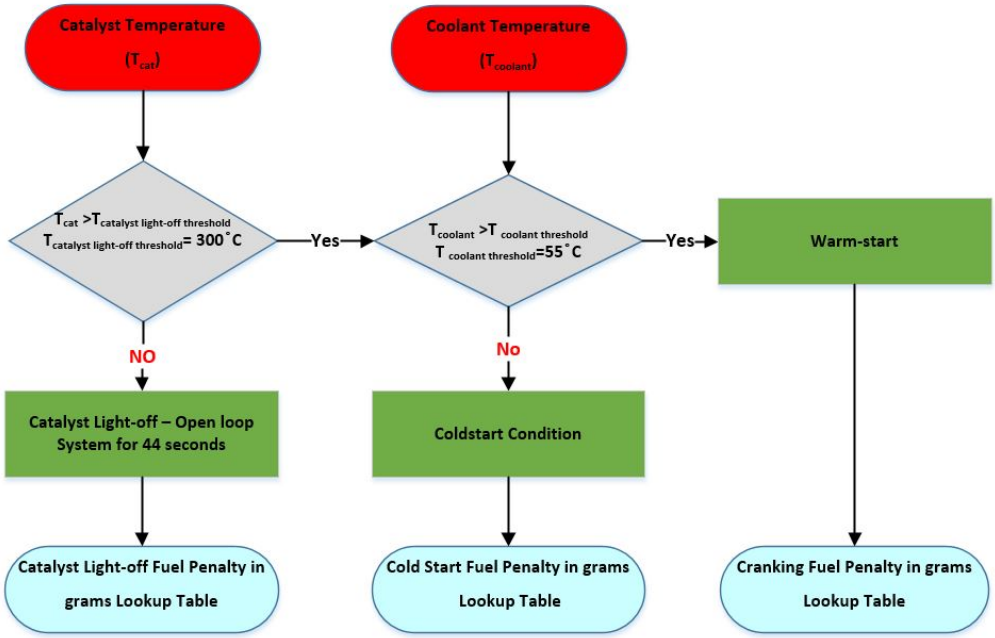

Figure 3.4: Flowchart to calculate fuel penalty depending on TWC temperature and engine coolant temperature

This fuel penalty strategy was implemented in the engine model and Figures 3.5(a) and 3.5(b) show validation of fuel flow rate with and without fuel penalty strategy for charge sustaining (CS) Urban Dynamometer Driving Schedule (UDDS) drive cycle.

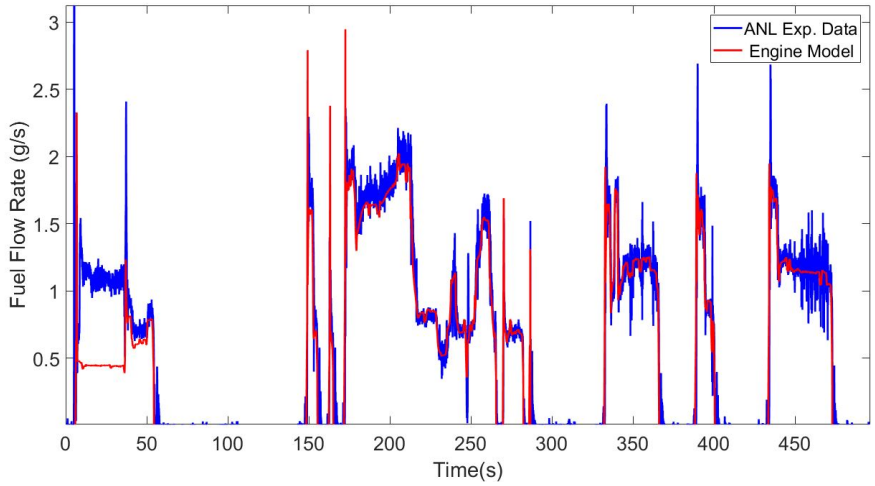

(a) Engine model without fuel penalty strategy

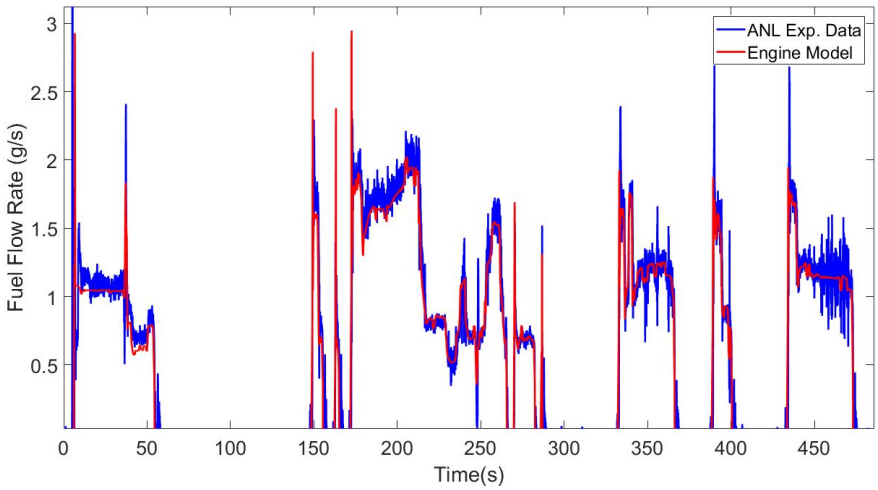

(b) Engine model with fuel penalty strategy

Figure 3.5: Comparison of two engine models with and without fuel penalty strategy for UDDS charge sustaining drive cycle.Test details are provided in Appendix B.7 (Filename: 61607029.mat)

Cumulative fuel consumed by the engine as per ANL test data was calculated to be 405 grams during the whole test cycle. From analysis of engine simulations (shown in Figures 3.5(a) and 3.5(b)), it is found that total fuel consumption prediction by the engine model with fuel penalty factor (401 grams) was more accurate than the

engine model without fuel penalty factor (367 grams). This shows an improvement in fuel consumption prediction in the engine model by incorporating the discussed fuel penalties.

3.2.1.7 Engine Coolant Temperature Model

Engine coolant temperature model is important to predict the fuel penalty associated to cold-startups in the engine. GM Premix DEX-COOL coolant (Appendix A) is used for engine cooling application. A simple lumped coolant model has been developed as function of heat loss from combustion of fuel and ambient temperature [31]. Figure 3.6 shows the heat flow for prediction of coolant temperature.

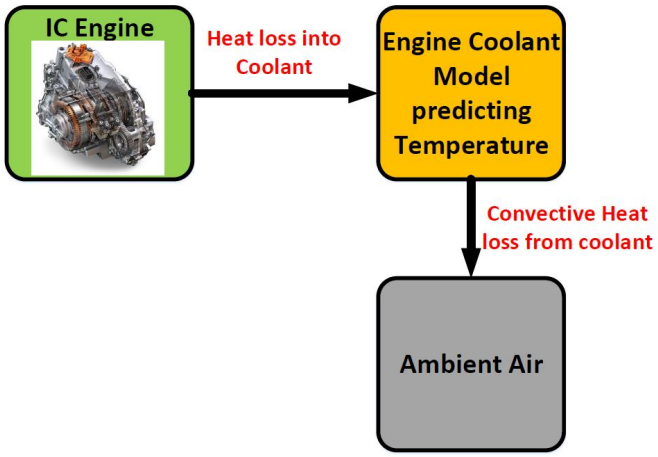

Figure 3.6: Lumped coolant temperature model

Considering engine coolant as the control volume, conservation of energy gives the

following equation :

$$\alpha \dot{m}_f Q_{LHV} = M_{coolant} C_{coolant} \frac{dT_{coolant}}{dt} + hA\delta T \tag{3.9}$$

where, α is fraction of fuel energy supplied to coolant heating, $\dot{m}_f$ is injected fuel flow rate, Q_{LHV} is lower heating value of gasoline, $M_{coolant}$ is mass of coolant liquid, $C_{coolant}$ is specific heat capacity of coolant liquid, $T_{coolant}$ is coolant temperature, h is convective heat transfer coefficient, A is the area of coolant exposed to air, δT is the difference between coolant temperature and ambient air temperature. Only $\dot{m}_f$, Q_{LHV}, initial coolant temperature and ambient temperature are known, rest of the parameters are found using experimental ANL test data. Figure 3.7 shows the coolant temperature model prediction.

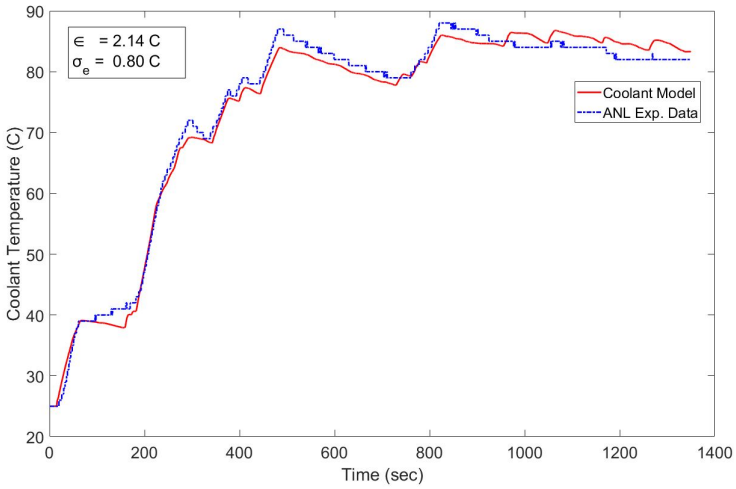

Figure 3.7: Comparison of predicted coolant temperature versus ANL test data (UDDS) CS. Operating condition: T_{amb}=22 °C. Test details are provided in Appendix B.7 (Filename: 61607029.mat)

Model with tuned parameters ($C_{coolant}$,$M_{coolant}$, A and h) was validated with APS test data which is shown in the Figure 3.8

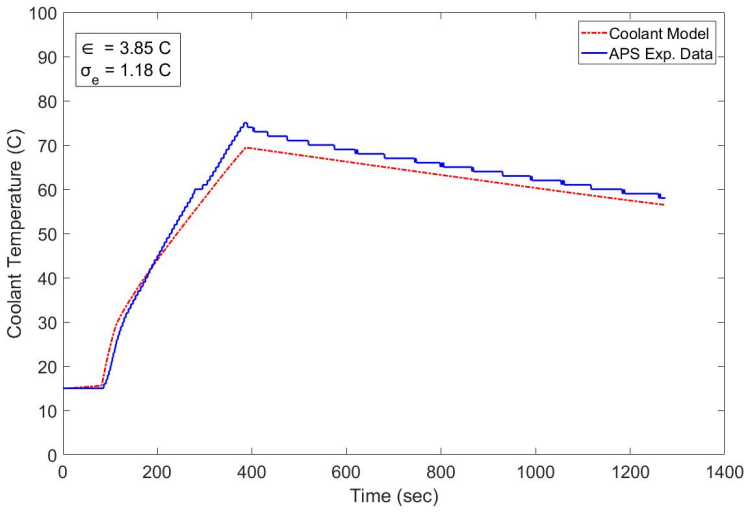

Figure 3.8: Validation of coolant temperature for the vehicle test data collected at APS labs. Operating Condition: T_{amb}=-5 °C. Test details are provided in Appendix B.7 (Filename: datacooling.xls)

The model developed predicts coolant temperature well with $\epsilon = 3.85$ °C (average error) and $\sigma_e = 1.18$ °C (standard deviation of error), and will play an important role in determining cold-start fuel penalty.

3.2.1.8 Catalyst Temperature Model

To predict catalyst fuel penalty, it is important to estimate TWC temperature. A catalyst heating model has been developed to predict TWC temperature. To achieve light-off temperature, engine initially runs at higher speed to heat up TWC. Hence,

TWC temperature (T_{cat}) is proportional to the engine speed (as fuel flow rate increases, both engine speed and TWC temperature increases) and a model was developed (as a function of engine speed (ω_e)) to predict TWC heating. Figure 3.9 shows a plot of TWC heating which the model was tuned to predict (ANL test data) and Figure 3.10 shows validation of model with APS Labs test data.

$$T_{cat} = f(\omega_e) \tag{3.10}$$

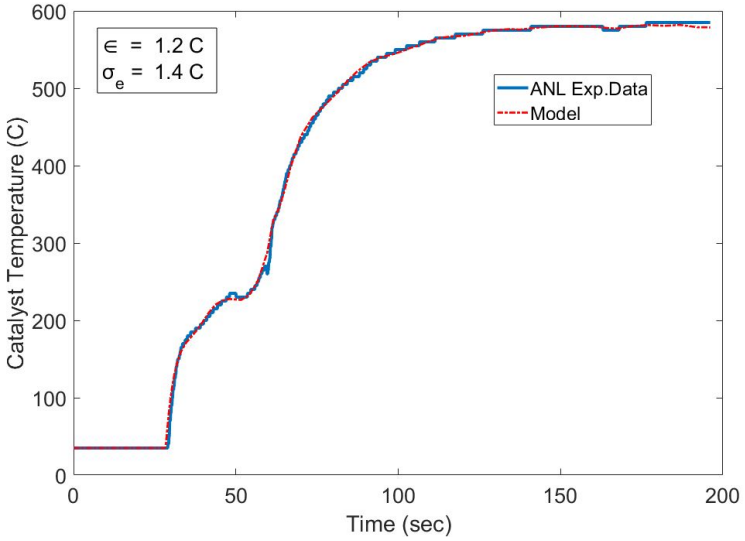

Figure 3.9: Comparison of catalyst heating model with ANL test data. Test details are provided in Appendix B.7 (Filename: 61607012.mat)

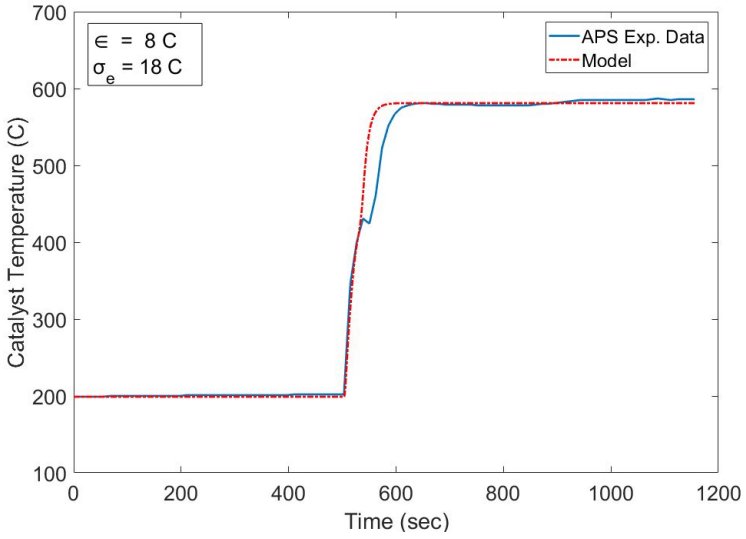

Figure 3.10: Validation of catalyst heating profile for the vehicle test data collected at APS labs. Test details are provided in Appendix B.7 (Filename: Catalystheating.xls)

The model developed predicts catalyst heating temperature well with $\epsilon = 8$ °C (average error) and $\sigma_e = 18$ °C (standard deviation of error).

Catalyst cooling depends on ambient temperature and vehicle speed. The convective heat transfer loss in TWC depends on the ambient temperature and vehicle speed. The equation used to estimate TWC cooling temperature is given by:

$$M_{TWC}C_{TWC}T_i - hA_{TWC}(T_i - T_{amb}) \;=\; M_{TWC}C_{TWC}T_{i+1} \tag{3.11}$$

$$T_{i+1} = T_i - \frac{hA_{TWC}}{M_{TWC}C_{TWC}}(T_i - T_{amb}) \tag{3.12}$$

$$h = f(T_{amb}, v) \tag{3.13}$$

where, M_{TWC} is mass of TWC, C_{TWC} is specific heat capacity of TWC, T_i is initial TWC temperature, h is convective heat transfer coefficient which is a function of ambient temperature (T_{amb}) and vehicle speed (v), A_{TWC} is area of TWC and T_{i+1} is TWC temperature in next time step. Figure 3.11 shows catalyst cooling curve for which the parameters (M_{TWC}, C_{TWC}, h) of catalyst model were tuned and Figure 3.12 shows validation of catalyst model (with tuned parameters) with ANL test data.

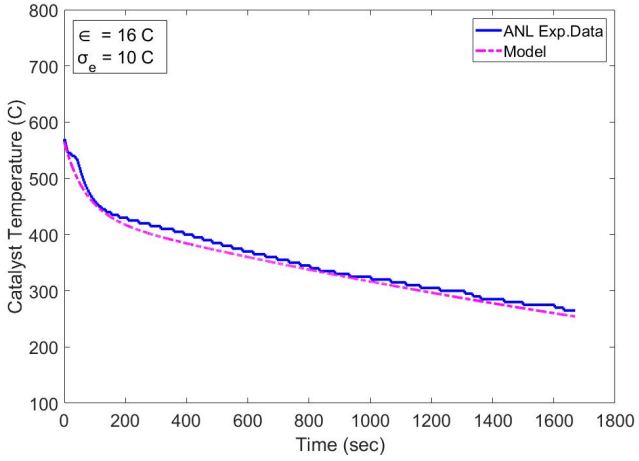

Figure 3.11: Comparison of predicted catalyst cooling profile with ANL test data. Test details are provided in Appendix B.7 (Filename: 61607004.mat)

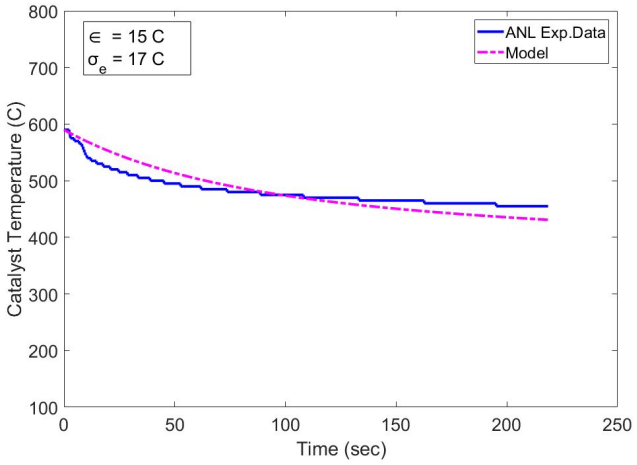

Figure 3.12: Validation of catalyst cooling profile with ANL test data. Test details are provided in Appendix B.7 (Filename: 61607009.mat)

The model developed predicts catalyst cooling temperature well with $\epsilon = 15$ °C (average error) and $\sigma_e = 17$ °C (standard deviation of error)

3.2.1.9 Experimental Validation

The engine Simulink model was validated with CS test data provided by Argonne National Laboratory. Validation of air flow rate, engine torque delivered and fuel flow rate for US06 has been shown in Figures 3.13(a), 3.13(b) and 3.13(c), respectively.

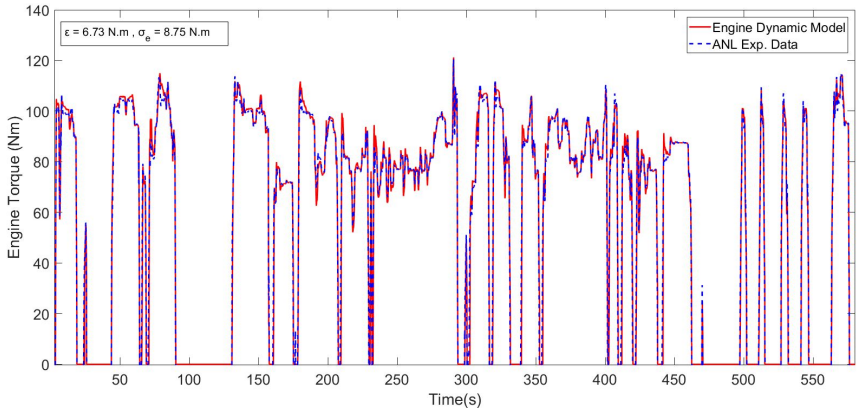

(a) Validation of engine torque

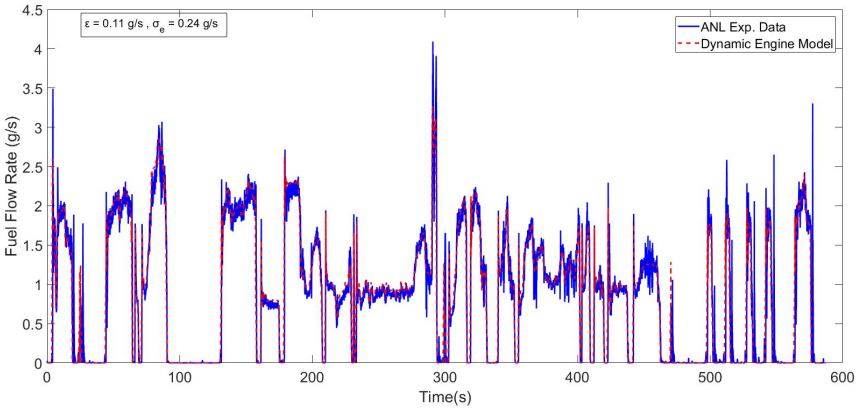

(b) Validation of fuel flow rate

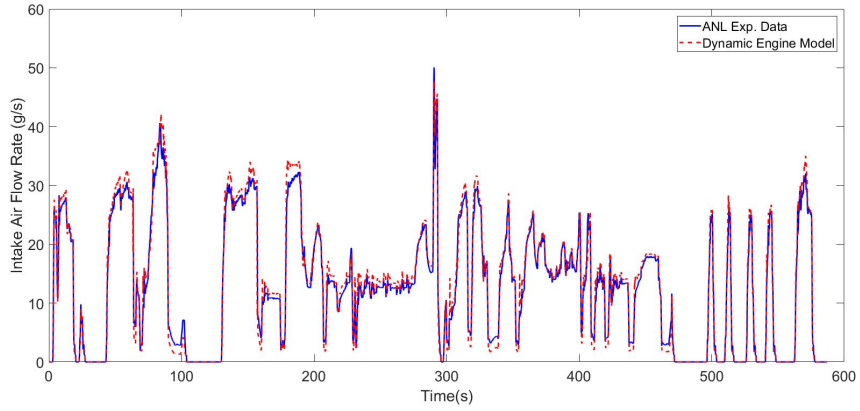

(c) Validation of intake air flow rate

Figure 3.13: Validation of engine dynamic model with CS US06 ANL test data ($\bar{\epsilon}$ =average error, σ_e = standard deviation of error).Test details are provided in Appendix B.7 (Filename: 61607019.mat)

.

Further three CS test cycle provided by ANL were validated with the engine model and Table 3.8 shows fuel consumption prediction for three CS test cycles.

Table 3.8
Fuel consumption validation of Chevy Volt engine dynamic model for three CS test cycles. Test details are provided in Appendices B.7 and B.8 (Grade Passing Filename: 61607008.mat, HWFET Filename: 61607025.mat, UDDS Filename: 61607029.mat)

Drive Cycle	**Average error (g/s)**	**Standard deviation (g/s)**	**Total Error (%)**
Grade Passing	0.12	0.28	0.1
HWFET	0.09	0.21	1.4
UDDS	0.05	0.20	0.1

3.2.2 Electric Motor and TPIM Model

Chevy Volt Gen II has two electric motor-generators (motor-generator A (MGA) and motor-generator B (MGB)) for propulsion as well as regeneration, both having mass and volume reduction of 40% and 20% respectively when compared to GEN I motors [17]. Each motor specification has been provided in Table 3.9 [17].

Table 3.9
Motor A and Motor B specifications of Chevy Volt Gen II

Parameters	Specifications
Motor A material	Ferrite magnet with distributed bar wound
Motor B material	NdFeB magnet with distributed bar wound
Motor A peak torque	118 Nm
Motor B peak torque	280 Nm
Motor A peak power	48 kW
Motor B peak power	87 kW

Traction Power Inverter Module (TPIM) is a package, containing three inverter modules; traction power inverter module-A (TPIM-A), power inverter module-B (TPIM-B) and oil pump inverter, is present between motor generators and battery.

3.2.2.1 Model Description

The Simulink subsystems of MGA and MGB consist efficiency maps that were created by data extraction from [32]. Inputs to the model is motor speed and torque (Figure 3.1), correspondingly battery power request is the output. Motor generator A and Motor generator B maps have been shown in the Figures 3.14 and 3.15 respectively.

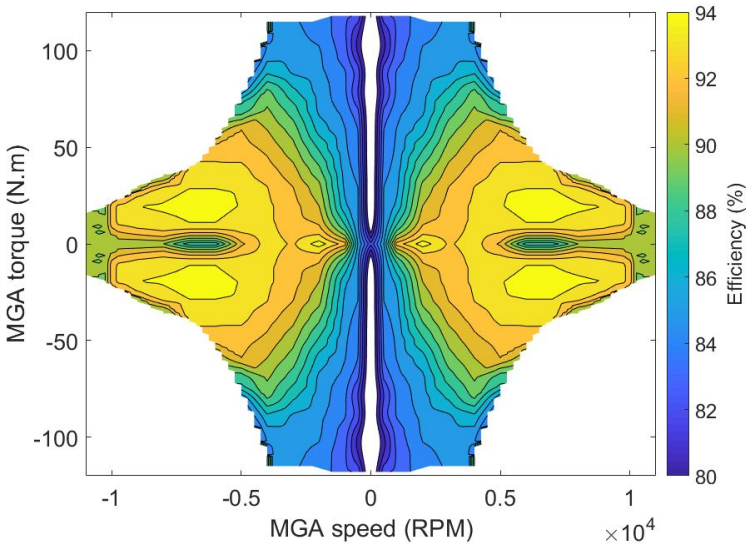

Figure 3.14: MGA efficiency map for 406 V battery voltage

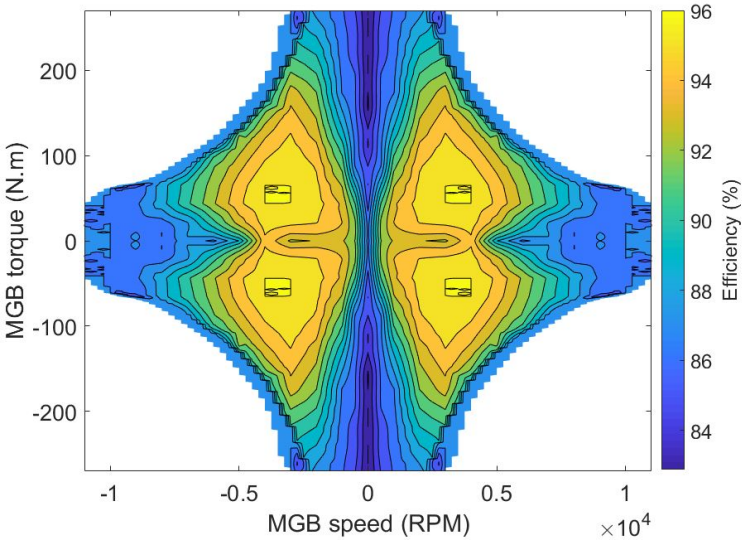

Figure 3.15: MGB efficiency map for 410 V battery voltage

TPIM efficiency maps for MGA and MGB were created by extracting data from [33].

TPIM-A and TPIM-B are shown in the Figures 3.16 and 3.17.

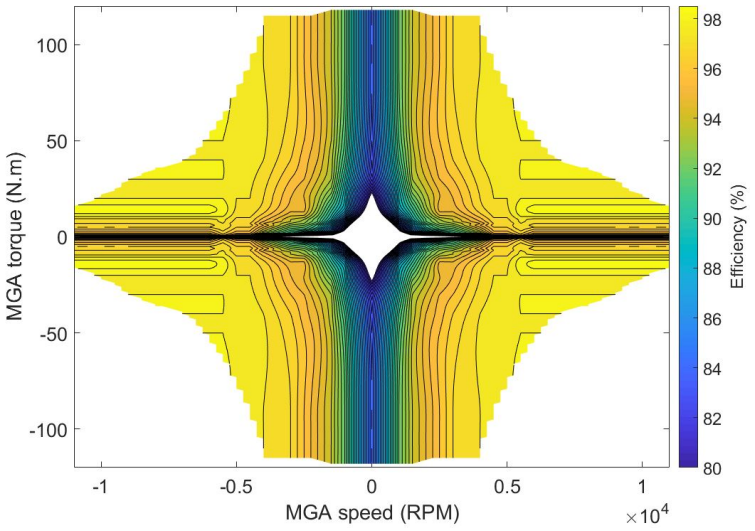

Figure 3.16: TPIM-A efficiency map for 406 V battery voltage

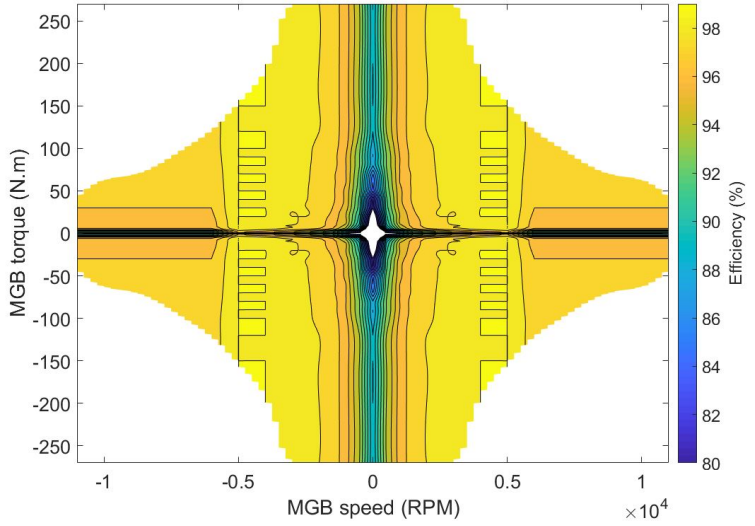

Figure 3.17: TPIM-B efficiency map for 410 V battery voltage

3.2.2.2 Model Validation

Electric load consumed by MGA and MGB from the battery is validated for CD case provided by ANL. Power supplied by the battery is first converted into alternating current (AC) power then supplied to the motors. Figures 3.18 and 3.19 show validation of battery power load consumed by MGA and MGB cumulatively, which also includes efficiency of TPIM-A and TPIM-B, for UDDS (CD) and US06(CD) test cycles.

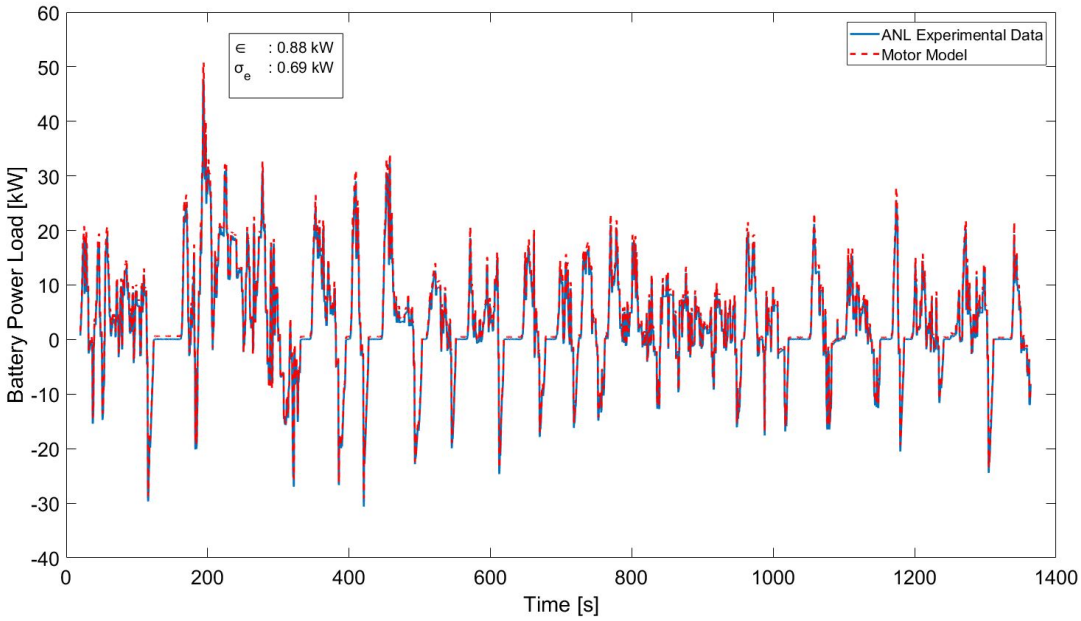

Figure 3.18: Motor model validation with UDDS (CD) test cycle.Test details are provided in Appendix B.7 (Filename: 61608022.mat)

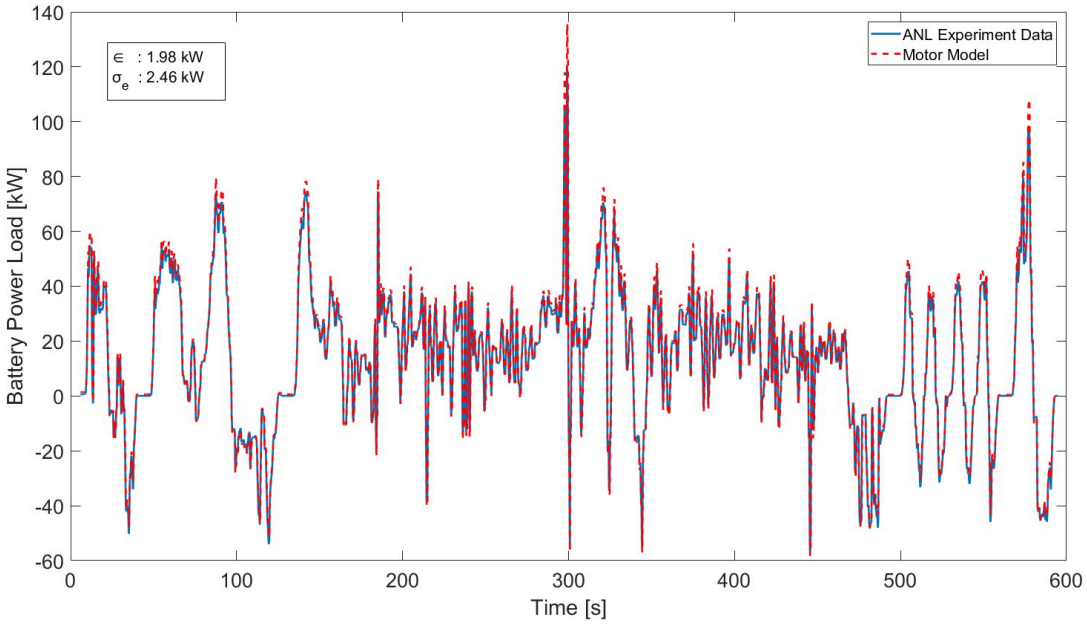

Figure 3.19: Motor generator model validation with US06 (CD) test cycle. Test details are provided in Appendix B.7 (Filename: 61608021.mat)

3.2.3 Li-ion Battery Model

Chevy Volt includes a 18.4 kWhr Li-ion battery to supply electrical energy for propulsion and auxiliary devices functioning. It has 2 cell in parallel configuration compared to Gen I which improved packaging efficiency and energy density [17]. Battery specifications have been provided in Table 3.10.

Table 3.10
Li-ion Battery specifications of Chevy Volt Gen II [17]

Parameters	Specifications
Energy (kWh)	18.4
Maximum Power (kW)	120
Peak Capacity (Ah)	52
Cell Chemistry	Li-Ion
Configuration	2 parallel,96 series
Mass,Pack (kg)	183
Volume, Pack (L)	148
Cooling (L)	Liquid

3.2.3.1 Model Description

A simulink model, based on electrical and thermal dynamics, of 18.4 kWh Li-Ion battery was developed using the battery parameters provided by GM. Further validation of model was performed with CD test cases provided by ANL.

The circuit diagram of cell is shown in the Figure 3.20. The model consists two circuits, one determining capacity of the battery and other with a series internal resistance and two RC circuits [34]. The electrical equations used for determining battery voltage and state of charge (SOC) are given by the following equations:

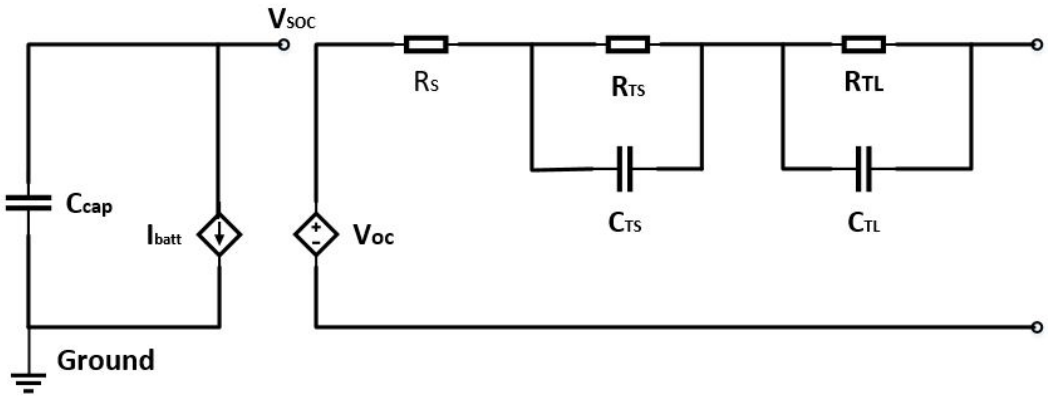

Figure 3.20: Circuit diagram of a cell

$$P_{batt} = V_{batt} I_{batt} \tag{3.14}$$

P_{batt}, V_{batt} and I_{batt} are battery power, battery voltage and battery current respectively.

$$\frac{dV_{CTS}}{dt} = \frac{-V_{CTS}}{R_{TS}C_{TS}} - \frac{I_{batt}}{C_{TS}} \tag{3.15}$$

$$\frac{dV_{CTL}}{dt} = \frac{-V_{CTL}}{R_{TL}C_{TL}} - \frac{I_{batt}}{C_{TL}} \tag{3.16}$$

$$V_{batt} = g(x) + V_{CTL} + V_{CTS} + R_s I_{batt} \tag{3.17}$$

$$SOC = SOC_i - \frac{\int I_{batt} dt}{Q} \tag{3.18}$$

where, R_{TS}, R_{TS} and V_{CTS} represent the resistance, capacitance and voltage drop in the shorter time constant RC circuit respectively, R_{TL}, R_{TL} and R_{CTL} represent the resistance, capacitance and voltage drop in the longer time constant RC circuit

respectively, R_s is series resistance, $g(x)$ is open circuit voltage (OCV), Q is battery capacity, I_{batt} is battery current, SOC_i is initial SOC of the battery. All these parameters, dependent on temperature and SOC, are determined using maps which were created using GM given data. Figure 3.21 show the overall Simulink model of the Li-Ion battery.

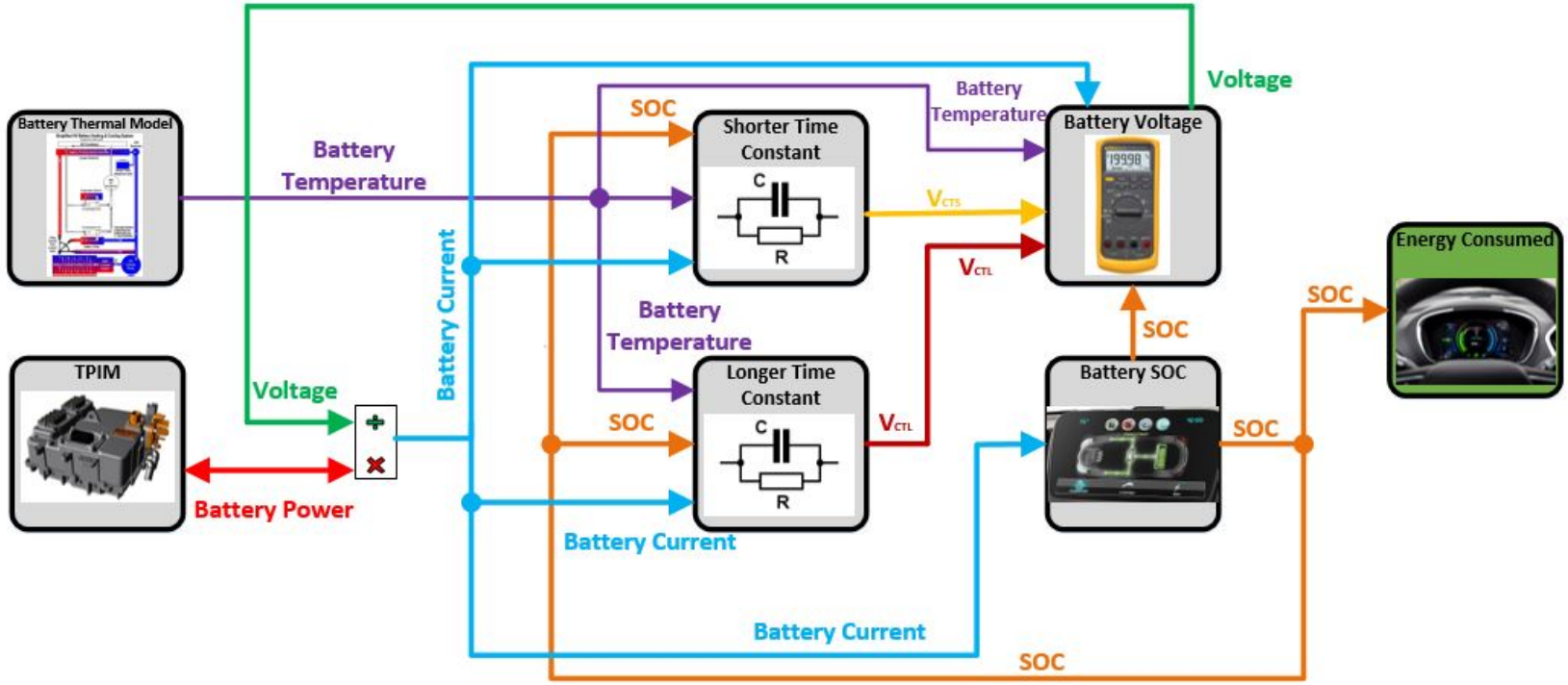

Figure 3.21: Li-Ion battery model of Chevy Volt GEN II

3.2.3.2 Model Validation

Li-ion battery model was validated for CD test case provided by ANL. Validation of SOC for UDDS and US06 have been shown in Figures 3.22 and 3.23 respectively.

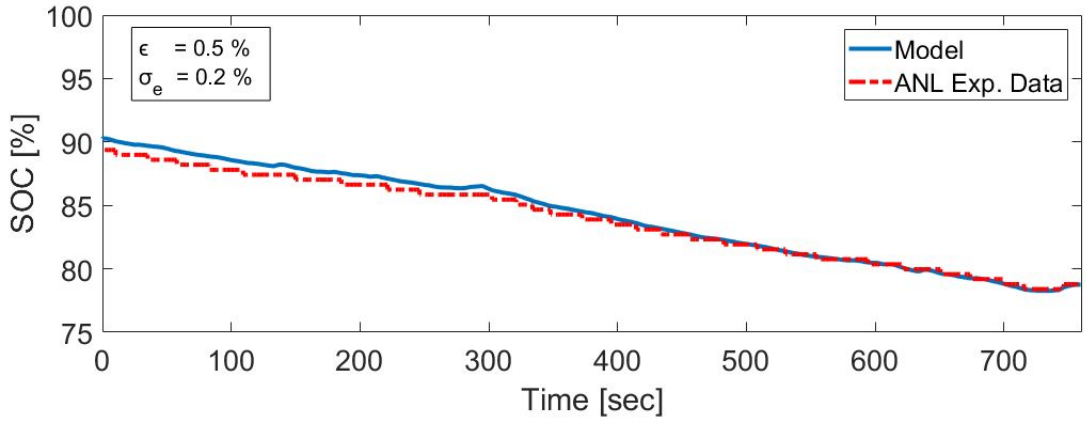

Figure 3.22: Validation of battery model with CD UDDS ANL test data (ϵ =average error, σ_e = standard deviation of error). Test details are provided in Appendix B.7(Filename: 61608022.mat)

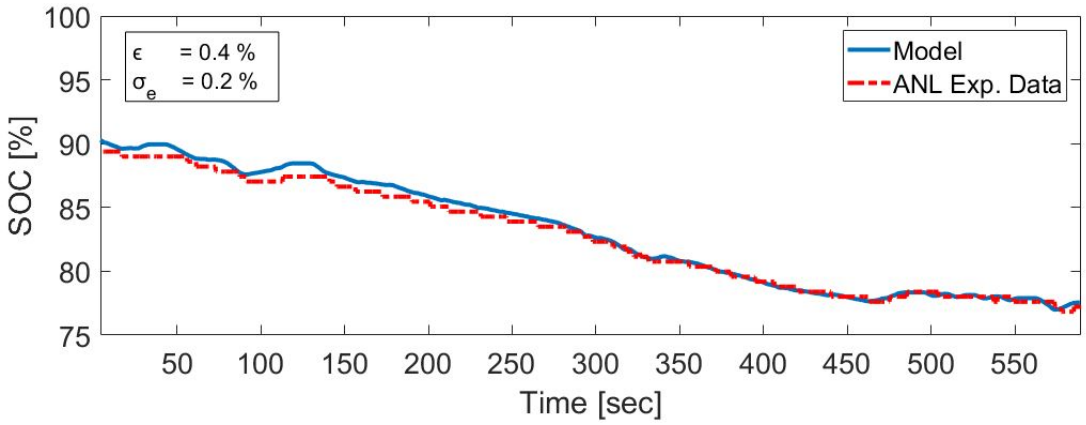

Figure 3.23: Validation of battery model with CD US06 ANL test data (ϵ =average error, σ_e = standard deviation of error). Test details are provided in Appendix B.7 (Filename: 61608021.mat)

3.2.4 Drive unit and Operating Modes

Drive unit with powertrain components are shown in the Figure 3.24. Three clutches and two planetary gear set enable vehicle to operate in five different modes. Different combination of clutch positions allow different power flow directions in the drive unit. Figure 3.25 shows one motor EV mode power flow in which MGB carries out propulsion and regeneration braking. Figure 3.26 shows two motor EV power flow in which both MGB and MGA carry out propulsion of vehicle. Figure 3.27 shows low extended range mode power flow in which ICE assist MGB in vehicle propulsion and fraction of engine fuel energy is converted into electrical energy by MGA. Figure 3.28 shows fixed ratio extended range mode power flow in which both ICE and MGB propel the vehicle. Figure 3.29 shows high extended range mode power flow in which ICE, MGA and MGB propel the vehicle. These modes are decided by supervisory controller based on driver speed request and battery SOC.

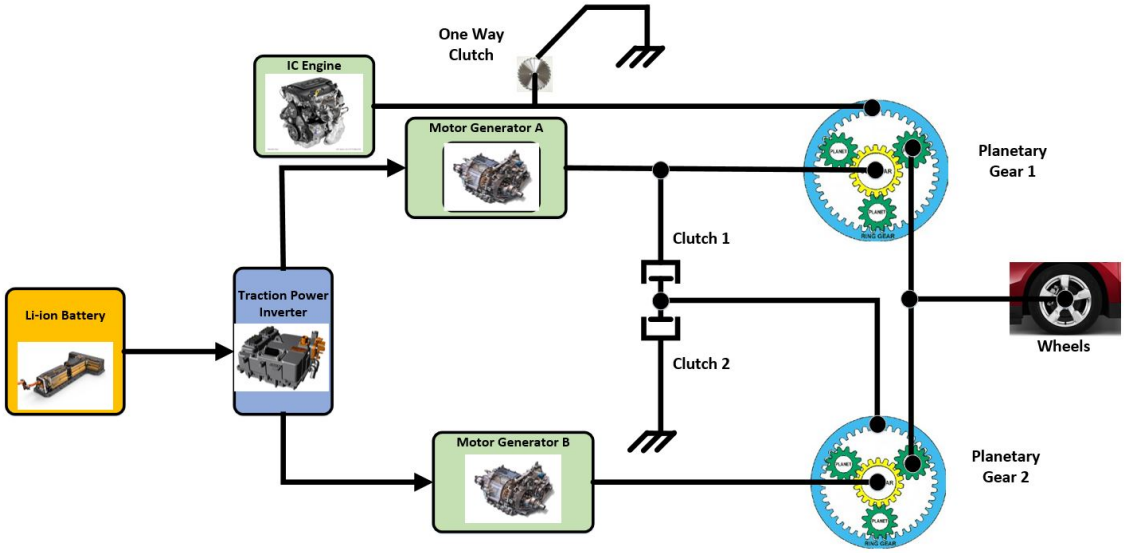

Figure 3.24: Schematic of the Chevy Volt Gen II drive unit

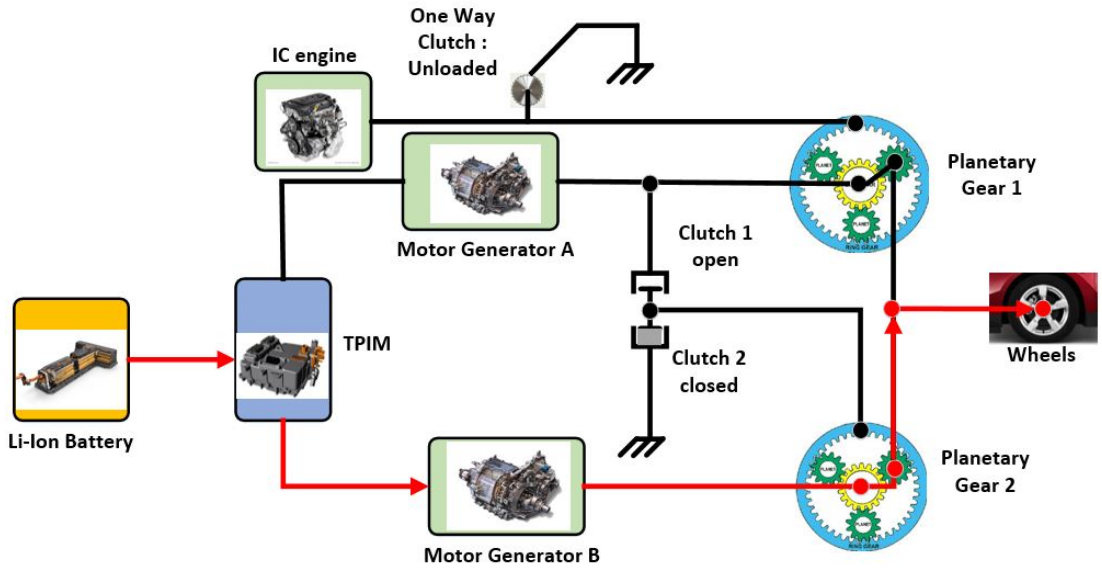

Figure 3.25: Chevy Volt GEN II - One motor EV

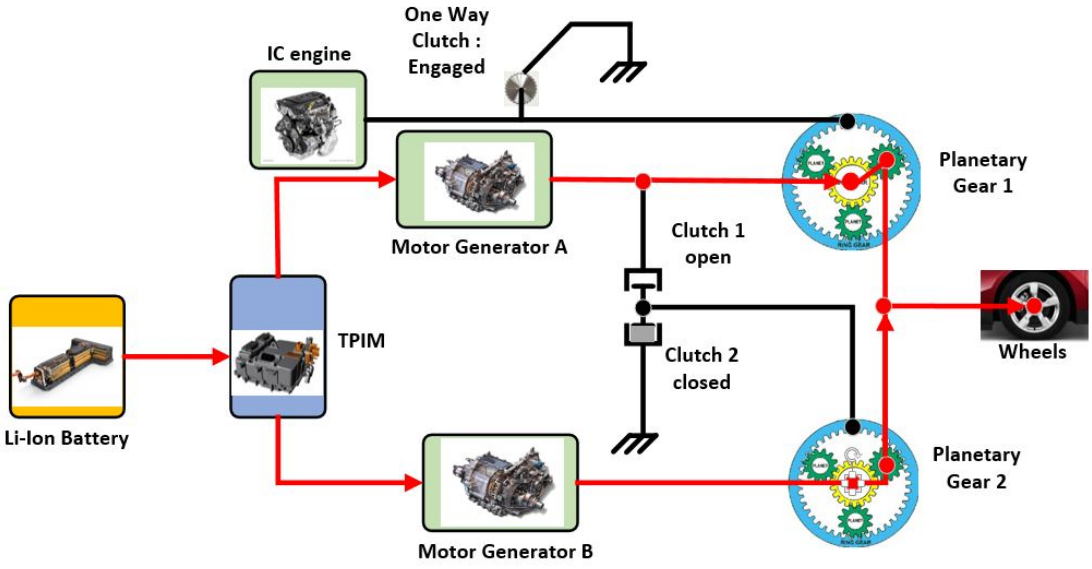

Figure 3.26: Chevy Volt GEN II -Two motor EV

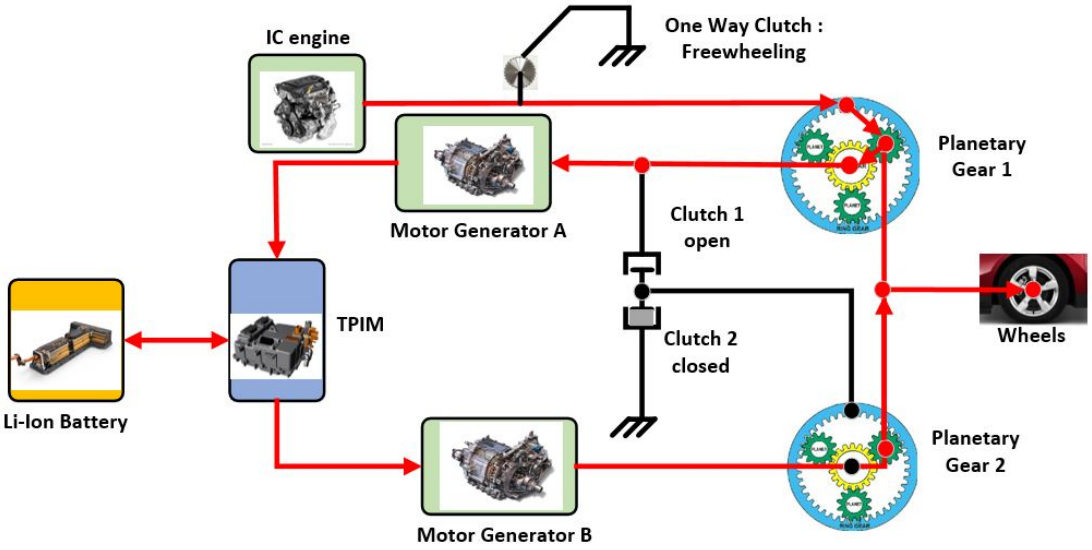

Figure 3.27: Chevy Volt GEN II -Low extended range

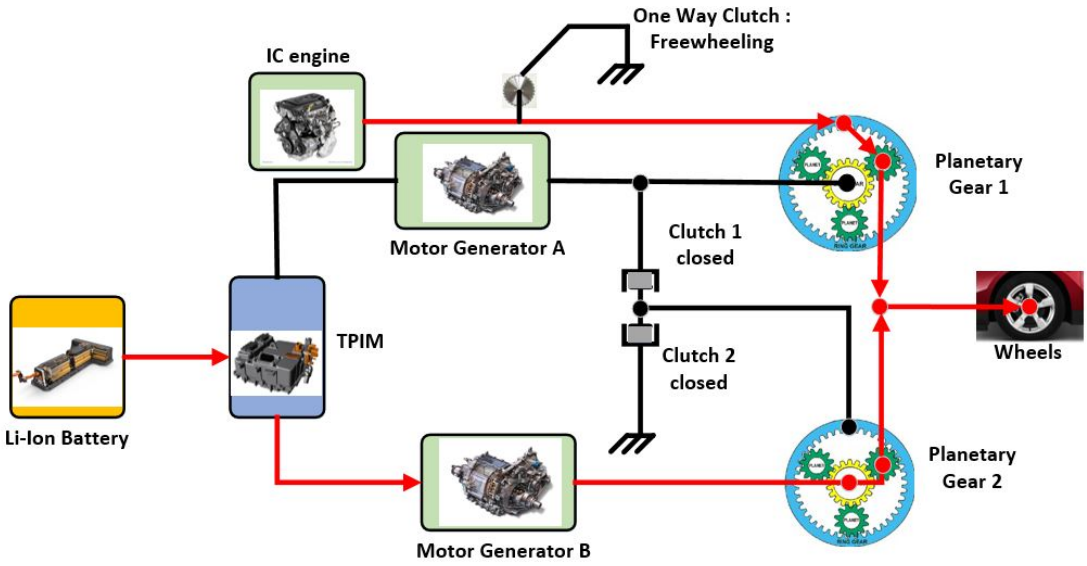

Figure 3.28: Chevy Volt GEN II -Fixed ratio extended range

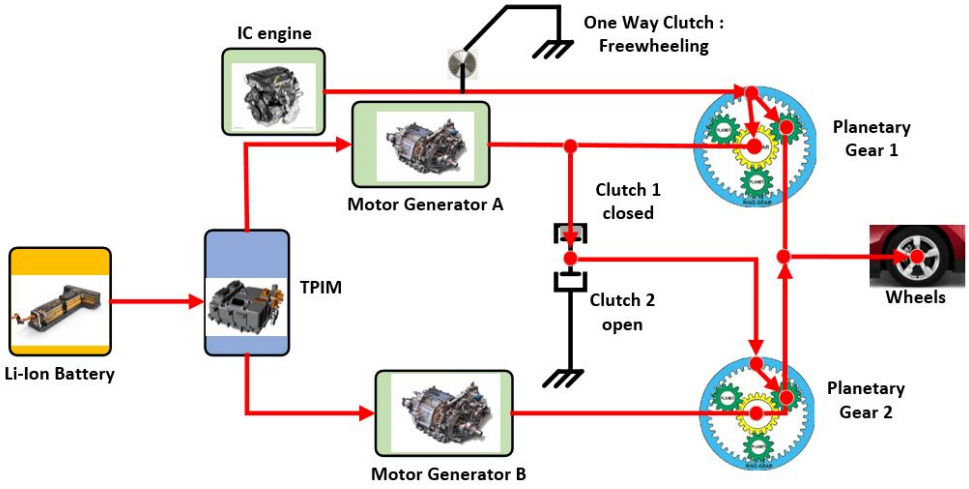

Figure 3.29: Chevy Volt GEN II -High extended range

3.2.4.1 Model Description

Chevy Volt Gen II has five operating modes , which are achieved by using two planetary gear sets and three clutches, depending on the vehicle speed and torque requirements. The dynamic equations for operating modes were obtained from [16]. Figure 3.30 shows planetary gear set with ring gear, planet carrier, pinion gear and sun gear. The kinematic constraints of the planetary gear set are given by:

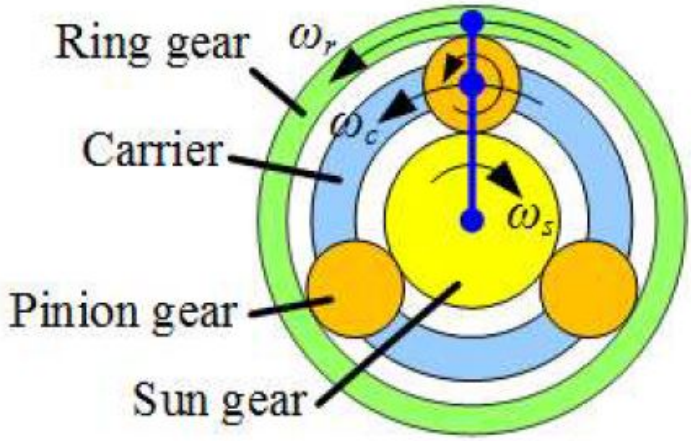

Figure 3.30: Planetary gear set [16]

$$\omega_r R + \omega_s S = \omega_c (R + S) \tag{3.19}$$

where, ω_r , ω_s and ω_s are angular speeds of the ring, sun and carrier gears respectively. S and R denote the radii of sun and ring gear, respectively.

The dynamic equations of each gear node is given by [35]:

$$\dot{\omega_r} I_r = FR - T_r \tag{3.20}$$

$$\dot{\omega_c} I_c = -FR - FS + T_c \tag{3.21}$$

$$\dot{\omega_s} I_s = FS - T_s \tag{3.22}$$

where, $\dot{\omega_r}$, $\dot{\omega_s}$ and $\dot{\omega_c}$ are angular acceleration of the ring, sun and carrier gears respectively. I_r, I_s and I_c are inertias of propulsion components connected at ring, sun and carrier respectively. The dynamic equations for each operating modes are discussed as follows;

† One motor EV : MGB is only used for propulsion at light loads in this operating mode. As shown in the Figure 3.25, clutch 2 (C2) is closed with clutch 1 (C1) and one way clutch (OWC), open and unloaded respectively. Figure 3.31 shows lever diagram of this mode. The dynamic equation of this mode is given as;

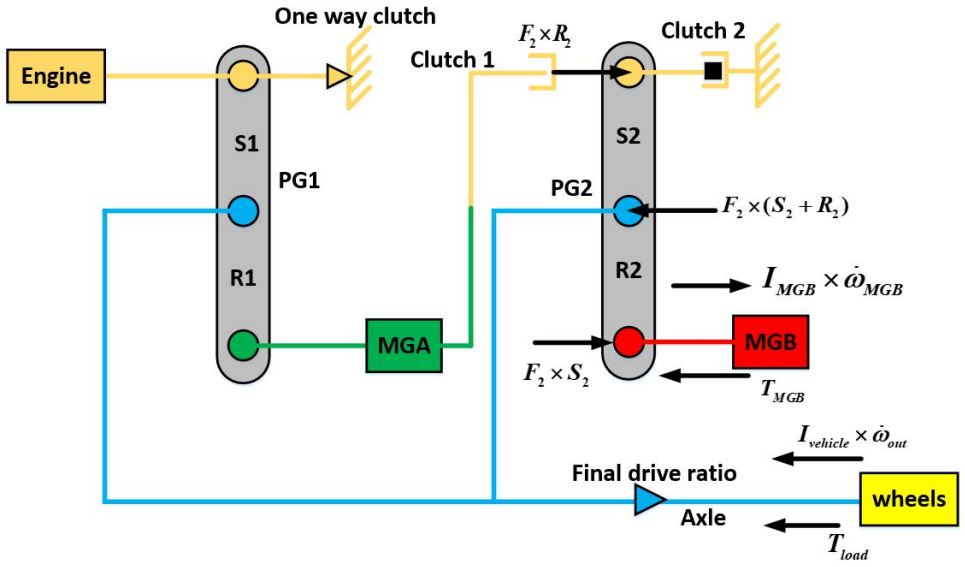

Figure 3.31: Lever diagram on one motor EV mode

$$\begin{bmatrix} I_{vehicle} & 0 & S_2 + R_2 \\ 0 & I_{MGB} & -S_2 \\ S_2 + R_2 & -S_2 & 0 \end{bmatrix} \begin{bmatrix} \dot{\omega}_{out} \\ \dot{\omega}_{MGB} \\ F_2 \end{bmatrix} = \begin{bmatrix} -T_{load} \\ T_{MGB} \\ 0 \end{bmatrix}$$

where, $I_{vehicle}$ and I_{MGB} are inertia of vehicle and MGB respectively. F_2 is internal force acting between the gears of planetary gear 2 and , T_{load} and T_{MGB} are sum of vehicle resistance (rolling, aerodynamic and gradient resistance) and T_{MGB} is torque generated by MGB. S_2 and R_2 are radii of sun and ring gear for planetary gear 2 (PG2). $\dot{w}_{out}$ and $\dot{w}_{MGB}$ are angular acceleration of axle and MGB.

† Two motor EV : MGB and MGA are used for propulsion at higher loads in this operating mode. As shown in the Figure 3.26, C1 is open, C2 is closed and

OWC is engaged. Figure 3.32 shows lever diagram of this mode. The dynamic equation of this mode is given as;

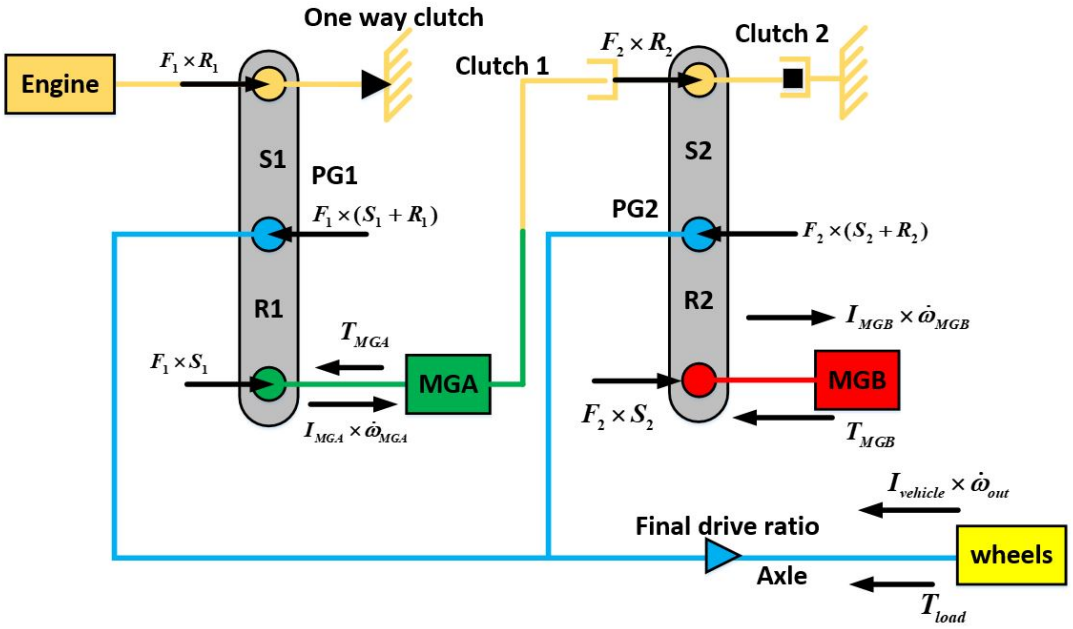

Figure 3.32: Lever diagram of two motor EV mode

$$\begin{bmatrix} I_{vehicle} & 0 & 0 & S_1+R_1 & S_2+R_2 \\ 0 & I_{MGA} & 0 & -S_1 & 0 \\ 0 & 0 & I_{MGB} & 0 & -S_2 \\ S_1+R_1 & -S_1 & 0 & 0 & 0 \\ S_2+R_2 & 0 & -S_2 & 0 & 0 \end{bmatrix} \begin{bmatrix} \dot{\omega}_{out} \\ \dot{\omega}_{MGA} \\ \dot{\omega}_{MGB} \\ F_1 \\ F_2 \end{bmatrix} = \begin{bmatrix} -T_{load} \\ T_{MGA} \\ T_{MGB} \\ 0 \\ 0 \end{bmatrix}$$

where, I_{MGA} is inertia of MGA. F_1 is internal force acting between the gears of planetary gear 1 (PG1) and, T_{MGA} is torque generated by MGA. S_1 and R_1

are radii of sun and ring gear for planetary gear 1 (PG1). $\dot{\omega}_{MGA}$ is angular acceleration of MGA.

† Low extended range: MGB and Engine propel the vehicle with fraction of engine fuel energy converted into electrical energy by MGA in this operating mode. As shown in the Figure 3.27, C1 is open, C2 is closed and OWC is freewheeling. Figure 3.33 shows lever diagram of this mode. The dynamic equation of this mode is given as;

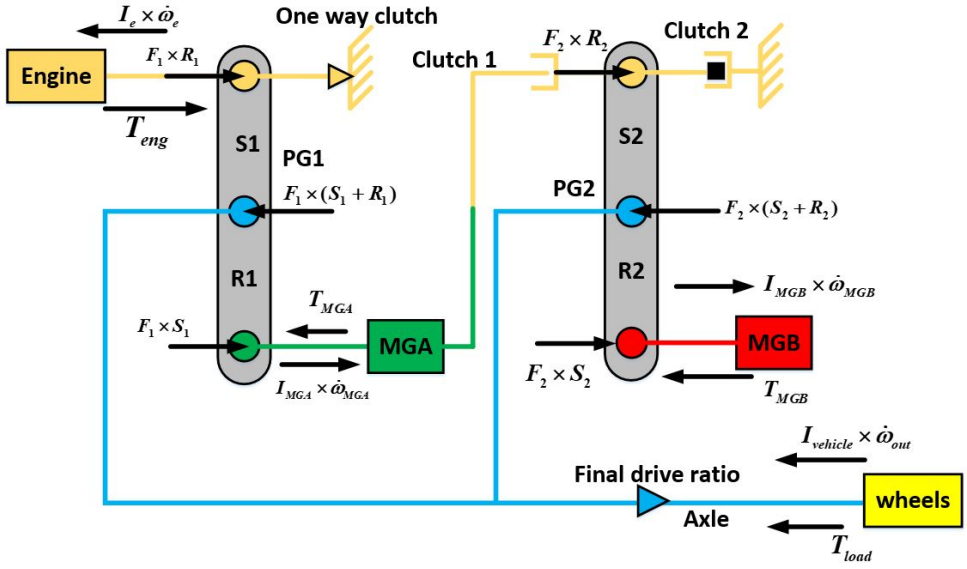

Figure 3.33: Lever diagram of low extended range mode

$$\begin{bmatrix} I_{vehicle} & 0 & 0 & 0 & S_1+R_1 & S_2+R_2 \\ 0 & I_e & 0 & 0 & -R_1 & 0 \\ 0 & 0 & I_{MGA} & 0 & -S_1 & 0 \\ 0 & 0 & 0 & I_{MGB} & 0 & -S_2 \\ S_1+R_1 & -R_1 & -S_1 & 0 & 0 & 0 \\ S_2+R_2 & 0 & 0 & -S_2 & 0 & 0 \end{bmatrix} \begin{bmatrix} \dot{\omega}_{out} \\ \dot{\omega}_e \\ \dot{\omega}_{MGA} \\ \dot{\omega}_{MGB} \\ F_1 \\ F_2 \end{bmatrix} = \begin{bmatrix} -T_{load} \\ T_e \\ T_{MGA} \\ T_{MGB} \\ 0 \\ 0 \end{bmatrix}$$

where, I_e, T_e and $\dot{\omega}_e$ is inertia, torque generated and angular acceleration of ICE.

† Fixed ratio extended range: Both MGB and engine propels the vehicle and is used mostly for moderate power demands in this operating mode. As shown in the Figure 3.28, C1 is closed, C2 is closed and OWC is freewheeling. Figure 3.34 shows lever diagram of this mode. The dynamic equation of this mode is given as;

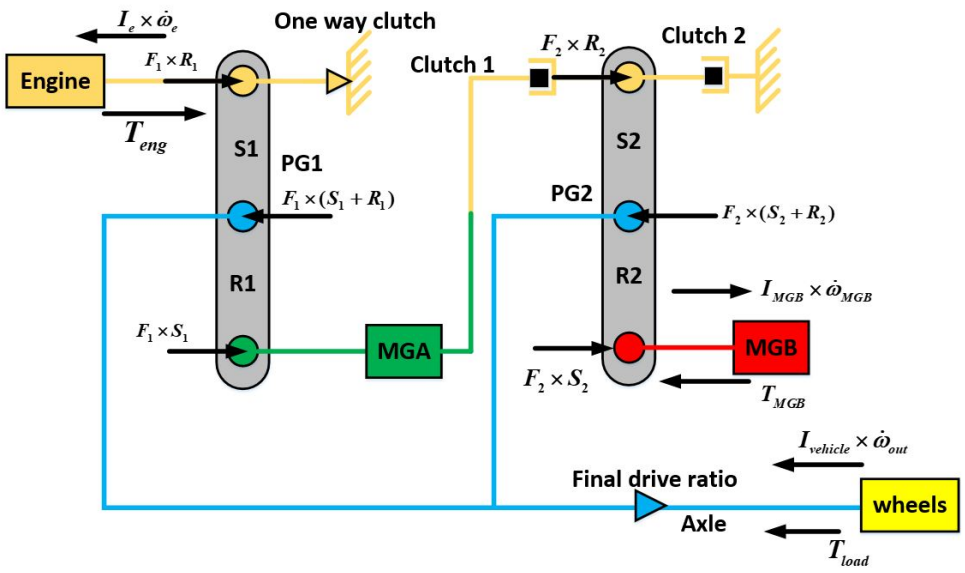

Figure 3.34: Lever diagram of fixed ratio extended range mode

$$\begin{bmatrix} I_{vehicle} & 0 & 0 & S_1+R_1 & S_2+R_2 \\ 0 & I_e & 0 & -R_1 & 0 \\ 0 & 0 & I_{MGB} & 0 & -S_2 \\ S_1+R_1 & -S_1 & 0 & 0 & 0 \\ S_2+R_2 & 0 & -S_2 & 0 & 0 \end{bmatrix} \begin{bmatrix} \dot{\omega}_{out} \\ \dot{\omega}_e \\ \dot{\omega}_{MGB} \\ F_1 \\ F_2 \end{bmatrix} = \begin{bmatrix} -T_{load} \\ T_e \\ T_{MGB} \\ 0 \\ 0 \end{bmatrix}$$

† High extended range : MGB, MGA and engine propel the vehicle due to peak power demands in this operating mode. As shown in the Figure 3.29, C1 is closed, C2 is open and OWC is freewheeling. Figure 3.35 shows lever diagram of this mode. The dynamic equation of this mode is given as;

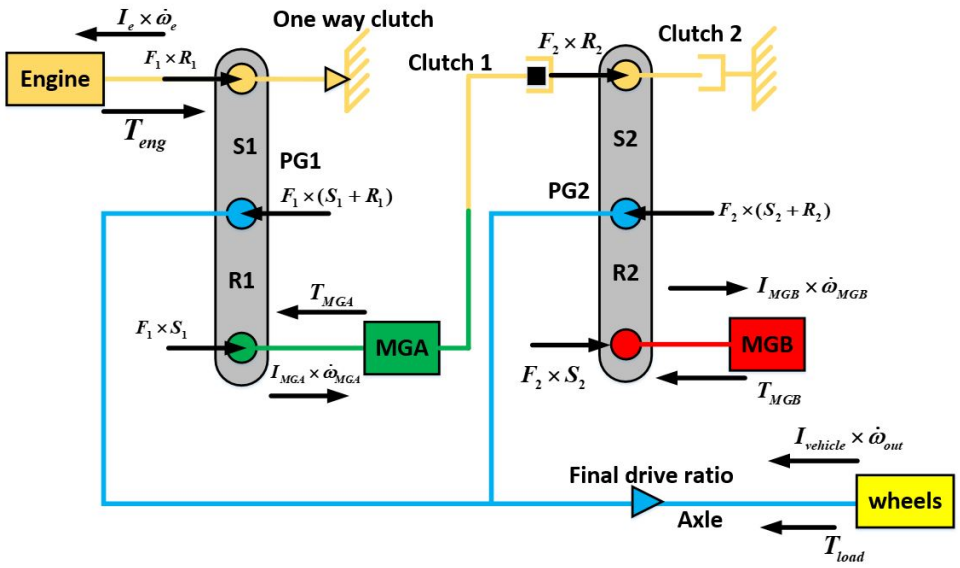

Figure 3.35: Lever diagram of high extended range mode

$$\begin{bmatrix} I_{vehicle} & 0 & 0 & 0 & S_1+R_1 & S_2+R_2 \\ 0 & I_e & 0 & 0 & -R_1 & 0 \\ 0 & 0 & I_{MGA} & 0 & -S_1 & -R_2 \\ 0 & 0 & 0 & I_{MGB} & 0 & -S_2 \\ S_1+R_1 & -R_1 & -S_1 & 0 & 0 & 0 \\ S_2+R_2 & 0 & -R_2 & -S_2 & 0 & 0 \end{bmatrix} \begin{bmatrix} \dot{\omega}_{out} \\ \dot{\omega}_e \\ \dot{\omega}_{MGA} \\ \dot{\omega}_{MGB} \\ F_1 \\ F_2 \end{bmatrix} = \begin{bmatrix} -T_{load} \\ T_e \\ T_{MGA} \\ T_{MGB} \\ 0 \\ 0 \end{bmatrix}$$

3.2.5 Auxiliary Pump Model

Drive unit auxiliary pump is one of the devices that consumes electrical energy from that battery to maintain lubrication of the 4ET50 transaxle. The drive unit auxiliary pump provides pressurized automatic transmission fluid (Dexron VI) to actuate clutches, lubricate gears, bearings and bushings, and cool the motor generators[36].

3.2.5.1 Model Description

Using ANL test data, a model predicting auxiliary pump power was created. On analysis of test data it was inferred that the power consumed by auxiliary pump depended on the axle torque, vehicle speed and powertrain mode. Figure 3.36 shows the overview of the auxiliary pump model which is an empirical model.

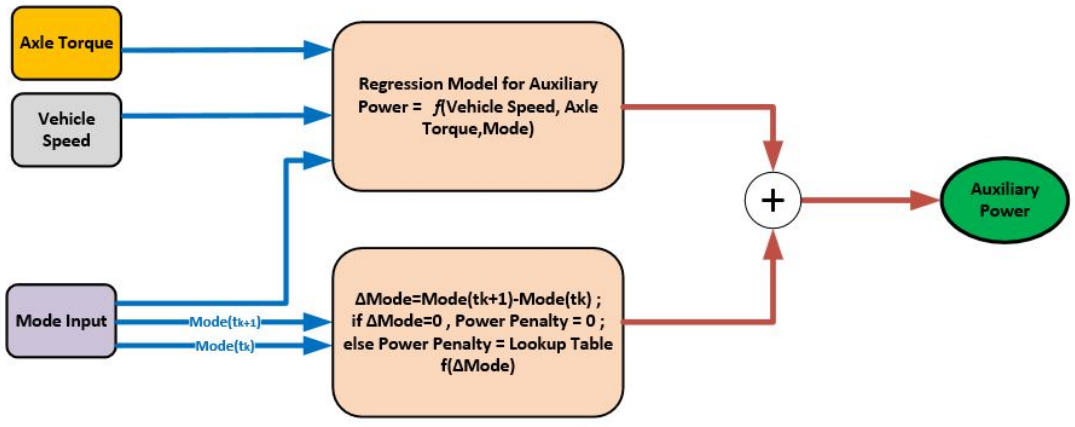

Figure 3.36: Auxiliary pump model

Auxiliary power calculated from the above model is converted into auxiliary battery load by following equations:

$$P_{load} = \frac{AuxiliaryPower}{\eta_{motor}\eta_{inverter}} \tag{3.23}$$

where, P_{load} is auxiliary battery load, η_{motor} is auxiliary pump motor efficiency and $\eta_{inverter}$ is auxiliary pump inverter efficiency provided by GM.

3.2.5.2 Model Validation

Figure 3.37(a) and Figure 3.37(b) show validation of auxiliary pump power with ANL data.

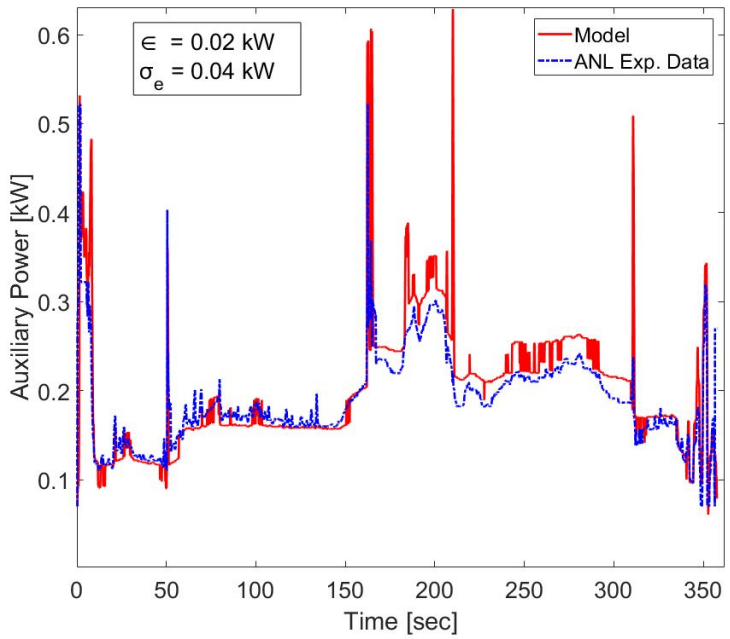

(a) Auxiliary pump power vs time for CD test (ANL)

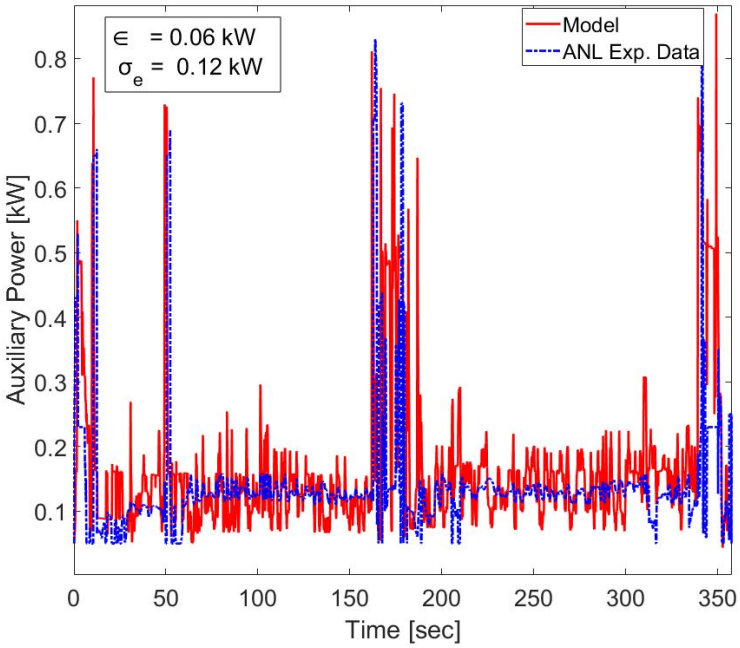

(b) Auxiliary pump power vs time for CS test (ANL)

Figure 3.37: Validation of drive unit auxiliary pump model with ANL test data (ϵ =average error, σ_e = standard deviation of error). Test details are provided in B.7(CD Filename: 61608022.mat and CS Filename: 61607029.mat)

3.2.6 Longitudinal Vehicle Dynamics

Longitudinal vehicle dynamics (LVD) estimates speed of the vehicle. It takes into account two important resistive forces acting on the vehicle, namely; rolling resistance and aerodynamic drag resistance.

3.2.6.1 Model Description

Figure 3.38 shows the forces acting on a moving vehicle.

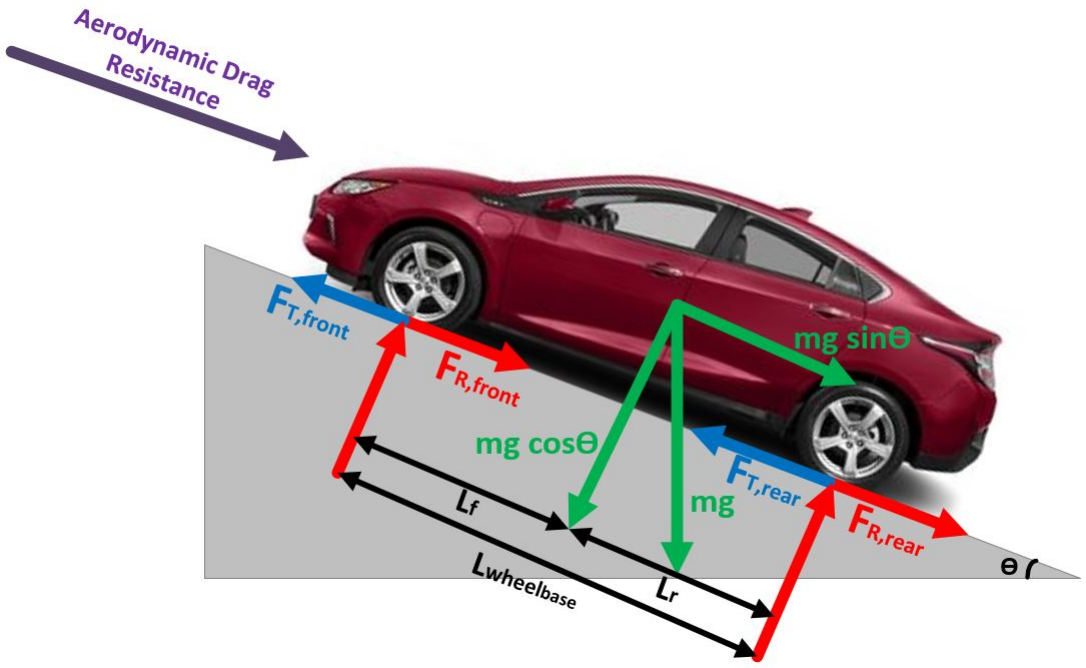

Figure 3.38: Longitudinal vehicle dynamics of Chevy Volt Gen II

Using Newton's second law on the vehicle, vehicle acceleration can be found using following equation;

$$m\frac{dv}{dt} = F_T - F_R \tag{3.24}$$

$$F_R = F_{R,front} + F_{R,rear} + F_{aero} + mgsin\theta \tag{3.25}$$

where, m is mass of the vehicle, v is vehicle velocity, F_T is total traction force on the wheels, F_R is total resistive force acting on the wheels, $F_{R,front}$ is rolling resistance on front wheels, $F_{R,rear}$ is rolling resistance on rear wheels, F_{aero} is aerodynamic drag resistance, g is acceleration due to gravity and θ is the gradient angle.

The resistive forces in the model are found by the Road–load equation provided by GM. This equation is determined from vehicle testing and consequently an equation dependent on vehicle speed, using regression tool, is found. The equation only includes the effect of rolling resistance and aerodynamic drag resistance. As testing to determine road load equation is performed on flat roads (θ=0), gradient resistance is zero. Road load is given by:

$$F_R = F_0 + F_1 v + F_2 v^2 \tag{3.26}$$

where, v is vehicle velocity, F_0, F_1 and F_0, are coefficients found through regression (determine the effect of aerodynamic drag resistance and rolling resistance). These coefficients, also known as road load coefficients, are provided by GM.

3.3 Charge Depleting Drive Cycle Validation

Energy consumption analysis has been carried out in this section. Fuel energy, used by the engine, and electrical energy, used by the battery, are two sources of energy available for vehicle propulsion. Total energy consumed by the vehicle has been calculated using following equations:

$$P_{batt} = V_{batt} I_{batt} \tag{3.27}$$

$$E_{batt} = \int_0^T P_{batt} dt \tag{3.28}$$

where, P_{batt} is battery power consumed, E_{batt} is total battery energy consumed during the drive cycle and T is duration of drive cycle. Similarly, total fuel energy is calculated by following equation:

$$M_{fuel} = \int_0^T \dot{m}_{fuel} dt \tag{3.29}$$

$$E_{fuel} = M_{fuel} \times LHV \tag{3.30}$$

where, M_{fuel} is total fuel consumed, $\dot{m}_{fuel}$ is fuel flow rate and LHV is the lower heating value of gasoline. Total energy (E_{total}) consumed during a test cycle is given by:

$$E_{total} = E_{fuel} + E_{batt} \tag{3.31}$$

Model validation of two CD test drive cycles have been performed and corresponding energy consumption have been compared to that of ANL test data. Vehicle speed, battery power and SOC have been validated. Performance of vehicle model against ANL test data has been shown in Figures 3.39 and 3.40 for US06 and HWFET drive cycles respectively.

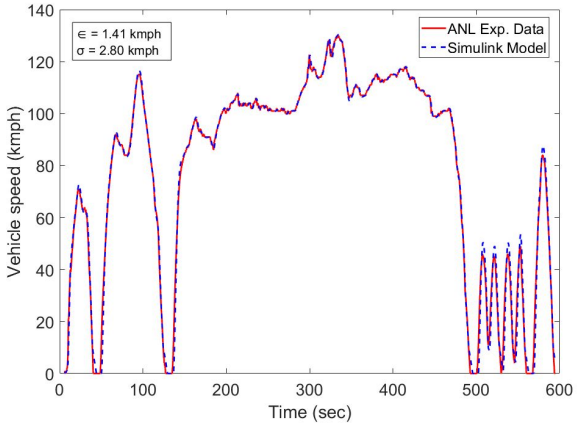

(a) Validation of vehicle speed

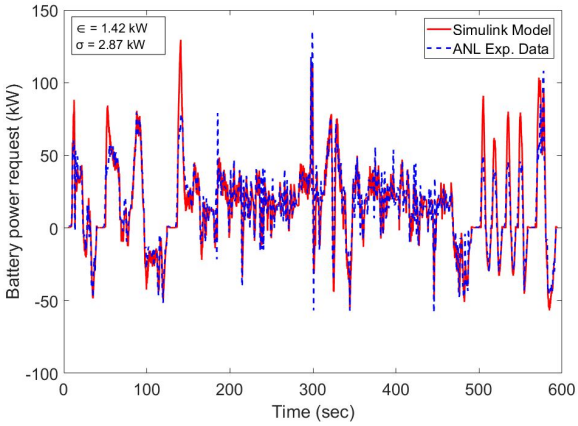

(b) Validation of battery power request

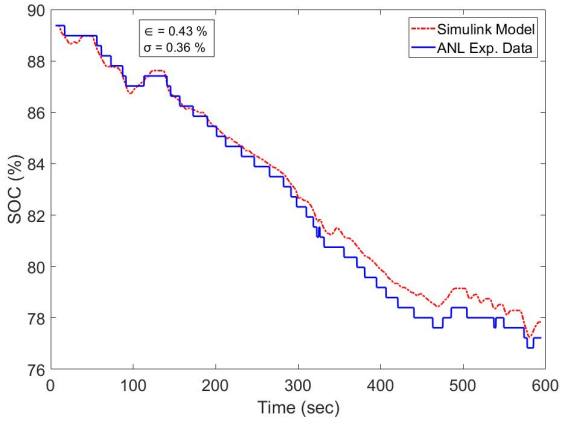

(c) Validation of SOC

Figure 3.39: Validation of vehicle model with CD US06 ANL test data (ϵ =average error, σ_e = standard deviation of error). Test details are provided in Appendix B.8 (Filename: 61608021.mat)

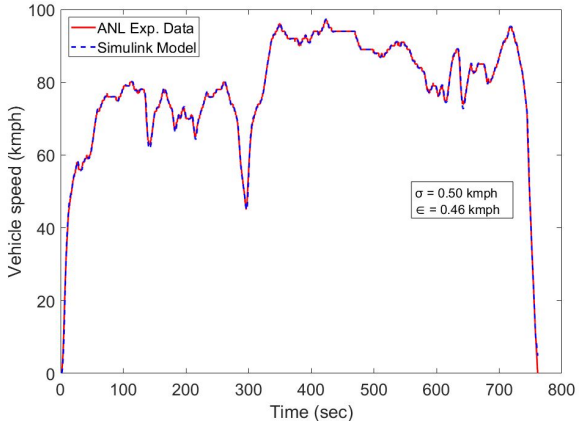

(a) Validation of vehicle speed

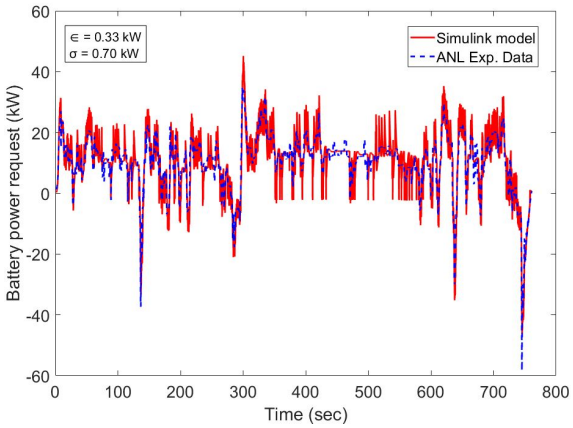

(b) Validation of battery power request

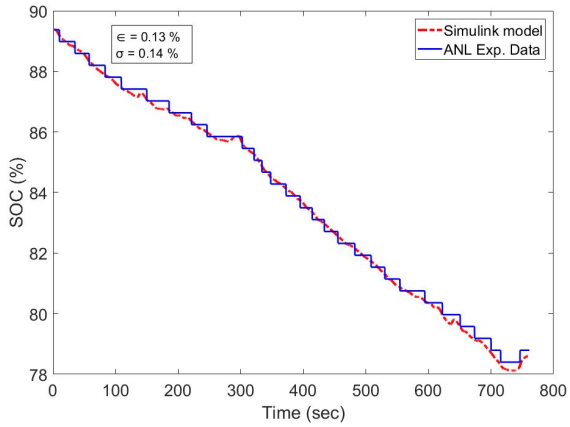

(c) Validation of SOC

Figure 3.40: Validation of vehicle model with CD HWFET ANL test data (ϵ =average error, σ_e = standard deviation of error). Test details are provided in Appendix B.8 (Filename: 61607018.mat)

3.4 Charge Sustaining Drive Cycle Validation

Model validation of two CS test drive cycles have been performed and corresponding energy consumption have been compared to that of ANL test data. Vehicle speed, fuel flow rate and SOC have been validated. Performance of vehicle model against ANL test data has been shown in Figures 3.41 and 3.42 for US06 and HWFET drive cycle respectively.

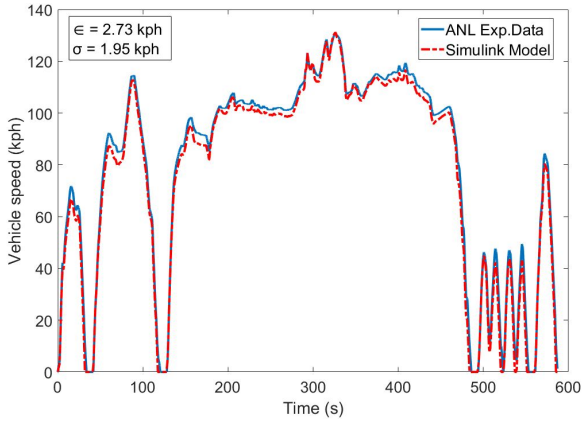

(a) Validation of vehicle speed

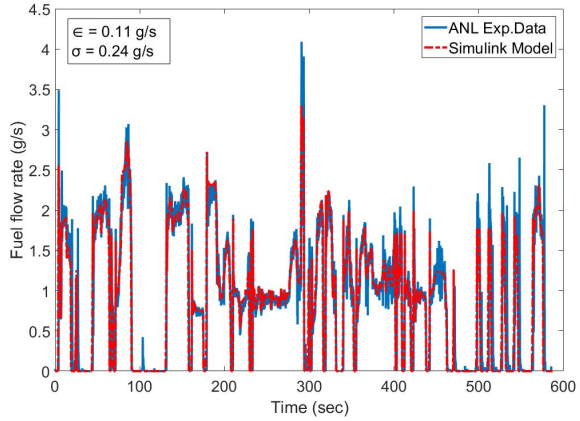

(b) Validation of fuel flow rate

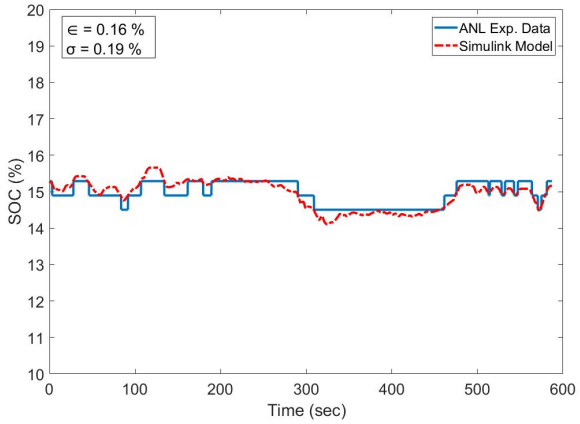

(c) Validation of SOC

Figure 3.41: Validation of vehicle model with CS US06 ANL test data (ϵ =average error, σ_e = standard deviation of error). Test details are provided in Appendix B.8 (Filename: 61607019.mat)

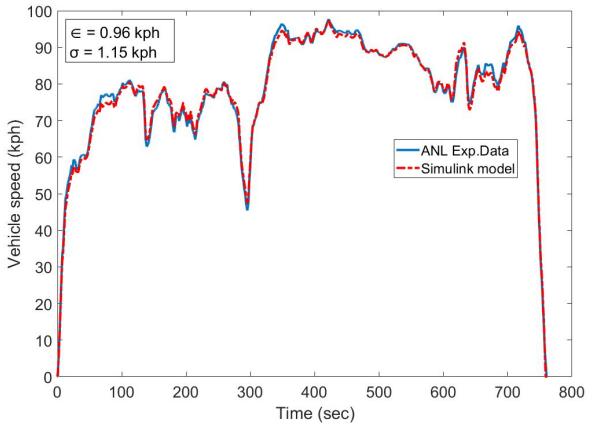

(a) Validation of vehicle speed

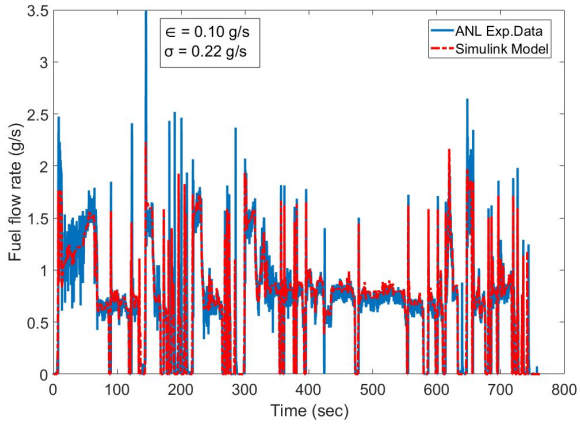

(b) Validation of fuel flow rate

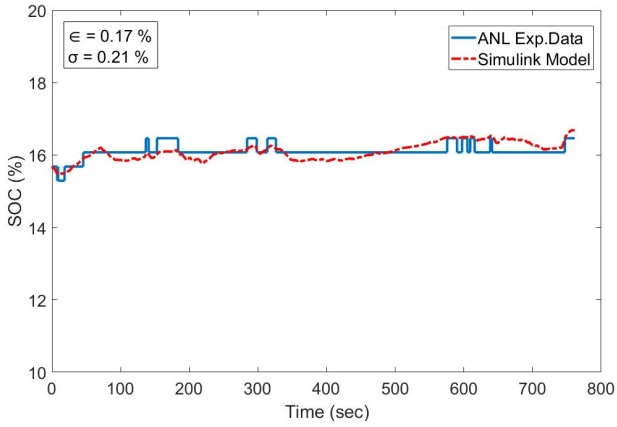

(c) Validation of SOC

Figure 3.42: Validation of vehicle model with CS HWFET ANL test data (ϵ =average error, σ_e = standard deviation of error). Test details are provided in Appendix B.8 (Filename: 61607025.mat)

Tables 3.11 and 3.12 shows quantitative validation of overall energy consumption of vehicle model with ANL test data for CD and CS test cycles respectively.

Table 3.11
Comparison of fuel consumed and electrical energy consumed by vehicle model (simulation) with ANL CD test data (experimental data)

	Simulation		Experimental		
Drive cycle	Fuel (MJ)	Electrical (MJ)	Fuel(MJ)	Electrical(MJ)	Error(%)
US06	0	7.91	0	7.85	0.76
HWFET	0	8.59	0	8.72	1.46

Table 3.12
Comparison of fuel consumed and electrical energy consumed by vehicle model (simulation) with ANL CS test data (experimental data)

	Simulation		Experimental		
Drive cycle	Fuel (MJ)	Electrical (MJ)	Fuel(MJ)	Electrical(MJ)	Error(%)
US06	22.31	-0.17	22.87	-0.29	1.94
HWFET	23.19	-0.61	22.93	-0.66	1.39

Mean absolute error and standard deviation error of vehicle velocity for CS test cases (Figures 3.41 and 3.42) is high compared to that of CD test cases (Figures 3.39 and 3.40). For CD test cases, vehicle velocity is controlled using a PID controller, leading to less error in vehicle speed. In CS test cases, MGB torque, engine torque, MGA speed and mode inputs are provided with no control action on the vehicle velocity.

Chapter 4

Analysis of Energy Consumption for Charge Sustaining and Charge Depleting Drive Cycles

4.1 Analysis of Mode Operation

Chevy Volt GEN II model was created by integrating the validated components discussed in previous Chapter 3. Overall model was validated for four drive cycles, two for each CS and CD test cases was also validated. The inputs to the model, as shown in the Figure 2.2, were extracted from ANL test data and fed to the model. MGB

torque, engine torque, MGA speed, mode and friction brake are five inputs given to the overall model. In the real vehicle, these inputs are generated by the supervisory controller according to the speed and torque requests of the driver. In this section, mode operation of Chevy Volt Gen II is analyzed for different drive cycles provided by ANL. The vehicle operating mode depend on driver speed and torque request. Additionally, vehicle operation also depends on SOC of the battery and operates in CD mode till lower SOC limit is not achieved [17]. When lower SOC limit is achieved, engine starts and vehicle operates in extended range modes [17].

Figures 4.1, 4.2 and 4.3 show modes during UDDS drive cycle, MGB operating points on MGB efficiency map for different modes and MGA operating points on MGA efficiency map for different modes.

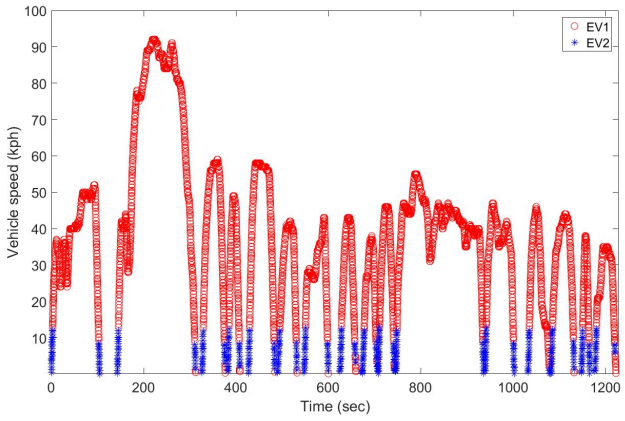

Figure 4.1: Vehicle speed versus time showing EV1 and EV2 operating modes for UDDS drive cycle Appendix B.10 (Filename: 61608022.mat)

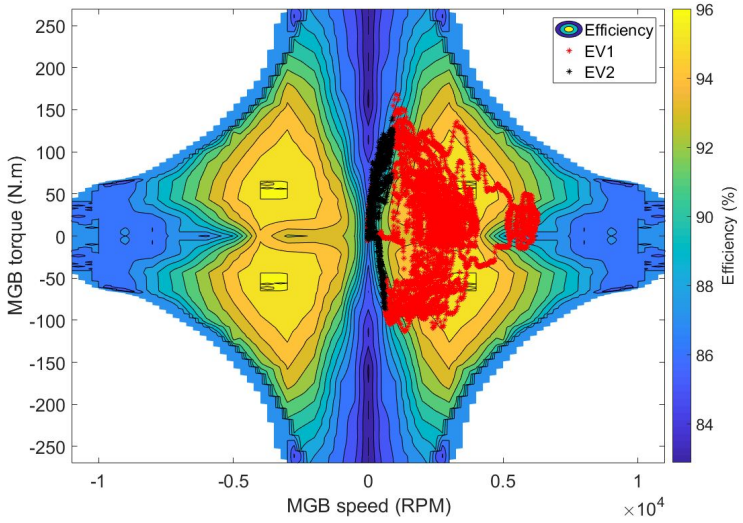

Figure 4.2: MGB Operating points on MGB efficiency map with EV operating modes for UDDS drive cycle. Test details are provided in Appendix B.10 (Filename: 61608022.mat)

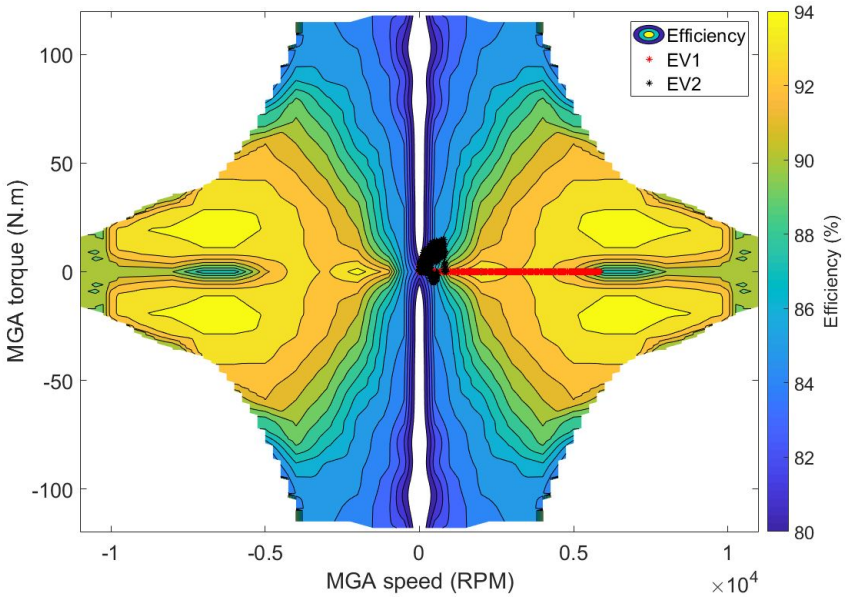

Figure 4.3: MGA Operating points on MGA efficiency map with EV operating modes for UDDS drive cycle. Test details are provided in Appendix B.10 (Filename: 61608022.mat)

The vehicle operates in CD mode throughout the drive cycle and Figure 4.1 shows EV operating modes during the drive cycle. To provide instant torque [17], EV2 mode operates and then vehicle runs in EV1 mode as MGB operation is enough to fulfill axle torque request. Figure 4.2 shows MGB operating points at different EV modes. MGB is mostly provided torque (positive torque) during propulsion and also charging (negative torque) the battery through regeneration. Figure 4.3 shows MGA is mostly off during the drive cycle and only assisting MGB during vehicle startup.

Figures 4.4, 4.5, 4.6 and 4.7 show modes during UDDS drive cycle, MGB operating points on MGB efficiency map for different modes, MGA operating points on MGA efficiency map for different modes and engine operating points on BSFC map (BSFC map was created by extracting data from [17]).

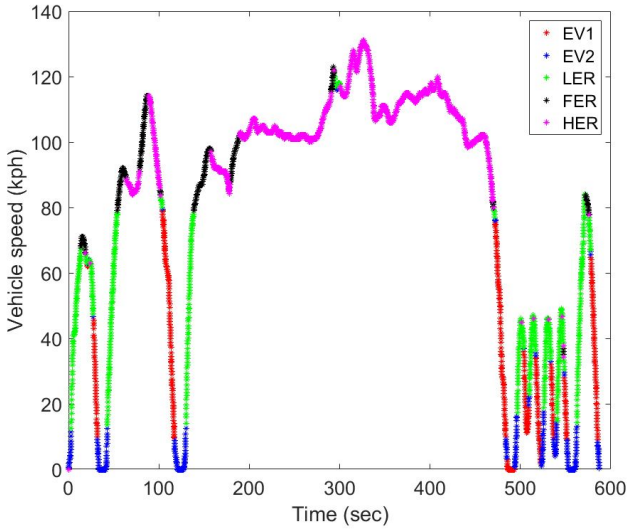

Figure 4.4: Vehicle speed versus time showing five operating modes for US06 drive cycle . Test details are provided in Appendix B.10 (Filename: 61607019.mat)

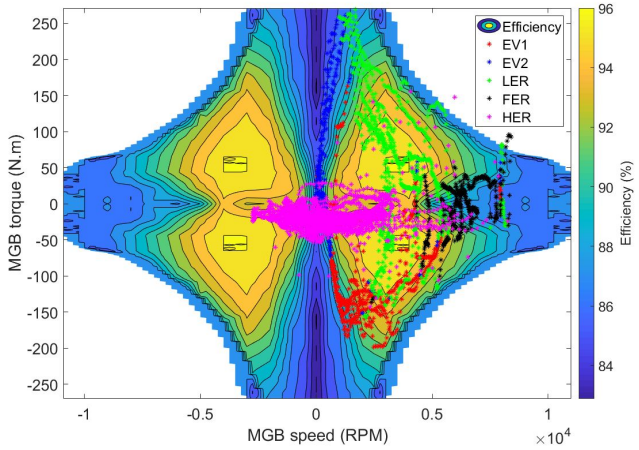

Figure 4.5: MGB Operating points on MGB efficiency map with five operating modes for US06 drive cycle. Test details are provided in Appendix B.10 (Filename: 61607019.mat)

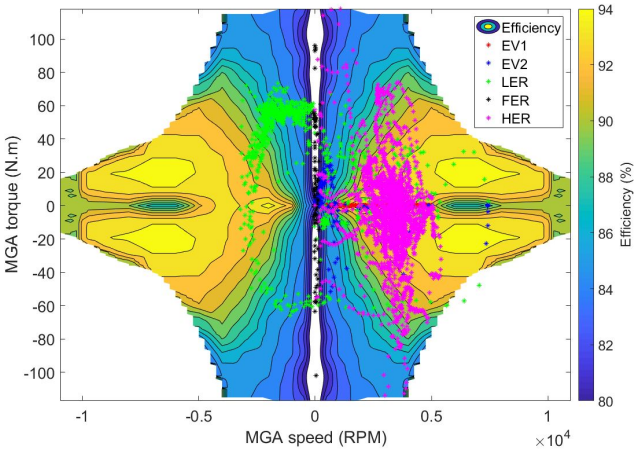

Figure 4.6: MGA Operating points on MGA efficiency map with five operating modes for US06 drive cycle. Test details are provided in Appendix B.10 (Filename: 61607019.mat)

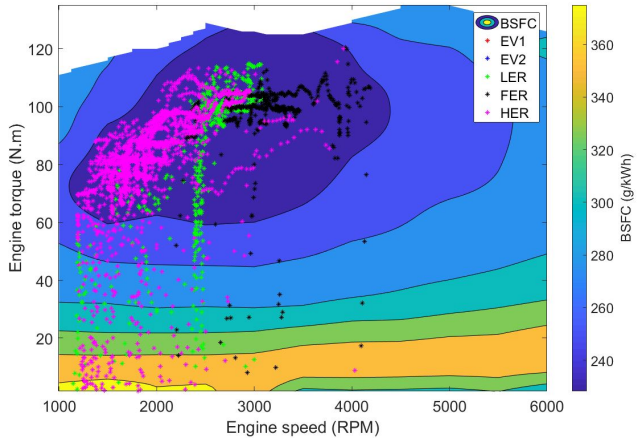

Figure 4.7: Engine Operating points on Engine BSFC map with five operating modes for US06 drive cycle. Test details are provided in Appendix B.10 (Filename: 61607019.mat)

Figure 4.4 shows vehicle is operating in CS mode during the drive cycle. From Figure 4.4 we can infer that vehicle starts EV1 or EV2 mode due to light loads and low velocity [17], and regeneration being carried out in EV1 mode. It shows LER mode being used for propulsion at low velocity (20 to 80 kmph). It also shows FER mode operating at high vehicle speed to provide acceleration and HER mode operating at high cruising velocities [17]. Figure 4.5 shows MGB mostly regenerating during HER mode and propelling the vehicle in LER mode. All the operating points are located in efficient operating zones of MGB. Figure 4.6 shows MGA assisting engine for propulsion and also regenerating in the HER mode. Figure 4.7 shows engine operating points during the drive cycle. It can be seen that all the CS operating modes are very well located in efficient BSFC region. This infers that engine has been calibrated to work in efficient zones for the desired vehicle speed and torque requests. Since in FER mode, engine is providing all power for propulsion, the operating points

during this mode are located at higher engine speed range compared to HER mode.

4.2 Analysis of fuel consumption during engine transients

To implement energy management control strategy, it is important to work on a high fidelity model, which includes dynamics. Such model will help in accurate prediction of energy consumption for varying vehicle conditions. The model developed in this work consists of map based TPIM and motor generator models as losses due to dynamics in these electric machines don't affect the final energy consumption by considerable amount. Whereas in engine, dynamics play an important role in determining overall energy consumption. Since brake fuel conversion efficiency is significantly smaller compared to combined efficiency of motor generator and TPIM, an engine dynamic model is necessary to develop and incorporate in vehicle controller to know associated penalty for command changes in powertrain / engine operating conditions. Furthermore, there is a fuel penalty associated to each engine transient operation. Figure 4.8 shows experimental data of engine transient operation. This transient operation causes fuel penalty due to transient control action to reach the resultant engine torque[37].

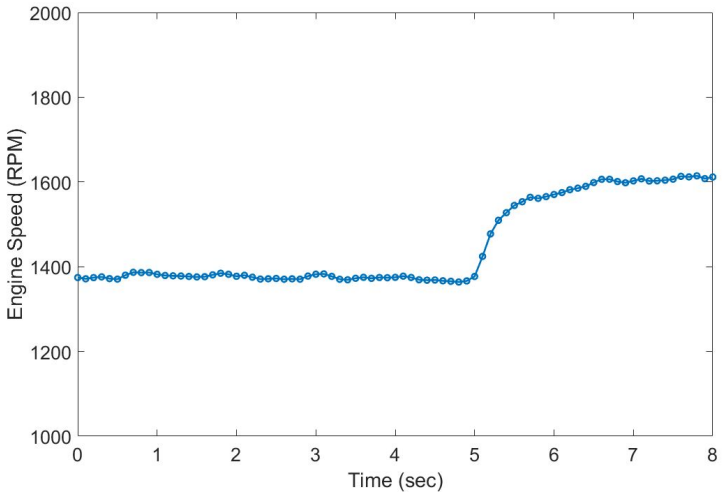

(a) Transient operation of engine speed

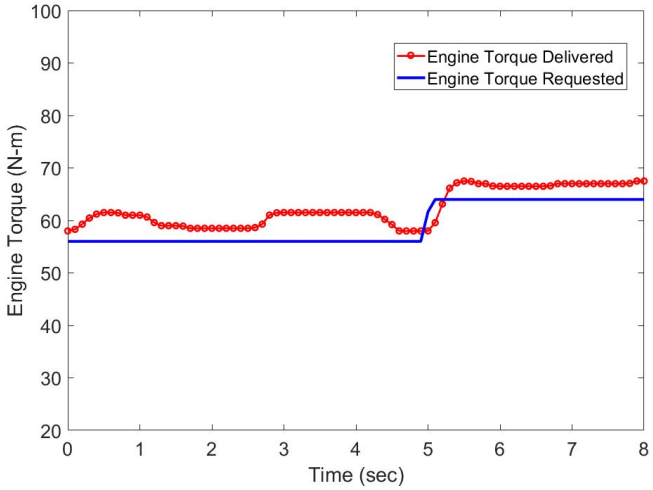

(b) Transient operation of engine torque

Figure 4.8: Transient operation of engine causing fuel penalty of 0.52 grams

Figure 4.9 shows all the operating points of the engine in the test data provided by ANL. To analyze fuel penalty between each operating point, it is necessary to have a dynamic engine model which has the capability to predict such transient behavior.

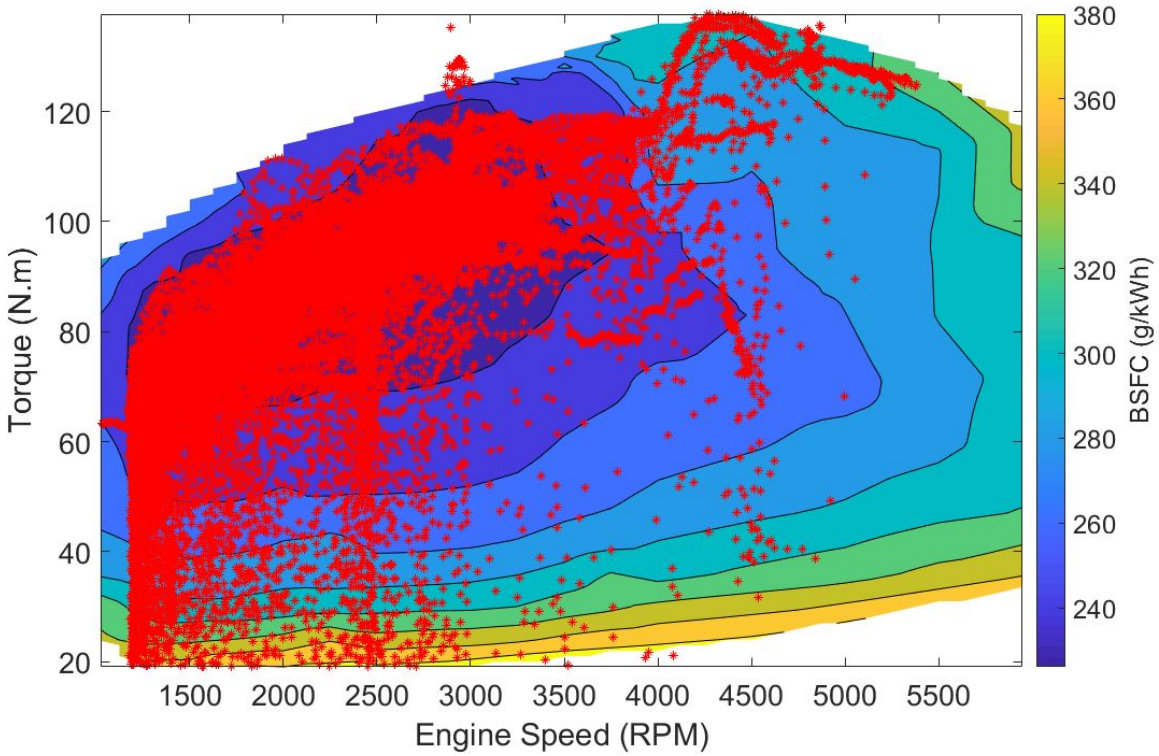

Figure 4.9: Operating points of engine on BSFC map [17] using the ANL test data

Transient fuel penalty analysis was carried out by giving a step torque command from 50 N to 60 N and Figure 4.10 shows torque response and commanded throttle position for this step input. A fuel penalty of 0.054 grams was observed for this step change in engine torque.

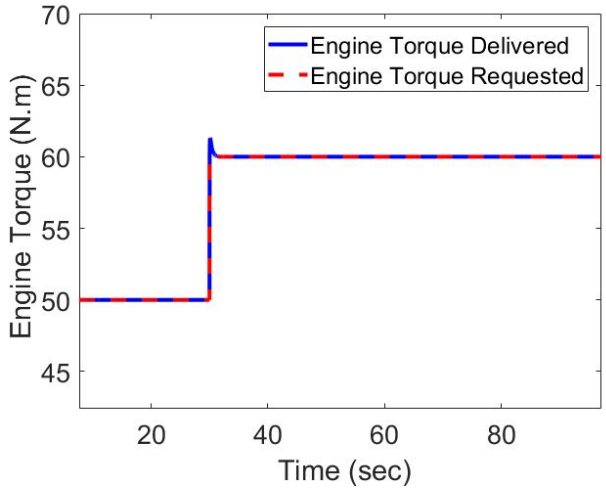

(a) Response of engine torque for step torque request

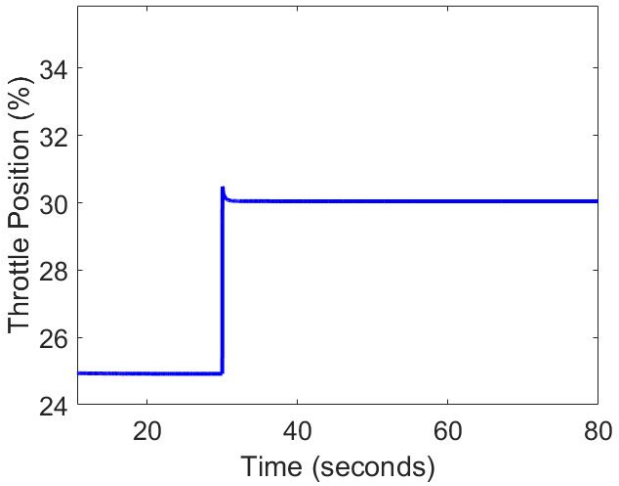

(b) Commanded throttle position for step torque request

Figure 4.10: Transient response of engine for step torque request

Such simulation tests can be used to generate a fuel penalty lookup map which can be utilized for HEV energy management controller, and also developing a simplified engine model to predict fuel consumption during engine transients. Figures 4.11 show transient fuel penalty plot for a step response of engine model for a specific initial condition. Figure 4.12 shows transient fuel penalty map for average change in speed

(Δ Engine Speed) and torque (Δ Engine Torque).

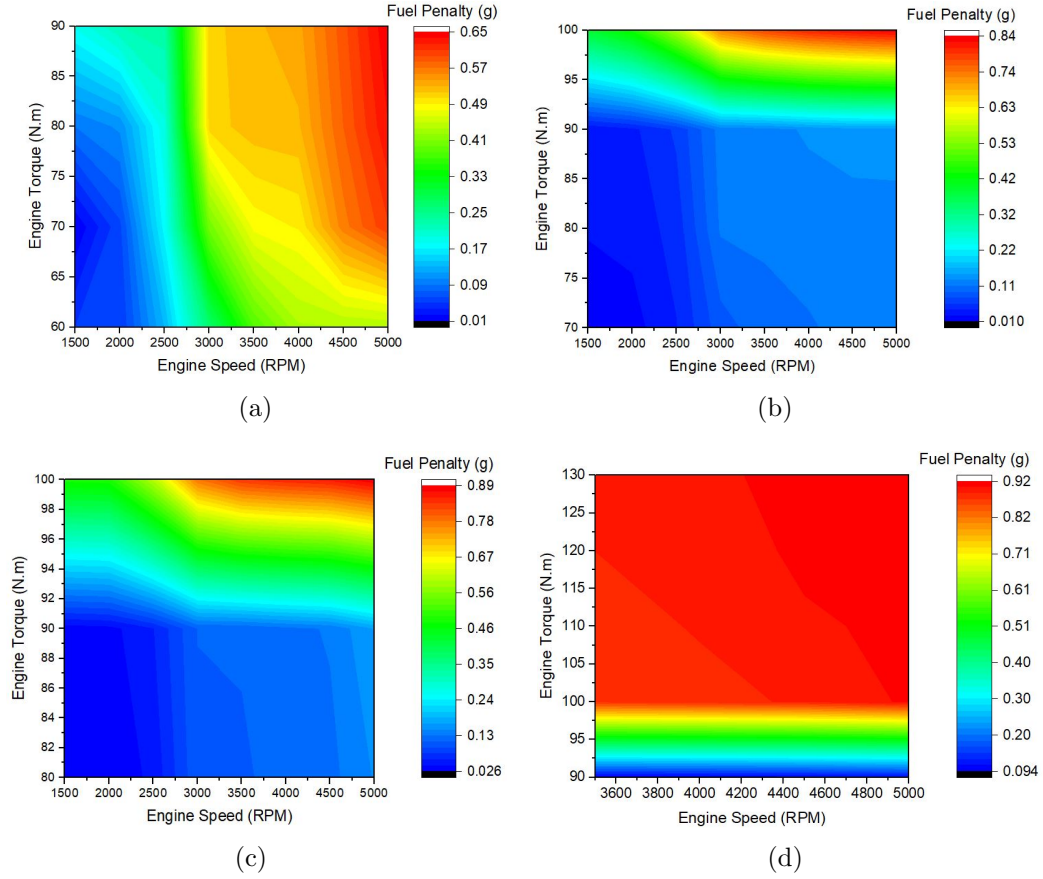

Figure 4.11: Fuel penalty due to transients with initial conditions (a) Engine torque = 50 Nm and engine speed = 1000 RPM; (b) Engine torque = 60 Nm and engine speed = 1000 RPM; (c) Engine torque = 70 Nm and engine speed = 1000 RPM; (d) Engine torque = 80 Nm and engine speed = 1000 RPM

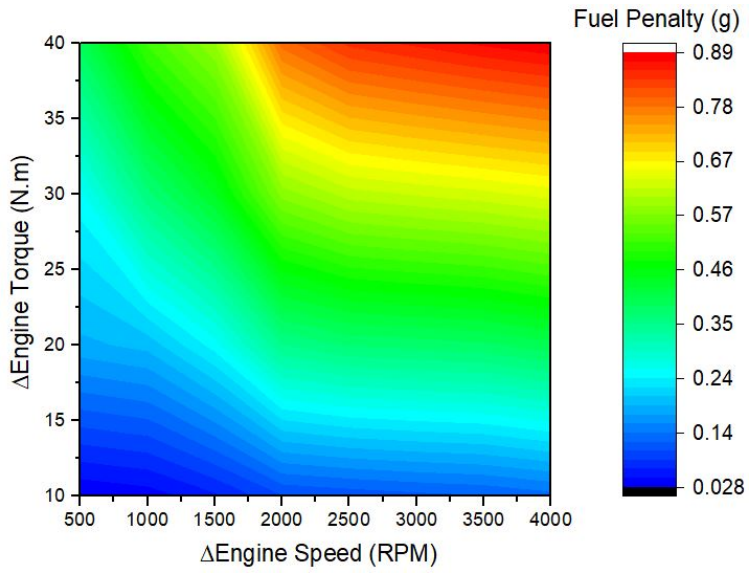

Figure 4.12: Average fuel penalty map for Δ Engine Torque and Δ Engine Speed change in engine operating conditions

To predict engine transient fuel penalty, a lookup map can be generated out of the average fuel penalty map (shown in Figure 4.12) and can be incorporated in static map based engine model. This will make the model give same output as a dynamic engine model, predicting transient fuel penalties. This makes engine model simple, computationally efficient and enables vehicle energy management controller to optimally select engine operating modes and minimize engine transients. Though average fuel penalty map is good predictor of engine transient fuel penalties, it has few uncertainties:

† Same Δ input change in speed and torque does not have close fuel penalties

† Average value of same Δ input change has been considered which is not an accurate method

Table 4.1 shows uncertainties in average fuel penalty map.

Table 4.1
Uncertainties in average fuel penalty map

Δ Engine Speed (RPM)	**Δ Engine Torque (N)**	**Uncertainty (%)**
500-1500	10-40	3
2000-4000	40-60	5

4.3 Mode switch penalties

Vehicle components require extra energy to perform mode transition. If this energy penalty information is known, strategies can be incorporated in the supervisory controller to minimize such energy penalties and optimize energy consumption. During mode transition, test data of auxiliary pump showed an instant increase (spike) in auxiliary pump power for few seconds. This spike in power corresponds to mode switch penalty and has been incorporated in auxiliary pump model. Furthermore, engine fuel penalties discussed in Chapter 3 takes place whenever engine is turned on (vehicle switches from two motor EV mode to LER mode). Figure 4.13 shows mode switch penalties flow chart which have been incorporated in the model.

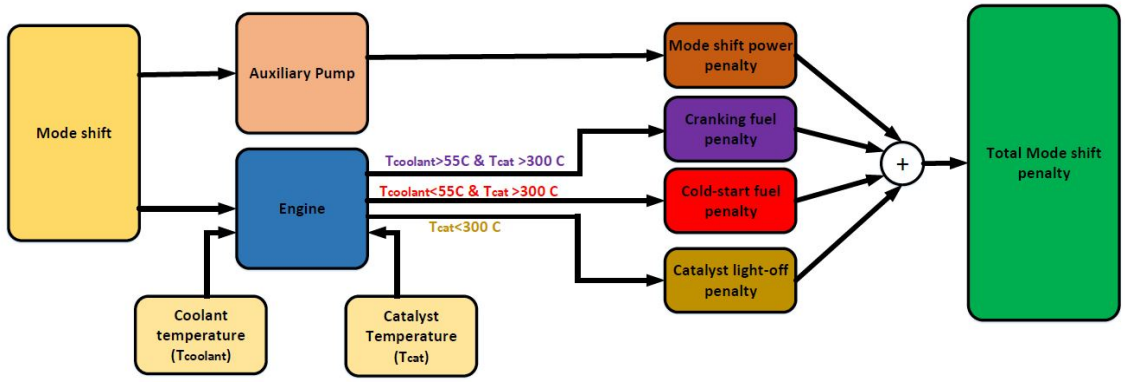

Figure 4.13: Flowchart showing mode shift penalty

Figures 4.14 and 4.15 show energy penalty caused to due to mode transition in auxiliary pump model and engine fuel penalty caused due to cranking, cold-start and catalyst light off. Cold-start and cranking fuel penalties are coolant temperature dependent and maximum value of corresponding energy penalties is shown in the Figures 4.15(a) and 4.15(c).

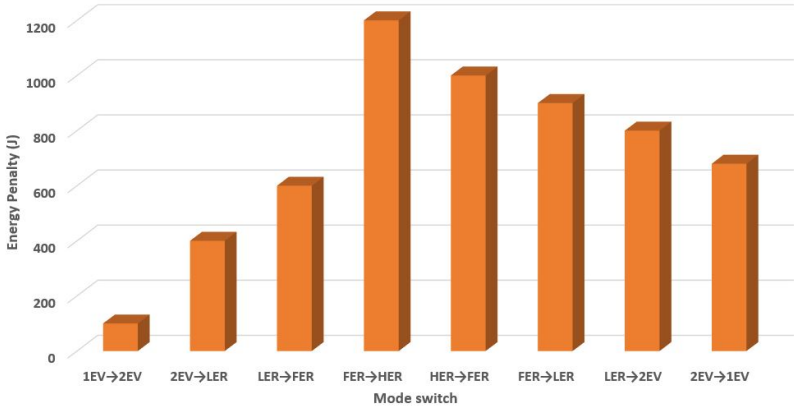

Figure 4.14: Mode switch energy penalty of auxiliary pump

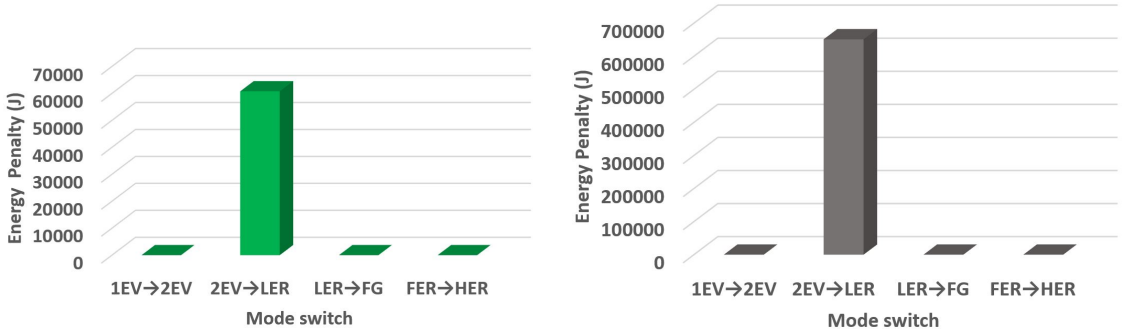

(a) Cold-start energy penalty

(b) Catalyst light-off energy penalty

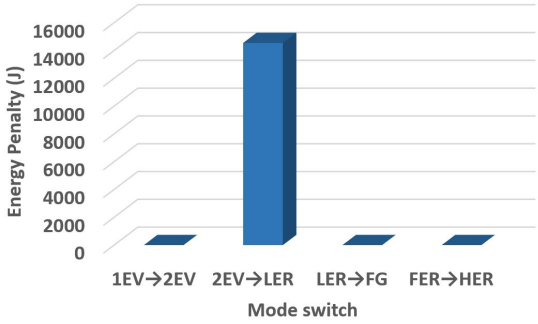

(c) Cranking energy penalty

Figure 4.15: Mode switch energy penalty of engine startup

Figures 4.14 and 4.15 show mode switch energy penalties which can play an important role in determining mode switches in the vehicle and help in reduction of energy consumption. Supervisory controller can be embedded with such strategies and will be essential in optimized propulsion of HEVs. Fuel penalty due to cranking is dependent on coolant temperature and engine speed requested. Figure 4.16 shows cranking fuel penalty (in grams) depending on coolant temperature and engine speed. As discussed earlier, this fuel penalty occurs during two motor EV to LER mode switch.

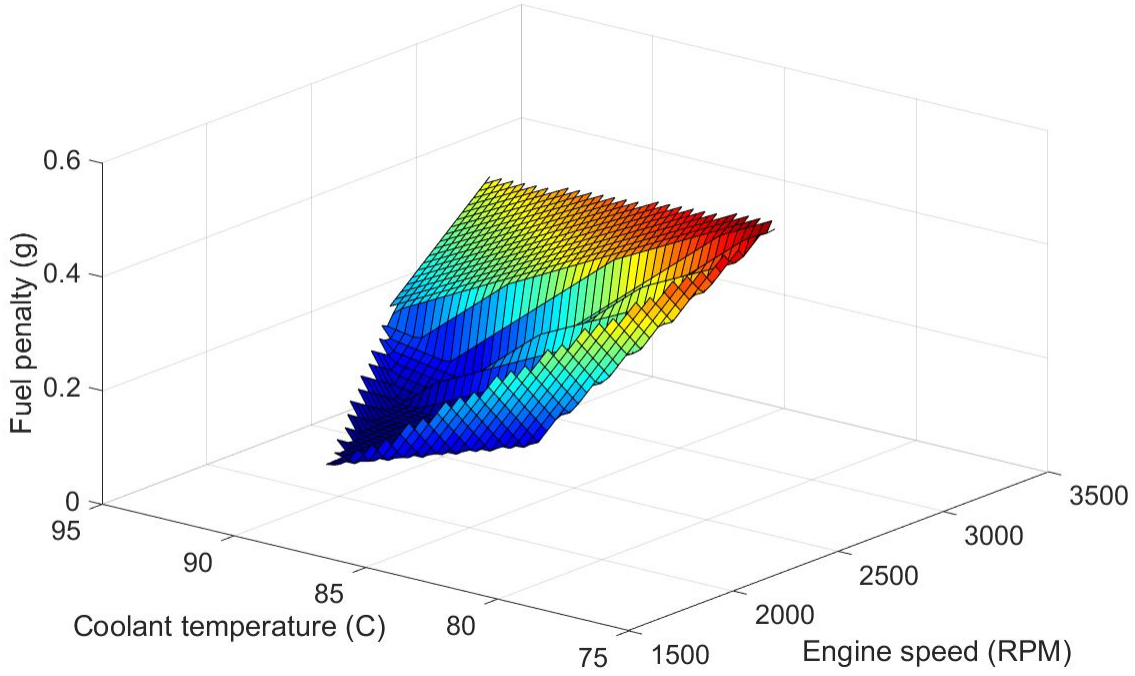

Figure 4.16: Cranking fuel penalty function of engine speed and coolant temperature

From Figure 4.16, it is evident that as startup engine speed is high or initial startup coolant temperature is low, cranking fuel penalty is high.

Chapter 5

Conclusion and Future Works

5.1 Conclusion

A Simulink/ MATLAB based model of Chevy Volt GEN II was developed using experimental data, ANL experimental data and maps/ parameters provided by GM. Few subsystems were developed through data analysis of ANL test data and others through in-vehicle testing conducted at APSRC. Model validation was performed using test data provided by ANL. The work done in this thesis is summarized as follows:

† A dynamic ICE model was developed which included air flow dynamics, torque generation, rotational dynamics, EGR subsystem, engine torque control and engine fuel penalty terms.

† In-vehicle testing was performed to understand the engine fuel penalties (Catalyst light–off , cold–start, cranking) based on engine temperature (TWC and coolant temperature) conditions and a rule based controller was developed to enhance accuracy of fuel consumption prediction.A simple lumped coolant model was developed to predict coolant temperature which would be necessary in order to predict engine startup fuel penalties.

† Map based electric motor (MGA and MGB) models, traction power inverter module (TPIM) models, lithium-ion battery model and transmission model consisting two planetary gears were created.

† Transmission auxiliary pump model predicting auxiliary pump power was developed using linear regression tool and experimental data.

All the subsystems were initially validated separately and then integrated in the vehicle model. The vehicle model, with all the major subsystems, was validated with ANL experimental test data for two charge sustaining (CS) and two charge depleting (CD) drive cycles. The developed model shows good accuracy in predicting vehicle energy consumption. Overall,the total error between the energy consumption of model with that of test data is well within 5 % for the tested drive cycles. This level of model

accuracy is suitable for MPC implementation in the NEXTCAR Project which aims to minimize energy consumption by 20 %.

Further, importance of engine dynamics model was analyzed and corresponding fuel penalties during transient operation, which a map based model is unable to predict, were analyzed. Maps describing fuel penalty based on mode transients in engine were developed which can be incorporated along with steady–state engine model, giving output as a dynamic model. This simplified computationally efficient model would be of utility for use in vehicle energy management controller to optimally choose engine operating mode and properly minimize engine transients with high fuel penalty.

5.2 Future Works

† Battery temperature plays an important role in battery performance.Since SOC, OCV, resistances and capacitances are all temperature dependent parameters, it is important to incorporate battery thermal model which predicts battery temperature. Moreover, battery temperature is not allowed to operate outside a certain temperature range as it hampers battery's performance. Hence a high voltage battery heating / cooling system can be incorporated in Chevy volt GEN II vehicle model.

† Heating, ventilation, and air conditioning (HVAC) is also a major energy consuming system in a vehicle that should be incorporated in the model to improve accuracy of energy consumption.An HVAC model can be incorporated in the vehicle to decide cabin heating and cooling strategies which will play an integral role in energy consumption reduction in Chevy Volt Gen II.

† Current vehicle model needs commanded MGB torque, engine torque, operating mode and MGA speed as inputs. To make the model independent and run with given vehicle velocity as input, one needs to add vehicle rule based control strategies to predict vehicle energy consumption.

† The developed model needs to be validated for broad operating conditions. This will require collecting vehicle data for various driving conditions.

† Currently friction braking is obtained from ANL test data. The model needs to predict friction braking by its own depending on the rule incorporated in the vehicle.

† Spin-losses play an important role in determining axle torque. Spin-losses depend on drive unit line pressure and transmission oil temperature. Models to predict oil temperature and line pressure will be developed to estimate spin-losses in the vehicle.

† To enhance energy prediction, it is important to incorporate electrical losses in the vehicle that occur during mode transition. Mode transition electrical losses will be incorporated in future.

References

[1] United States Environmental Protection Agency. "Green Vehicle Guide". 2017.

[2] Aaron Hula, Amy Bunker, Andrea Maguire, and Jeff Alson. "Light-Duty Automotive Technology, Carbon Dioxide Emissions, and Fuel Economy Trends: 1975 Through 2017". 2018.

[3] Namdoo Kim, Michael Duoba, Namwook Kim, and Aymeric Rousseau. "Validating Volt PHEV model with dynamometer test data using Autonomie". *SAE Int. J. Passeng. Cars - Mech. Syst*, 2013.

[4] Namwook Kim, Aymeric Rousseau, Daeheung Lee, and Henning Lohse-Busch. "Thermal Model Development and Validation for 2010 Toyota Prius". *SAE Technical Paper*, doi:10.4271/2014-01-1784, 2014.

[5] Jinming Liu and Huei Peng. "Modeling and Control of a Power-Split Hybrid Vehicle". *IEEE TRANSACTIONS ON CONTROL SYSTEMS TECHNOLOGY*, 16, 2008.

[6] B.K.Powell, K.E.Bailey, and S.R.Cikanek. "Dynamic modeling and control of hybrid electric vehicle powertrain systems". *IEEE*, 1998.

[7] Olivier Tremblay and Louis-A. Dessaint. "Experimental Validation of a Battery Dynamic Model for EV Applications". *World Electric Vehicle Journal*, 3, 2009.

[8] H Yeo and H Kim. "Hardware-in-the-loop simulation of regenerative braking for a hybrid electric vehicle". *Proc Instn Mech Engrs*, 216, 2002.

[9] Rui Xiong, Hongwen He, Fengchun Sun, and Kai Zhao. "Online Estimation of Peak Power Capability of Li-Ion Batteries in Electric Vehicles by a Hardware-in-Loop Approach". *Energies*, doi:10.3390/en5051455, 2012.

[10] Rui Xiong, Yanzhou Duan, Jiayi Cao, and Quanqing Yu. "Battery and ultracapacitor in-the-loop approach to validate a real-time power management method for an all-climate electric vehicle". *Applied Energy*, 2018.

[11] K. B. Wipke, M. R. Cuddy, and S. D. Burch. "BADVISOR 2.1: A user-friendly advanced powertrain simulation using a combined backward/forward approach". *EEE Trans. Vehicular Technol.*, 48, 1999.

[12] Jongryeol JEONG, Sungwook Choi, Namdoo Kim, Heeyun Lee, Kevin Stutenberg, and Aymeric Rousseau. "Model Validation of the Chevrolet Volt 2016". *SAE International*, doi:10.4271/2018-01-0420, 2018.

[13] L. Guzzella and A. Sciarretta. "Vehicle Propulsion Systems". *Springer*, ISBN: 978-3-642-35912-5, 2013.

[14] https://pluginamerica.org/plug-in-vehicle/chevrolet-volt/. .

[15] https://www.youtube.com/watch?v=8PSIzRQJQ2Y. .

[16] Weichao Zhuang, Liangmo Wang, Xiaowu Zhang, Daofei Li, and Yin. "Mode shift map design and integrated energy management control of a multi-mode hybrid electric vehicle". *Applied Energy*, 10.1016/j.apenergy.2017.07.059, 2017.

[17] Brendan M. Conlon, Trevor Blohm, Michael Harpster, Alan Holmes, Margaret Palardy, Steven Tarnowsky, and Leon Zhou. "The Next Generation Voltec Extended Range EV Propulsion System". *SAE Int. J. Alt. Power*, 0.4271/2015-01-1152, 2015.

[18] "Chevrolet Product Information". *media. chevrolet. com*, 2015.

[19] . *https: // www. getahelmet. com/ jeeps/ maint/ dexcool/*, .

[20] Office of Transportation and Air Quality U.S. Environmental Protection Agency. "Draft Technical Assessment Report: Midterm Evaluation of Light-Duty Vehicle Greenhouse Gas Emission Standards and Corporate Average Fuel Economy Standards for Model Years 2022-2025". *https: // www. nhtsa. gov/ sites/ nhtsa. dot. gov/ files/ draft-tar-final. pdf*, 2016.

[21] United States Environmental Protection Agency. "Light-Duty Vehicle CO2 and Fuel Economy Trends". pages `https://www.epa.gov/fuel--economy--trends`, 2017.

[22] J HEYWOOD. *INTERNAL COMBUSTION ENGINE FUNDAMENTALS*. MCGRAW-HILL EDUCATION, 2018.

[23] M. Shahbakhti A. Sahraeian, S.A. Jazayeri A. R. Aslani, S. Azadi, and A. H. Shamekhi. "Longitudinal Vehicle Dynamics Modeling on the Basis of Engine Modeling". *SAE Technical Paper Series*, 10.4271/2004-01-1620, 2004.

[24] Michael Fons, Martin Muller, Alain Chevalier, Christian Vigild, Elbert Hendricks, and Spencer C. Sorenson. "Mean Value Engine Modelling of an SI Engine with EGR". *SAE Technical Paper Series*, 10.4271/1999-01-0909, 1999.

[25] Elbert Hendricks and Spencer C. Sorenson. "Mean Value Modelling of Spark Ignition Engines". *SAE Technical Paper Series*, 10.4271/980784, 1998.

[26] Seyed Ali Jazayeri, Mohammad Sharifi Rad, and Shahram Azadi. "Development and Validation for Mean Value Engine Models". *SAE Technical Paper Series*, 2005.

[27] John J Moskwa. *"Automotive engine modeling for real time control"*. Massachusetts Institute of Technology, Massachusetts Institute of Technology. Dept. of Mechanical Engineering, 1988.

[28] Jeffrey Jocsak, David White, Cedric Armand, and Richard S. Davis. "Development of the Combustion System for General Motors' High-Efficiency Range Extender Ecotec Small Gas Engine". *SAE International Journal of Engines*, 10.4271/2015-01-1272, 2015.

[29] Martin Mller, Peter M. Olin, and Bart Schreurs. "Dynamic EGR Estimation for Production Engine Control". *SAE Technical Paper Series*, 10.4271/2001-01-0553, 2001.

[30] Andrew Roberts, Richard Brooks, and Philip Shipway. "Internal combustion engine cold-start efficiency: A review of the problem, causes and potential solutions". *Energy Conversion and Management*, 2014.

[31] Forrest Jehlik, Eric Rask, and Martha Christenson. "Simplified Methodology for Modeling Cold Temperature Effects on Engine Efficiency for Hybrid and Plug-in Hybrid Vehicles". *SAE Technical Paper Series*, 10.4271/2010-01-2213, 2010.

[32] Sinisa Jurkovic, Khwaja Rahman, Nitin Patel, and Peter Savagian. "Next Generation Voltec Electric Machines; Design and Optimization for Performance and Rare-Earth Mitigation". *SAE Int. J. Alt. Power*, doi:10.4271/2015-01-1208, 2015.

[33] Mohammad Anwar, Monty Hayes, Anthony Tata, Mehrdad Teimorzadeh, and Thomas Achatz. "Power Dense and Robust Traction Power Inverter for the

Second-Generation Chevrolet Volt Extended-Range EV". *SAE Int. J. Alt. Power*, doi:10.4271/2015-01-1201, 2015.

[34] Knauff, M McLaughlin, Jeffrey Dafis, Chris Niebur, Dagmar Singh, Pritpal Kwatny, Harry, Nwankpa, and Chika. "Simulink Model of a Lithium-Ion Battery for the Hybrid Power System Testbed". *Research Gate*, `https://www.researchgate.net/publication/253731796`, 2018.

[35] Xiaowu Zhang. 'Design of Power Split Hybrid Powertrains with Multiple Planetary Gears and Clutches". 2015.

[36] The Chevrolet Volt Cooling/Heating Systems Explained. *http://gm-volt.com*, 2017.

[37] M. Shahbakhti, M. Ghafuri, A. Sahraeian, S. A. Jazayeri, and S. Azadi. "A Method to Determine Fuel Transport Dynamics Model Parameters in Port Fuel Injected Gasoline Engines During Cold Start and Warm- Up Conditions". *Journal of Engineering for Gas Turbines and Power*, 10.1115/1.4000150, 2010.

[38] Manfred Przybilla, Christian Kunze, Serdar Celik, and Shachindra Dongaonkar. "Combined Simulation Approach For Dry Clutch Systems". *SAE International*, doi:10.4271/2011-01-1232, 2011.

[39] Charles R. Cornell. "Dynamic Simulation of a Hydrostatically Propelled Vehicle". *SAE Technical Paper Series*, doi:10.4271/811253, 1981.

[40] Autonomie. *https://www.autonomie.net/expertise/Autonomie.html*, 2017.

[41] NamdooKim, Neeraj Shidore, and Aymeric Rousseau. "Sizing Algorithm Validation for Several Vehicle Powertrains". 2017.

[42] Namdoo Kim, Michael Duoba, Namwook Kim, and Aymeric Rousseau. "Validating Volt PHEV Model with Dynamometer Test Data Using Autonomie". *SAE Int. J. Passeng. Cars - Mech. Syst.*, doi:10.4271/2013-01-1458, 2013.

[43] Namwook Kim, Jongryeol Jeong, Aymeric Rousseau, and Henning Lohse-Busch. "Control Analysis and Thermal Model Development for Plug-In Hybrid Electric Vehicles". *SAE Int. J. Alt. Power*, doi:10.4271/2015-01-1157, 2015.

[44] Tiegang Hu, Yanjv Wei, Shenghua Liu, and Longbao Zhou. "Improvement of Spark-Ignition (SI) Engine Combustion and Emission during Cold Start, Fueled with Methanol/Gasoline Blends". *Energy and Fuels*, 10.1021/ef0603479, 2007.

[45] Dr. Darrell Robinette and Dr. John Beard. "Introduction to Propulsion Systems and HEV: Lecture 37". 2017.

Appendix A

Experimental Study

A.1 Experimental data fuel penalty

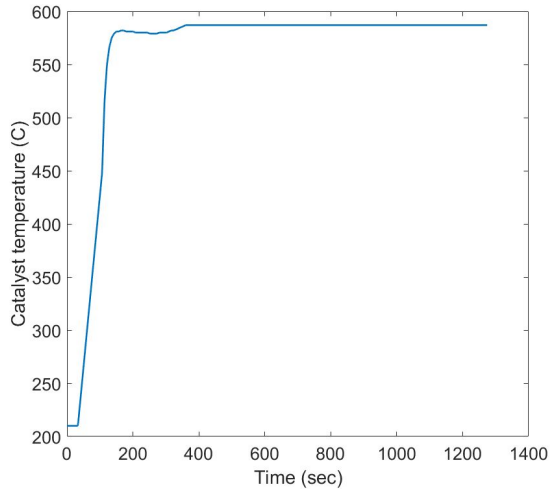

(a) Catalyst temperature Vs Time

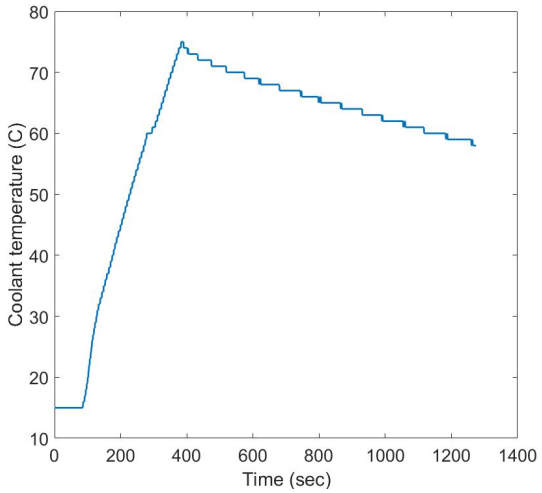

(b) Coolant temperature Vs Time

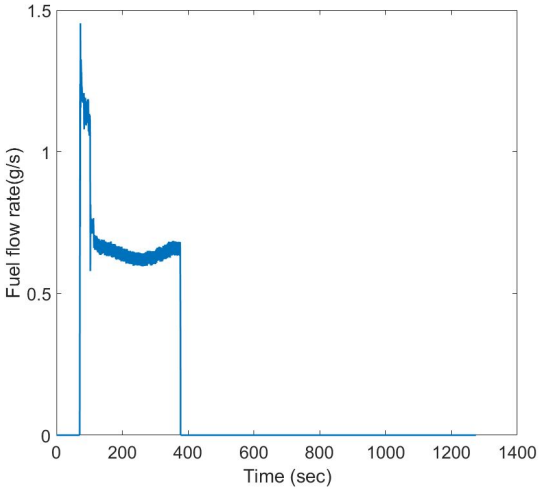

(c) Fuel flow rate Vs Time

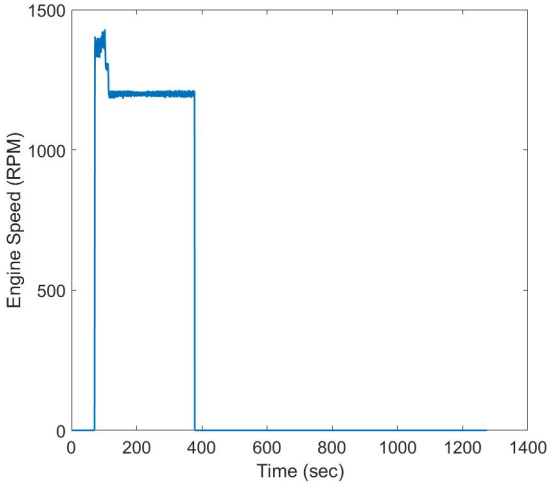

(d) Fuel flow rate Vs Time

Figure A.1: Data acquired for coldstart and catalyst lightoff conditions

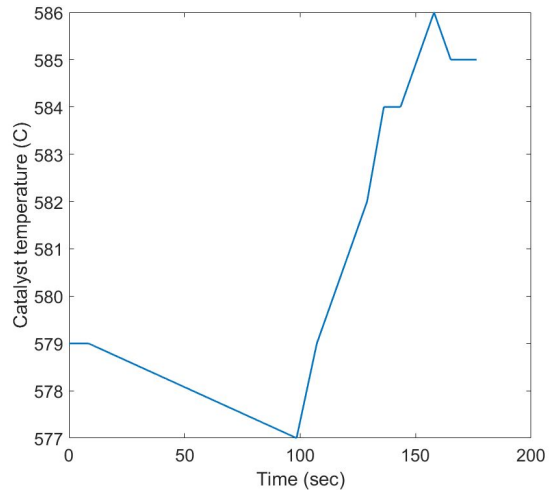

(a) Catalyst temperature Vs Time

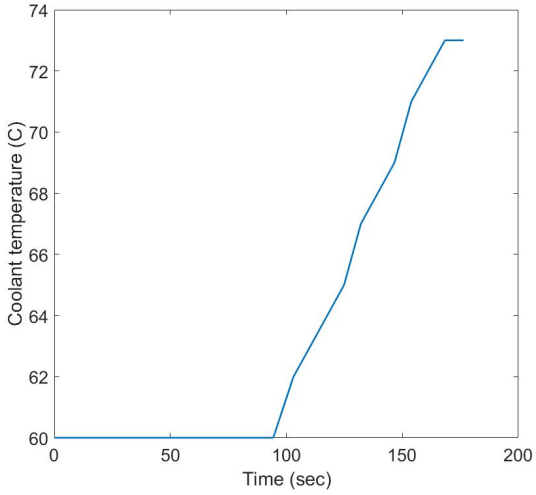

(b) Coolant temperature Vs Time

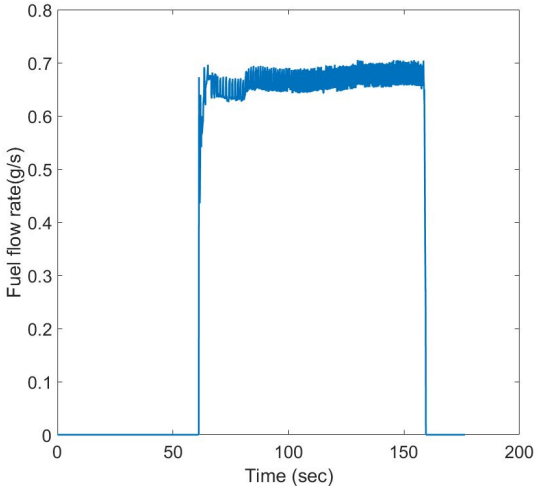

(c) Fuel flow rate Vs Time

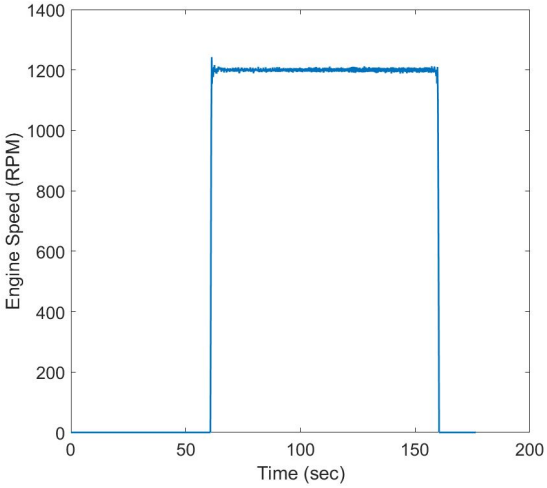

(d) Fuel flow rate Vs Time

Figure A.2: Data acquired for completely warmed up engine with only cranking fuel penalty

A.2 Specifications of Chevy Volt Gen II

Chevrolet Product Information

2016 CHEVROLET VOLT SPECIFICATIONS

Overview

Model:	Chevrolet Volt
Body style / driveline:	front-wheel-drive, five-door/five-passenger hatchback extended-range electric vehicle
Construction:	single body-frame-integral (unibody) with front and rear crumple zones; galvanized steel front fenders; hood, roof, door panels; one-piece bodyside outer panel; thermal plastic olefin (TPO) bumper fascias
EPA vehicle class:	compact car
Key competitors:	Toyota Prius Plug-in, Ford C-Max energi, clean diesels, mid-luxury sport sedans
Vehicle manufacturing location:	Detroit-Hamtramck Assembly, Hamtramck, Mich.
Battery manufacturing location:	Brownstown Township, Mich.

Battery system

Type:	rechargeable energy storage system comprising multiple linked modules
Size/case:	5.5-foot-long T-shaped; glass-filled polyester structural composite with aluminum thermal radiation shield and steel
Mass (lb / kg):	405 / 183
Battery chemistry:	lithium-ion
Thermal system:	liquid active thermal control
Cells:	192 prismatic
Combined electric/extended driving range (miles / km):	420 / 676 (estimate including EV on fully charged battery and full tank of fuel
Warranty:	eight years / 100,000 miles (10 years / 100,000 miles in ARB states)
Energy:	18.4 kWh

Engine

Type:	1.5L DOHC I-4
Displacement (cu in / cc):	91 / 1490
Bore & stroke (in / mm):	2.90 x 3.40 / 74 x 86.6
Block material:	cast aluminum
Cylinder head material:	cast aluminum
Valvetrain:	overhead camshafts; four valves per cylinder, continuously variable intake and exhaust cam phaser
Ignition system:	individual coil-on-plug
Fuel delivery:	direct injection with electronic throttle control
Compression ratio:	12.5:1
Output (kW / hp @ rpm):	75 / 101 @ 5600
Max engine speed (rpm):	5600
Emissions controls:	close-coupled catalytic converters; 58x ignition system; returnless fuel rail; fast light-off O2 sensor
Fuel type:	regular unleaded
EPA-estimated fuel economy (combined city / hwy):	42 mpg 106 mpg-e

Chevrolet Product Information

Electric drive

Type:	electric, two-wheel, front-drive
Motors (two):	twin-motor arrangement, 110 kW
Transaxle:	Voltec electric drive system
Power (kW / hp):	111 / 149
Torque: (lb-ft / Nm):	294 / 398

Charging times

120 V:	about 13 hours (based on charge level and outside temperature)
240 V:	about 4.5 hours (actual charge times may vary)

Performance

Top speed (mph):	98 (electronically limited)
0-60 mph:	8.4 sec.
EV range (city):	53 miles / 85 km (based on estimated fuel economy)
EV / extended range:	420 miles / 675 km including EV on fully charged battery and full tank of fuel

Chassis / Suspension

Front:	independent MacPherson strut-type with side-loaded strut modules, specially tuned coil springs, direct-acting hollow stabilizer bar; hydraulic ride bushings
Rear:	specially adapted compound crank (torsion beam) with double-walled, U-shaped profile at the rear; specifically tuned coil springs, hydraulic bushings
Chassis control:	four-channel ABS; all-speed traction control; StabiliTrak; drag control
Steering type:	rack-mounted electric power steering with ZF steering gear
Steering wheel turns, lock-to-lock:	3
Turning circle, curb-to-curb (ft / m):	36.4 / 11.1
Steering ratio:	15.7

Brakes

Type:	power four-wheel vented disc with ABS; electro-hydraulic; fully regenerative to maximize energy capture; dynamic rear brake proportioning
Brake rotor diameter front (in / mm):	11 / 276; vented, single 60-mm piston w/ steel body caliper
Brake rotor diameter rear (in / mm):	10 / 264; solid; steel body caliper with single 38-mm piston, with park brake motor on caliper
Total swept area (cu cm):	front: 350 rear: 277

Wheels / Tires

Wheel size and type:	17-in. 5-spoke painted aluminum wheels 17-in. Split-Y Ultra Bright Machined aluminum wheels with painted pockets
Tires:	Michelin Energy Saver A/S 215/50R17 all-season

Chevrolet Product Information

Dimensions

Exterior

Wheelbase (in / mm):	106.1 / 2694
Overall length (in / mm):	180.4 / 4582
Overall width (in / mm):	71.2 / 1809
Height (in / mm):	56.4 / 1432
Track front (in / mm):	60.6 / 1540 (front) 61.8 / 1570 (rear)

Interior

Seating capacity (front / rear):	2 / 3
Headroom (in / mm):	37.8 / 961 (front) 35.8 / 909 (rear)
Shoulder room (in / mm):	56.5 / 1434 (front) 53.2 / 1351 (rear)
Hip room (in / mm):	53.7 / 1365 (front) 51.3 / 1304 (rear)
Legroom (in / mm):	42.1 / 1068 (front) 34.7 / 882 (rear)
Cargo volume (cu ft / L):	10.6 / 301

Capacities

Curb weight (lb / kg):	3543 / 1607
Generator cooling (qt / L):	7.4 / 7.0
Battery pack cooling (qt / L):	4.5 / 4.25
Power electronics cooling (qt / L):	5.1 / 4.8
Fuel tank (gal / L):	8.9 / 33.7
Engine oil w/ filter (qt / L):	4.2 / 4
Drive unit fluid (qt / L):	7.1 / 6.7 (including cooling loop)

Note: Information shown is current at time of publication. Please visit our GM Media web site at http://media.gm.com for updates.

A.3 Specifications of Vector CANoe VN5610A

VECTOR

Technical Data VN5610A/VN5640

	VN5610A	VN5640
Ethernet: Channels/transceiver	2x BCM89811, 2x BCM54810 (selectively 2 usable)	12x NXP TJA1100, 4x Atheros AR8031
Ethernet: Physical layer	100BASE-T1 (BroadR-Reach) and 10BASE-T/100BASE-TX/1000BASE-T	
Ethernet: Connectors	2x RJ45 for 10BASE-T/100BASE-TX/1000BASE-T 1x D-SUB9 for 100BASE-T1 (BroadR-Reach; dual channel)	4 x RJ45 for 10BASE-T/100BASE-TX/1000BASE-T 6 x D-SUB9 for 100BASE-T1 (BroadR-Reach; dual channel)
Ethernet: Baudrates	10 Mbit/s, 100 Mbit/s, 1000 Mbit/s	
CAN (FD): Cannels/transceiver	2 x NXP TJA1051	
CAN (FD): Physical layer	CAN Highspeed (CAN FD capable)	
CAN (FD): Connectors	1x D-SUB9 (dual channel)	
CAN (FD): Baudrates	up to 8 Mbit/s	
Analog and Digital I/O	1 x Digital in/out, e.g. for DoIP Activation Line	1 x Analog input 2 x Digital input 1 x Digital output (open collector) 2 x Digital in/out, e.g. for DoIP Activation Line
Time stamp accuracy: within one device synchr. of multiple devices with sync cable	 1µs typ. 50µs typ. 1µs	
Mean reaction time	250µs	
Operating system	Windows 7/8 (32 and 64 Bit), Windows 10 (64 Bit)	
PC interface	USB 2.0	USB 3.0
Power supply	without external power supply: (bus-powered) at 100 Mbit operation mode, with external power supply: 7...50 V DC, typ. 12 V DC, power-up: 8 V DC	8...50 V (typ. 12 V) power-up: min. 5 V, voltage drop down (< 1 min) to 5 V
Driver libraries	XL Driver Library for CAN and Ethernet	
Temperature range	Operating: -40..+65 °C, storage: -40..+85 °C	Operating: -40..+60 °C, storage: -40..+85 °C
Dimensions(L/W/H)	125mm x 106mm x 32mm	186 mm x 172 mm x 55 mm
Weight	330g	1300g

https://vector.com/vi_vn5610a_vn5640_tdata_iframe_en.druck

A.4 Specifications of DEX COOL

Table A.1
Physical Properties DEX-COOL[19]

Color	Orange
Physical State	Liquid
Odor	Faint or Mild (sweet/sugary smell)
pH	8.0-8.6
Vapor Pressure	<0.01 mmHg @ 20 °C
Vapor Density (Air=1)	2.1
Boiling Point	108.9 °C
Solubility	Miscible
Freezing Point	-36.7 °C
Melting Point	NDA
Flashpoint	(Pensky-Mertens Closed Cup) 127 °C
Autoignition	400 °C
Specific Gravity	1.12 @ 15.6 °C
Viscosity	8cSt @ 40 °C

Table A.2
Chemical Properties DEX-COOL[19]

Ethylene Glycol	80-97 % weight
Diethylene Glycol	1-5 % weight
Potassium 2-ethylhexanoate	1-5% weight

Appendix B

Summary of Program and Data Files

B.1 Chapter 1

Table B.1
Figure Files

Files name	File description
Emissiondata.JPG	1.1
vehicleemissiondata.JPG	1.2
technologies.JPG	1.3
vehicletech.JPG	1.4
hybridvsnonhybrid.JPG	1.5
NEXCARproject.jpg	1.6
modelingapproach.JPG	1.7
thesisorganisation.JPG	1.7

B.2 Chapter 2

Table B.2
Visio Files

Files name	File description
connections.vsdx	2.2
ANL_usage.vsdx	2.5
literature.vsdx	1.7
organization.vsdx	1.8

Table B.3
Figure Files

Files name	File description
2016-Chevrolet-Volt-045-1024x683.JPG	2.1
OBD_port.jpg	2.3

B.3 Chapter 3

Table B.4
Visio Files

Files name	File description
Whole Model.vsdx	3.1
Dynamic engine model.vsdx	3.2
Engine model_fig1.vsdx	3.3
FLOW CHART FUEL PENALTY.vsdx	3.4
circuit diagram.vsdx	3.20
Battery model.vsdx	3.21
transmission.vsdx	3.24
transmission-Mode 1.vsdx	3.25
transmission-Mode 2.vsdx	3.26
transmission-Mode 3.vsdx	3.27
transmission-Mode 4.vsdx	3.28
transmission-Mode 5.vsdx	3.29
1ev.vsdx	3.31
2ev.vsdx	3.32
ler.vsdx	3.33
FG.vsdx	3.34
HER.vsdx	3.35
Auxiliary Pump.vsdx	3.36
LVD.vsdx	3.38
coolant model.vsdx	3.6

Table B.5
Figure Files

Files name	File description
wofuelpenalty.fig	3.5(a)
withfuelpenalty.fig	3.5(b)
enginetorque_figure4.fig	3.13(a)
fuel_figure4.fig	3.13(b)
Manifold_air_flow rate_figure4.fig	3.13(c)
MtrAmap_wo.fig	3.14
mtrBmap_wo.fig	3.15
TPIM A_wo.fig	3.16
TPIMB_wo.fig	3.17
UDDS_Figure7.fig	3.18
US06_Figure7.fig	3.19
batterySOCudds.JPG	3.22
batterySOCus06.JPG	3.23
planetarygear.JPG	3.30
CD.fig	3.37(a)
CS.fig	3.37(b)
base_coolant.JPG	3.7
cooling_plot.fig	3.8
catlystheating.JPG	3.9
catalyst_heatingprofilevalid.JPG	3.10
cooling_profile.JPG	3.11
cooling_validation.JPG	3.12
vehVel.fig	3.41(a)
Fuel Eng.fig	3.41(b)
SOC.fig	3.41(c)
HWFET_vehVel.fig	3.42(a)
HWFET_SOC.fig	3.42(b)
HWFET_Fuel Eng.fig	3.42(c)
speed_CD_us06.fig	3.39(a)
batterypower_CD_us06.fig	3.39(b)
soc_CD_us06.fig	3.39(c)
speed_CD_HWFET.fig	3.40(a)
batterypower_CD_HWFET.fig	3.40(b)
soc_CD_HWFET.fig	3.40(c)

Table B.6
MATLAB/Simulink Files

Files name	File description
Engine_dynamic_model.slx	Engine simulink model file
run_file_engine.m	File needed to extract ANL test data for engine model validation
BatteryModel.slx	Battery model
Auxiliary_pump.slx	Auxiliary pump model
coolant_model.slx	Coolant model
fixMode5OutputTrq_add15.slx	Chevy volt model
parent_072117.m	Initialization m-file
extractModelInputs_072117.m	m-file for extracting inputs from saved ANL folders
DataToLoad_JCT_071417.mat	Parameter file includes all the parameters needed to run the model
validationAnalysisPlots_071217.m	Validation plotting m-file

Table B.7
Data Files

Files name	Test File	Condition
Figure 3.5	Load mat file 61607029.mat and run Engine_model.slx	UDDS CS, $T_{testcell}$=29°C Barometric pressure= 29 (in/Hg)
Figure 3.13	Load mat file 61607019.mat and run Engine_model.slx	US06 CS ,$T_{testcell}$=26°C Barometric pressure= 29 (in/Hg)
Figure3.18	Load mat file 61608022.mat and run Motor_model.slx	UDDS CD, $T_{testcell}$=-7°C Barometric pressure= 29 (in/Hg) Climate Control= 72F auto Constant vehicle speed fan
Figure3.19	Load mat file 61608021.mat and run Motor_model.slx	US06 CD, $T_{testcell}$=-7°C Barometric pressure= 29 (in/Hg) Climate Control= 72F auto Constant vehicle speed fan
Figure3.22	Load mat file 61608022.mat and run BatteryModel.slx	UDDS CD, $T_{testcell}$=-7°C Barometric pressure= 29 (in/Hg) Climate Control= 72F auto Constant vehicle speed fan
Figure3.23	Load mat file 61608021.mat and run BatteryModel.slx	US06 CD, $T_{testcell}$=-7°C Barometric pressure= 29 (in/Hg) Climate Control= 72F auto Constant vehicle speed fan
Figure3.37(a)	Load mat file 61608022.mat and run Auxiliary_pump.slx	UDDS CD, $T_{testcell}$=-7°C Barometric pressure= 29 (in/Hg) Climate Control= 72F auto Constant vehicle speed fan
Figure3.37(b)	Load mat file 61607029.mat and run Auxiliary_pump.slx	CS, $T_{testcell}$=29°C Barometric pressure= 29 (in/Hg)
Figure 3.7	Load mat file 61607029.mat and coolant_model.slx	CS, $T_{testcell}$=29°C Barometric pressure= 29 (in/Hg)
Figure 3.8	Import datacooling.xls in Matlab and run coolant_model.slx model	T_{amb}=-5°C

Table B.8
Data Files

Files name	Test File	Condition
Figure 3.9	Load mat file 61607012.mat and run catalyst model	WOT case, $T_{testcell}$=22°C Barometric pressure= 29 (in/Hg)
Figure 3.10	Import catalysttest.xls and run catalyst model	T_{amb}=-5°C
Figure3.11	Load mat file 61607004.mat and run catalyst model	US06 CD, $T_{testcell}$=25°C Barometric pressure= 29 (in/Hg)
Figure3.12	Load mat file 61607009.mat and run catalyst model	US06 CD, $T_{testcell}$=26°C Barometric pressure= 29 (in/Hg)
Figure3.39	Load mat file 61608021.mat and run chevy volt model	US06 CD, $T_{testcell}$=-7°C Barometric pressure= 29 (in/Hg) Climate Control= 72F auto Constant vehicle speed fan
Figure3.40	Load mat file 61607018.mat and run chevy volt model	HWFET CD, $T_{testcell}$=26°C Barometric pressure= 29 (in/Hg)
Figure 3.41	Load mat file 61607019.mat and run chevy volt model	US06 CS ,$T_{testcell}$=26°C Barometric pressure= 29 (in/Hg)
Figure 3.42	Load mat file 61607025.mat and run chevy volt model	HWFET CS ,$T_{testcell}$=25°C Barometric pressure= 29 (in/Hg)

B.4 Chapter 4

Table B.9
Figure Files

Files name	File description
UDDS_modes.fig	4.1
motorA.fig	4.3
motorB.fig	4.2
vehiclespeed_CS_drivecycle.fig	4.4
MGA_CS_drivecycle.fig	4.6
MGB_CS_drivecycle.fig	4.5
BSFC_CS_drivecycle.fig	4.7
SOC_CS_drivecycle.fig	4.11
transient_speed.jpg	4.8(a)
transient_torque.jpg	4.8(b)
operating_points.jpg	4.9
Engine_tr_del_comm.fig	4.10(a)
Throttle_pos_sim.fig	4.10(b)
tor_50_N_1000.jpg	4.11(a)
tor_60_N_1000.jpg	4.11(b)
tor_70_N_1000.jpg	4.11(c)
tor_80_N_1000.jpg	4.11(d)
Average.JPG	4.12
modeshift.JPG	4.13
auxiliary energy penalty.JPG	4.14
coldstart_energy.JPG	4.15(a)
catalyst energy penalty.JPG	4.15(b)
cranking energy penalty.JPG	4.15(c)
crankingpenaltygrams.JPG	4.16

Table B.10
Data Files

Files name	**Test File**	**Condition**
Figure4.2	Load mat file 61608022.mat and run Motor_model.slx	UDDS CD, $T_{testcell}$=-7°C Barometric pressure= 29 (in/Hg) Climate Control= 72F auto Constant vehicle speed fan
Figure 4.7	Load mat file 61607019.mat and run chevy volt model	US06 CS ,$T_{testcell}$=26°C Barometric pressure= 29 (in/Hg)